A TRIDENT SCHOLAR PROJECT REPORT

NO. 479

Development of Advanced Functional Biomaterials

by

Midshipman 1/C Robert T. Chung, USN

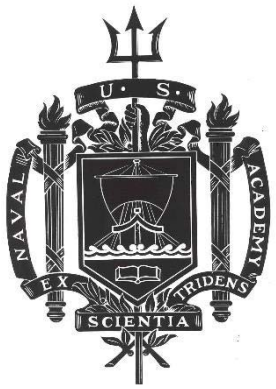

UNITED STATES NAVAL ACADEMY
ANNAPOLIS, MARYLAND

USNA-1531-2

REPORT DOCUMENTATION PAGE

Form Approved
OMB No. 0704-0188

1. REPORT DATE *(DD-MM-YYYY)*	**2. REPORT TYPE**	**3. DATES COVERED** *(From - To)*
5-20-19		

4. TITLE AND SUBTITLE
Development of Advanced Functional Biomaterials

5a. CONTRACT NUMBER

5b. GRANT NUMBER

5c. PROGRAM ELEMENT NUMBER

6. AUTHOR(S)
Chung, Robert T.

5d. PROJECT NUMBER

5e. TASK NUMBER

5f. WORK UNIT NUMBER

7. PERFORMING ORGANIZATION NAME(S) AND ADDRESS(ES)

8. PERFORMING ORGANIZATION REPORT NUMBER

9. SPONSORING / MONITORING AGENCY NAME(S) AND ADDRESS(ES)
U.S. Naval Academy
Annapolis, MD 21402

10. SPONSOR/MONITOR'S ACRONYM(S)

11. SPONSOR/MONITOR'S REPORT NUMBER(S)
Trident Scholar Report no. 479 (2019)

12. DISTRIBUTION / AVAILABILITY STATEMENT

This document has been approved for public release; its distribution is UNLIMITED.

13. SUPPLEMENTARY NOTES

14. ABSTRACT

The goal of this study was to develop novel ionic liquids (ILs) for the Natural Fiber Welding (NFW) process and use them to make advanced functional biocomposite materials with improved mechanical, chemical, and electrical properties. In this project, we synthesized three different classes of ILs containing either aromatic cations, cyclic (non-aromatic) cations, or polymerizable cations. These ILs were prepared to (i) evaluate their potential as novel NFW solvents to disrupt and reorganize biopolymer matrices, (ii) test their ability to polymerize ex-situ, and (iii) fiber-weld and subsequently polymerize within a biopolymer material to generate polyionic biocomposites.

After synthesizing nine different ILs and confirming their structure with nuclear magnetic resonance and infrared spectroscopies, we evaluated their welding potential through confocal fluorescence microscopy and scanning electron microscopy. These data confirmed that each class of ILs were viable NFW solvents. In this effort, we also developed a powerful, new method using atomic force microscopy (AFM) to map the nanomechanical properties of fiber-welded biomaterials. While evaluating each ILs' ability to polymerize ex-situ, we discovered that the acetate anion inhibits polymerization of acetate based polymerizable-ILs (poly-ILs). However, poly-ILs with chloride anions could be polymerized using either photo or thermal initiators. We then synthesized a polyionic biocomposite containing 1-ethyl-3-vinylimidazolium chloride and microcrystalline cellulose within a welded cotton matrix. Our novel results show that poly-ILs can be applied to the NFW process to fabricate advanced fiber-welded polyionic biocomposites. Due to the ionic character added by embedding poly-ILs within a biopolymer material (e.g. silk, cotton, hemp), these biocomposites have the potential for applications in solid battery electrolytes, biosensor technologies, ion-exchange materials, smart textiles, and fuel cell membranes.

15. SUBJECT TERMS
Polymerizable ionic liquids, Natural Fiber Welding, biopolymer materials, cellulose, cotton

16. SECURITY CLASSIFICATION OF:			**17. LIMITATION OF ABSTRACT**	**18. NUMBER OF PAGES**	**19a. NAME OF RESPONSIBLE PERSON**
a. REPORT	**b. ABSTRACT**	**c. THIS PAGE**		66	**19b. TELEPHONE NUMBER** *(include area code)*

U.S.N.A. --- Trident Scholar project report; no. 479 (2019)

Development of Advanced Functional Biomaterials

by
Midshipman 1/C Robert T. Chung
United States Naval Academy
Annapolis, Maryland

_____
(signature)

Certification of Adviser(s) Approval

Professor Paul C. Trulove
Chemistry Department

_____
(signature)

_____
(date)

CDR David P. Durkin, USN
Chemistry Department

_____
(signature)

_____
(date)

Assistant Professor Elizabeth A. Yates
Chemistry Department

_____
(signature)

_____
(date)

Acceptance for the Trident Scholar Committee

Professor Maria J. Schroeder
Associate Director of Midshipman Research

_____
(signature)

_____
(date)

1. Abstract

The goal of this study was to develop novel ionic liquids (ILs) for the Natural Fiber Welding (NFW) process and use them to make advanced functional biocomposite materials with improved mechanical, chemical, and electrical properties. In this project, we synthesized three different classes of ILs containing either aromatic cations, cyclic (non-aromatic) cations, or polymerizable cations. These ILs were prepared to (i) evaluate their potential as novel NFW solvents to disrupt and reorganize biopolymer matrices, (ii) test their ability to polymerize ex-situ, and (iii) fiber-weld and subsequently polymerize within a biopolymer material to generate polyionic biocomposites.

After synthesizing nine different ILs and confirming their structure with nuclear magnetic resonance and infrared spectroscopies, we evaluated their welding potential through confocal fluorescence microscopy and scanning electron microscopy. These data confirmed that each class of ILs were viable NFW solvents. In this effort, we also developed a powerful, new method using atomic force microscopy (AFM) to map the nanomechanical properties of fiber-welded biomaterials. While evaluating each ILs' ability to polymerize ex-situ, we discovered that the acetate anion inhibits polymerization of acetate based polymerizable-ILs (poly-ILs). However, poly-ILs with chloride anions could be polymerized using either photo or thermal initiators. We then synthesized a polyionic biocomposite containing 1-ethyl-3-vinylimidazolium chloride and microcrystalline cellulose within a welded cotton matrix. Our novel results show that poly-ILs can be applied to the NFW process to fabricate advanced fiber-welded polyionic biocomposites. Due to the ionic character added by embedding poly-ILs within a biopolymer material (e.g. silk, cotton, hemp), these biocomposites have the potential for applications in solid battery electrolytes, biosensor technologies, ion-exchange materials, smart textiles, and fuel cell membranes.

2. Keywords

Polymerizable ionic liquids, Natural Fiber Welding, biopolymer materials, cellulose, cotton

3. Acknowledgements

Funding for this work was provided by the Air Force Office of Scientific Research and the Office of Naval Research. Any opinions, findings, conclusions, or recommendations expressed herein are those of the authors and do not necessarily reflect the views of the U.S. Navy, the U.S. Air Force, the Department of Defense, or the U.S. Government.

While I recognize the futility of acknowledging people who will likely never read this work, I still feel an obligation to thank a few key people that have made all of this possible because it is the least I can do to show my gratitude for the endless support they have given me. First, my advisers provided the technical expertise when we ran in to any roadblocks. I definitely owe a lot to Professor Trulove, Commander Durkin, and Professor Yates because they have all been instrumental in developing the methods, conducting the experiments, and evaluating the results in this work. I am truly grateful for the technical skills, thought processes, and general laboratory organization that I developed over my time at this institution and in this lab in particular.

Beyond my advisers, I must also thank the countless numbers of instructors I have had in my educational experience. From Mr. Daschner to Mr. Pfeiffer, Professor Anderson to Professor Fulop, Professor Rehill to Professor Fleming, and everyone in between, I have learned well beyond the established curriculum to develop into who I am today.

Finally, I need to thank my friends and family for their unending support in helping me through this institution. Since day one of Plebe summer, my parents and brother were there to support me, whether I knew I needed it or not. Mom, Dad, and Michael: I love you all. If any of my contemporaries from First Company reads this, thank you for your support. I was moved by your support at my talk, and am continually moved by you all living up to the name of "First Fam." Last of all, I know they will never read this, but I am giving a shout out to Sam, Eli, Curtis, Trent, Dylan, Sean, and Adam. They know what that is for. Especially Sam and Eli.

Fun Fact: After having completed restoration this month, the Union Pacific Big Boy number 4014 is currently the largest and most powerful steam locomotive operating in the world today.

4. Table of Contents

5. Introduction

Synthetic polymers have been in the public's attention since the development of nylon just before the middle of the 20th century.[1] As one of the first mass-produced synthetic polymers, nylon freed textile manufacturing from its dependence on natural fiber materials (e.g. cotton, wool, or silk). Despite more than half a century of development, synthetic fibers often remain inferior to natural fibers. For example, the energy needed to break spider silk can be much greater than nylon or Kevlar on a mass basis.[2] Additionally, while natural cotton and synthetic rayon fibers both contain cellulose, the process to make rayon requires carbon disulfide, which is highly toxic.[3] The advantages of natural biopolymers over synthetic polymers arise from biopolymers' complex native structures that have developed through millions of years of evolution (see Figure 1, adapted from Haverhals, *et al*.[4]).

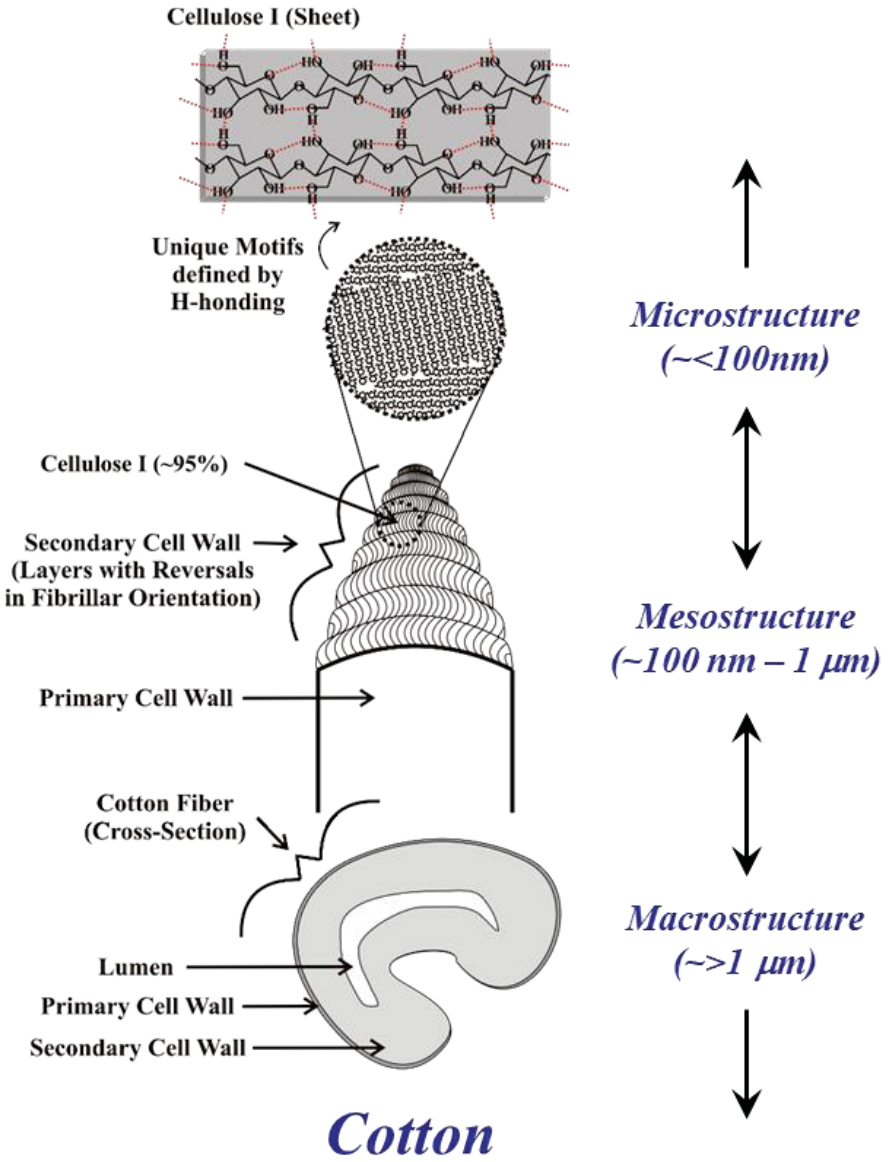

Figure 1. Diagram of hierarchical structure in cotton.

Processes that can manipulate biopolymers without destroying their underlying structure can deliver new materials that take advantage of native biopolymer physical properties. While such processes have been previously reported, most require noxious chemicals and often weaken the underlying biopolymer matrix. Recently, a more promising route has emerged that involves the use of ionic liquids (ILs).[3]

ILs are a class of ionic compounds that are liquid at relatively low temperatures (typically <100°C), allowing them to function as a unique type of solvent. There is a tremendous variety of ILs due to the wide range of cation and anion combinations that can be used to generate them, which enables the tailoring of ILs for specific applications.[5] Some examples of compounds that exist as ILs at low temperatures are shown in Figure 2.

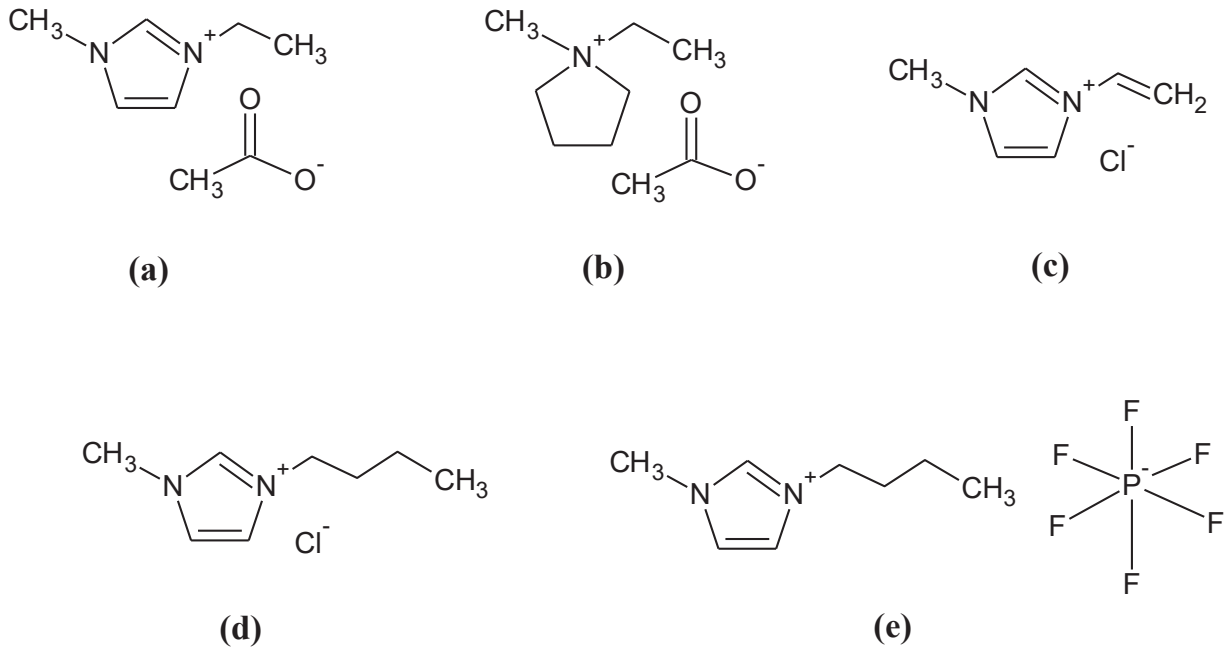

Figure 2. Structure of common ILs: (a) 1-ethyl-3-methylimidazolium acetate, (b) 1-ethyl-1-methylpyrrolidinium acetate, (c) 1-methyl-3-vinylimidazolium chloride, (d) 1-butyl-3-methylimidazolium chloride, (e) 1-butyl-3-methylimidazolium hexafluoro-phosphate.

ILs have been designed for and used in the modification and dissolution of biomaterials such as cellulose,[3] silk[6], chitin and chitosan,[4] wool keratin,[7] and starch.[8] ILs are a more environmentally friendly alternative to conventional solvents for biomaterial modification because they have an insignificant vapor pressure, and can easily be recycled.[9] While it is possible to dissolve biomaterials completely using ILs, doing so can destroy the complex native biomaterial structure that gives rise to many of their useful physical properties. By controlling treatment conditions with ILs, however, it is possible to alter the biopolymer matrix without destroying it.

Natural Fiber Welding (NFW) is a process developed in our laboratory to manipulate and modify natural biomaterials using ILs.[10] NFW involves the controlled application of an IL to a biopolymer material, such as cotton or silk, to modify its mechanical, chemical, and/or electrical properties. A key feature of this process is the alteration of only the outer portion of individual

fibers, resulting in a significant preservation of the material's native structure and properties.[4, 10] This process is illustrated in Figure 3.

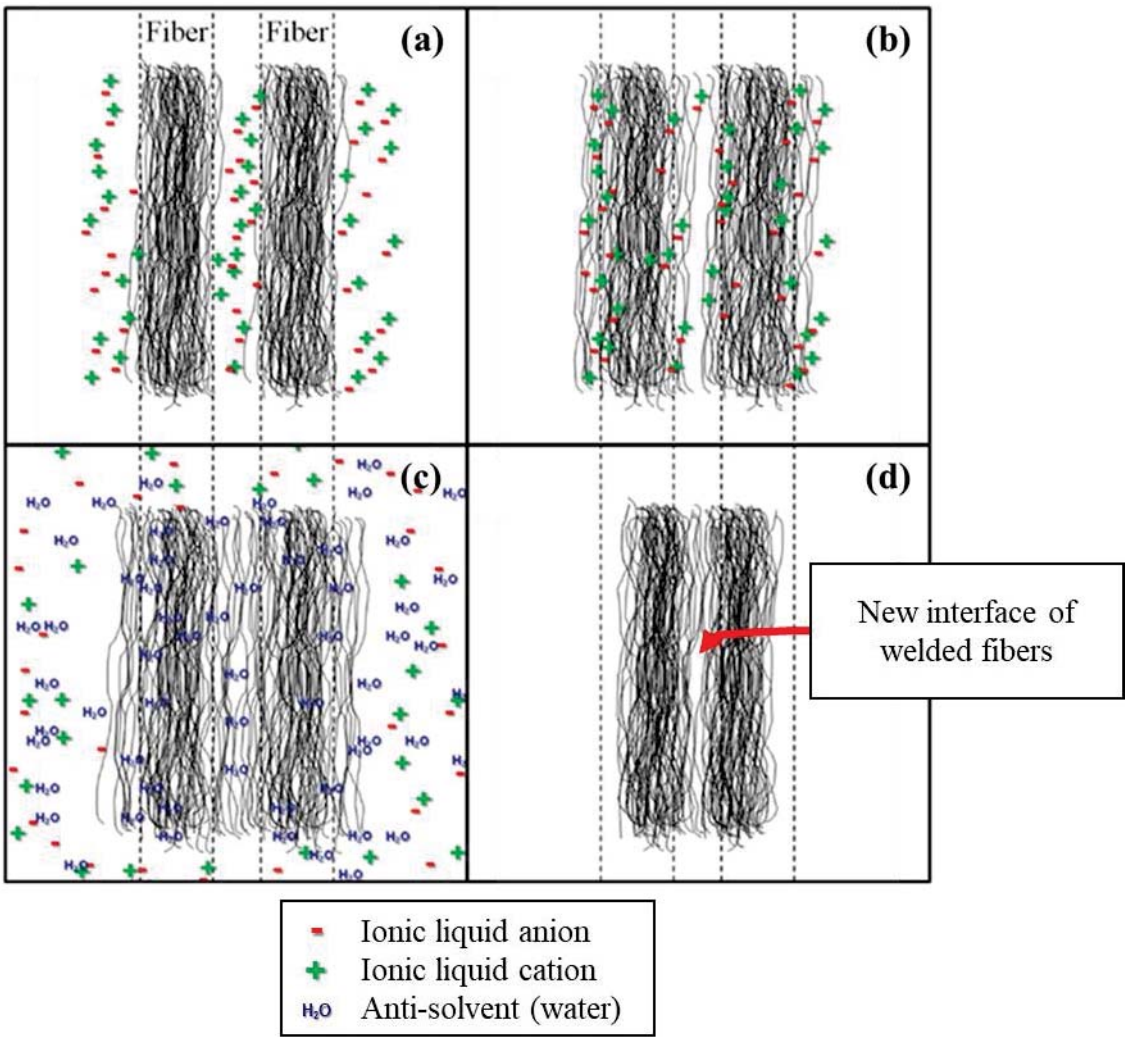

Figure 3. General scheme for the Natural Fiber Welding of two parallel fibers illustrating (a) the application of ionic liquid (IL), (b) the interaction of IL with the biopolymer, (c) the removal of IL using an anti-solvent, and (d) the modified biopolymer material. Solid vertical lines in each figure represent biopolymer chains while dashed vertical lines have been added to each figure as points of reference for resulting dimensional changes.

At the beginning of the NFW process, natural fibers are exposed to a controlled amount of IL at a desired temperature (Figure 3a). On the outer surface of each fiber, biopolymer chains (represented by the solid vertical lines making up the two fibers in Figure 3) are mobilized by disruption of their intermolecular hydrogen bonds by the added IL. The interaction between the fibers and the solvent is controlled for a given time (Figure 3b) before the IL is removed with an anti-solvent such as water (Figure 3c). After IL removal, the disrupted hydrogen bonds of the biopolymer chains are re-formed, giving fibers that have been welded at the fiber interface (Figure 3d). By carefully controlling the IL treatment conditions, this process can fuse individual biopolymer fibers, while retaining most of the native biopolymer structure.

NFW has proven to be a versatile engineering method for biopolymer manipulation, and over the years, several different ILs have proven to be capable welding solvents for a wide variety of biopolymer materials. The most common IL solvent used in NFW has been based off the 1-ethyl-3-methylimidazolium (EMI) cation.[4, 7-11] This is because it was believed that NFW could only be successful when performed using chaotropic anions and hydrogen-bonding cations that interact strongly with hydrogen bonding networks of cellulose.[4, 10] The present work challenges this paradigm by revealing a new non-aromatic IL, 1-ethyl-1-methylpyrrolidinium acetate (EMPyrAc), can also be an effective NFW solvent. This work then explores the viability of a series of polymerizable ILs (poly-ILs) in the NFW process.

There is strong evidence in the literature to suggest that poly-ILs may also be viable for NFW.[12, 13] Poly-ILs are so-named because one of their alkyl substituents, of the form $(CH_2)_nCH_3$, is replaced with an alkenyl group (e.g., vinyl ($-CH=CH_2$) or allyl ($-CH_2-CH=CH_2$)) that enables polymerization of the poly-IL cation. The alkenyl functional group present on a poly-IL cation can be initiated to undergo radical polymerization, generating a polymerized ionic liquid (Figure 4).

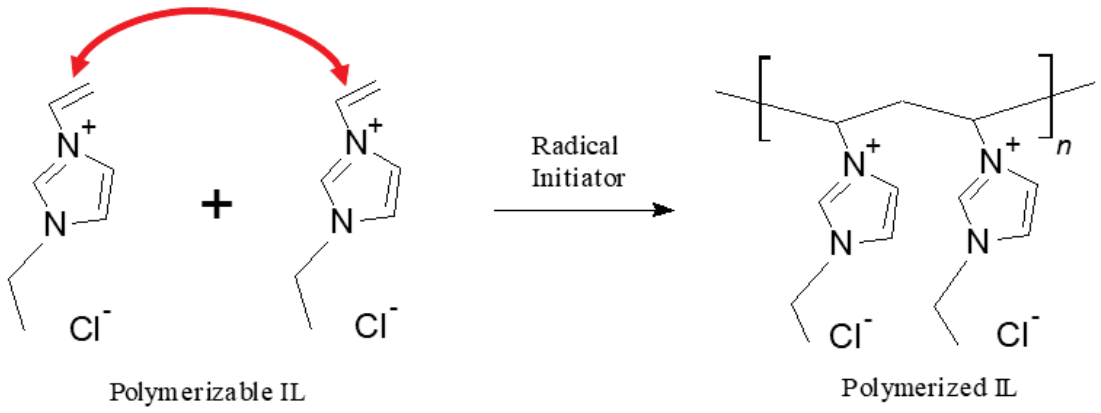

Figure 4. Polymerization scheme for using monomeric polymerizable ionic liquids (poly-ILs, left) to generate polymerized ionic liquids (right).

In short, this radical initiation process involves the formation of a radical from an initiator molecule and an appropriate stimulus. This radical can then react with the alkenyl group, forming another free radical which can undergo a chain-reaction with additional alkenyl groups.

While both the allyl and vinyl functional groups can be used in polymerization reactions, there is a difference in reactivity of these two groups caused by their chemical structure.[14] The allyl has an extra methylene group that allows it to form a resonance structure when the radical forms in the first step of a radical chain mechanism. While the resonance stability of the allyl functional group encourages the formation of the allylic radical, it also reduces this group's ability to produce a polymer by increasing the stability of the intermediate molecule. The vinyl functional group does not have this issue; instead, it is very reactive when it forms the vinylic radical. This stability can also create issues with preparing allylic and vinylic compounds; those containing the vinyl group have to be prepared with greater care to prevent side reactions involving the vinyl

group. This basic chemistry indicates that a vinylic poly-IL would be easier to polymerize than the allylic counterpart.

The poly-IL polymerization follows the same type of radical chain mechanism that is used to make synthetic polymers such as polystyrene (in Styrofoam) and polyvinylchloride (PVC) from their alkenyl precursors. Radical chain mechanisms require a radical initiator, which provides the initial stimulus for adjacent poly-IL molecules to react. One such radical initiator that depends on the addition of heat (azobisisobutyronitrile, AIBN) has been used to polymerize poly-ILs.[13, 15, 16] Our work examined the polymerization using AIBN, as well as another radical initiator (2-hydroxy-2-methylpropiophenone, HMPP) that uses UV light as the stimulus, based on work reported in the literature.[17, 18]

By polymerizing poly-ILs within a biopolymer material matrix, it becomes possible to generate new, charged biocomposites (Figure 5).

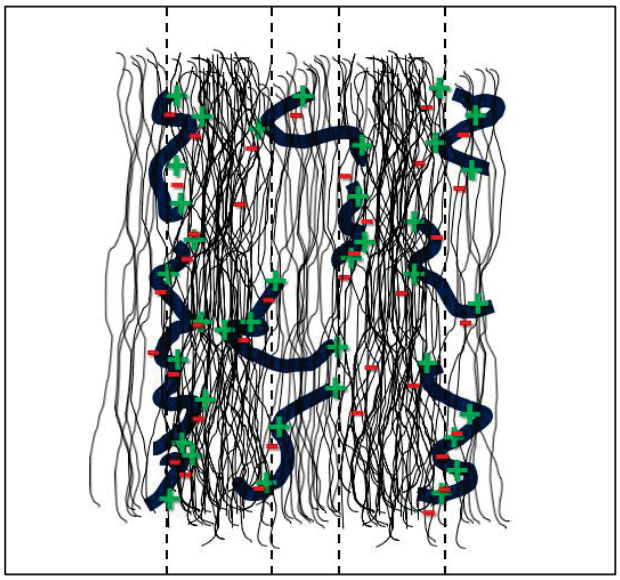

Figure 5. Illustration of the desired polyionic biocomposite material. The thick solid blue lines represent polymerized poly-IL cations in the biopolymer matrix, and the thin black lines represent biopolymer chains.

Because these generated biocomposites will have charged polymerized ILs within the biopolymer network that has been modified through the NFW process, these materials should have unique, functional properties. These properties would allow the polyionic biocomposites to be applied to fields of solid battery electrolytes, biosensor technologies, ion-exchange materials, smart textiles, and fuel cell membranes.

6. Experimental

6.1 Materials

Cotton yarns (white 100% mercerized Coats Cotton ART.8975 J7 150), microcrystalline cellulose (MCC, Sigma), and Aida Cloth (Sensations Article 335-4669) were used as received. The following chemicals were used: sodium hydroxide (98.0%), sodium borohydride (98.9%), sodium periodate (99.8%), (Fischer Chemical); concentrated hydrochloric acid (37.4%), ammonium acetate (99.0%), potassium acetate (>99.0%), iodomethane (99%), 1-vinylimidazole (100%), 1-methylimidazole (>98%), 2-hydroxy-2-methylpropiophenone (HMPP, 97%), dimethyl sulfoxide (DMSO, 98%) and azobisisobutyronitrile (AIBN, 98%), (Sigma-Aldrich); 1-methylpyrrolidine (>98%), 1-ethyl-1-methylpyrrolidinium bromide (99%), and 1-allyl-3-methylimidazolium chloride (>98%) (Iolitec); fluorescein-5-thiosemicarbazide (FTSC, >95%), and 7-diethylaminocoumarin-3-carboxylic acid hydrazide (DCCH, >95%), (Invitrogen); methanol (99%), acetonitrile (ACN) (99.9%) (Pharmco-Aaper); deuterium oxide (99.8%) and deuterated chloroform (99.8%), (Acros Organics). The 1-methylimidazole and the 1-methylpyrrolidine were redistilled prior to use, and the AIBN was recrystallized in methanol. All other chemicals and materials were used as received. An Eponate 12 kit with DMP-30 from PELCO was used as received for potting the modified biopolymer materials in epoxy.

6.2 Material synthesis and procedures

6.2.1 Dyeing cotton yarns

Most of the yarns used in this semester's project were prepared in the previous academic year (2017/2018) according to procedures described in MIDN Chung's SC495/496 report. In summary, cotton yarns were fluorescently labelled using FTSC and DCCH via a Schiff base mechanism using sodium periodate to oxidize the hydroxyl groups in cellulose and bind to the azo groups in FTSC and DCCH.[19] Subsequent reduction using sodium borohydride was followed by rinsing and drying to produce the labelled yarns.

6.2.2 Synthesis of ionic liquids

Nine ILs were synthesized in this project: 1-ethyl-3-methylimidazolium acetate (EMIAc), 1-ethyl-1-methylpyrrolidinium acetate (EMPyrAc), 1-allyl-3-methylimidazolium acetate (AMIAc), 1-allyl-1-methylpyrrolidinium acetate (AMPyrAc), 1-methyl-3-vinylimidazolium iodide (MVII), 1-methyl-3-vinylimidazolium acetate (MVIAc), 1-ethyl-3-vinylimidazolium bromide (EVIBr), 1-ethyl-3-vinylimidazolium acetate (EVIAc), and 1-ethyl-3-vinylimidazolium chloride (EVICl). The syntheses of EMIAc and EMPyrAc are described in MIDN Chung's SC495/496 report. In short, these two were prepared from their aqueous bromide salts. The aqueous ILs were generated after a two-step ion-exchange process followed by acetic acid neutralization. These ILs were used in experiments after removing the majority of the water through rotary evaporation followed by 1 week of drying under high vacuum.

The structural identities of pure EMIAc and EMPyrAc were confirmed using ^{1}H nuclear magnetic resonance (NMR) spectroscopy. The spectra of these compounds are included in Figures A-1 and A-2 in the Appendix.

Two other ILs, AMIAc and AMPyrAc, were synthesized using a different method than that used for the EMIAc and EMPyrAc. The AMIAc was prepared from 1-allyl-1-methylimidazolium

chloride (AMICl) directly using an anion exchange column charged with acetate anions, omitting the hydroxyl step used in the synthesis of EMIAc and EMPyrAc (see Figure 6).

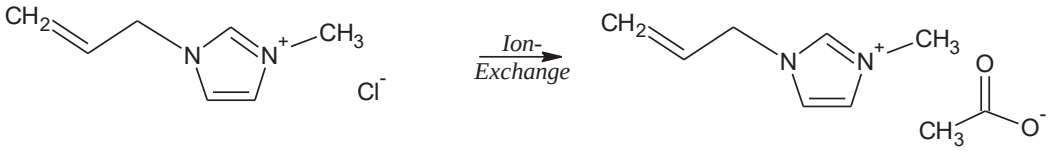

Figure 6. Ion exchange process for generation of AMIAc (right) from AMICl (left).

This omission was based on procedures in the literature describing simple, direct ion exchange of ILs.[20] The column was charged with 4 L of 1.5 M ammonium acetate ([NH_4][Ac]) which provided enough acetate to charge the anion exchange resin (IRA400, Alfa Aesar) via mass action. Excess [NH_4][Ac] was removed by rinsing the column with 5 L of 18 MΩ water. To generate AMIAc, AMICl was dissolved in water and transferred to the ion exchange column. The eluent was collected and brought to pH 6.54 using glacial acetic acid. After evaporating the water using high vacuum, the synthesis of AMIAc was confirmed using NMR (Figure A-3).

AMPyrAc was synthesized in two steps: quaternization reaction to form the pyrrolidinium halide (Figure 7a), and ion exchange to generate the acetate form (Figure 7b). The ion exchange step followed the same procedures described above for the AMIAc synthesis and purification. The synthesized AMPyrAc structure was confirmed using NMR (Figure A-4).

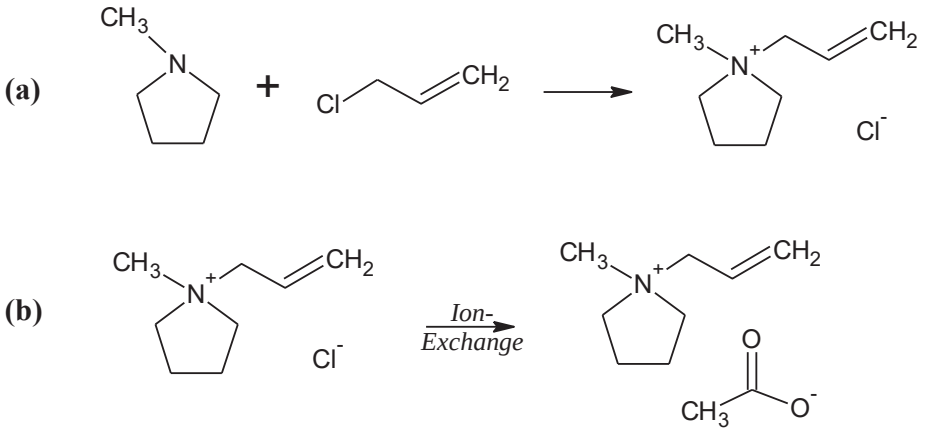

Figure 7. Reaction scheme for synthesis of AMPyrAc showing (a) the quaternization reaction between N-methylpyrrolidine and allyl chloride and (b) the anion exchange of 1-allyl-1-methylpyrrolidinium chloride to form AMPyrAc.

EMIAc was also generated using the direct anion exchange process (i.e., direct exchange to acetate form vice exchanging the salt to the hydroxide form followed by exchange of the hydroxide salt to acetate) described for AMIAc to compare the two methods for generating acetate forms of ILs. NMR found the EMIAc generated from both methods were identical, but EMIAc generated using the first method was used in the welding experiments described in this report.

MVIAc was synthesized through a two-step process from 1-vinylimidazole and iodomethane, according to the reaction scheme in Figure 8. This procedure is adapted from methods found in the literature.[21, 22]

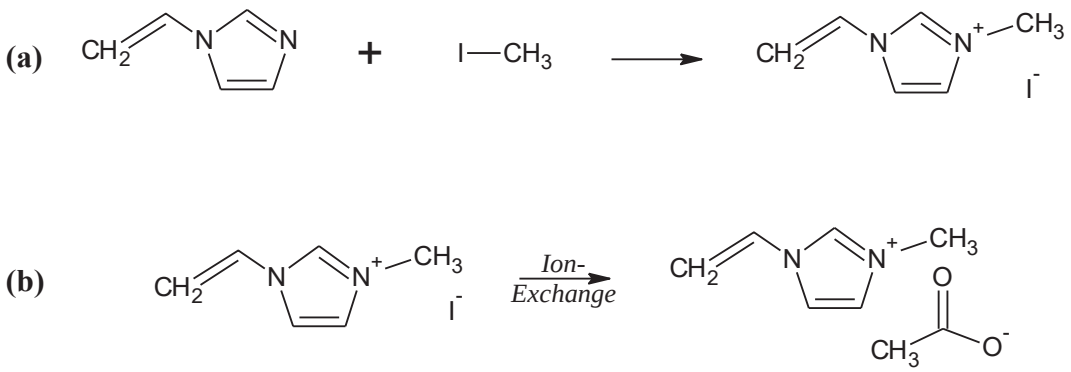

Figure 8. Reaction scheme for synthesis of MVIAc showing (a) the quaternization reaction between 1-vinylimidazole and iodomethane and (b) the anion exchange of 1-methyl-3-vinylimidazolium iodide to form MVIAc.

1-Vinylimidazole (25.0383 g) and iodomethane (20.1 mL) were reacted for 24 h in a round-bottom flask with a slight molar excess of iodomethane (1:1.2) in an ice bath to keep the reaction controlled (Figure 8a) in ACN and under a N_2 purge. This generated 1-methyl-3-vinylimidazolium iodide (MVII) in solution, which was crystallized with ethyl acetate. Drying the precipitate resulted in dry MVII – which was the intermediate compound in synthesizing MVIAc, but was an IL in and of itself. The MVII structure was confirmed using NMR (Figure A-5). The MVII was converted to the acetate form using the anion-exchange column (Figure 8b). The MVIAc structure was also confirmed using NMR (Figure A-6).

The synthesis process used for EVIBr and EVICl were both similar to the process used for MVIAc, with the modification of omitting the acetate ion-exchange step. In generating EVIBr, ethyl bromide was used instead of iodomethane. In this process, 1-vinylimidazole (25.0444 g) was reacted with ethyl bromide (37. mL), with the ethyl bromide in molar excess (2:1). This generated EVIBr in solution, which was crystallized with ethyl acetate, and dried to generate the pure IL. The EVIBr structure was confirmed using NMR (Figure A-7).

In the process for generating EVICl, ethyl chloride was used instead of iodomethane, generating 1-ethyl-3-vinylimidazolium chloride in solution, which was crystallized with ethyl acetate and dried to generate the pure IL. The EVICl structure was confirmed using NMR (Figure A-8).

To synthesize EVIAc, EVIBr was converted to the acetate form using the anion-exchange column described in the synthesis AMIAc and dried to remove excess water. This EVIAc structure was confirmed using NMR (Figure A-9).

6.2.3 Preparation and mounting of yarns on plates for treatment with ionic liquid

The method for conducting the NFW process used in this study is a variation on the technique developed by Haverhals, *et al.*[10] and described by Chung, *et al.*[23] In summary, an aluminum plate was designed and drilled with holes in such a way as to allow orientation of six sets of crossed yarns and six sets of parallel yarns. The distance spanned by each yarn was ~1 cm. An illustration of the setup and the demonstration of fluorescence of the dyed yarns is shown in Figure 9.

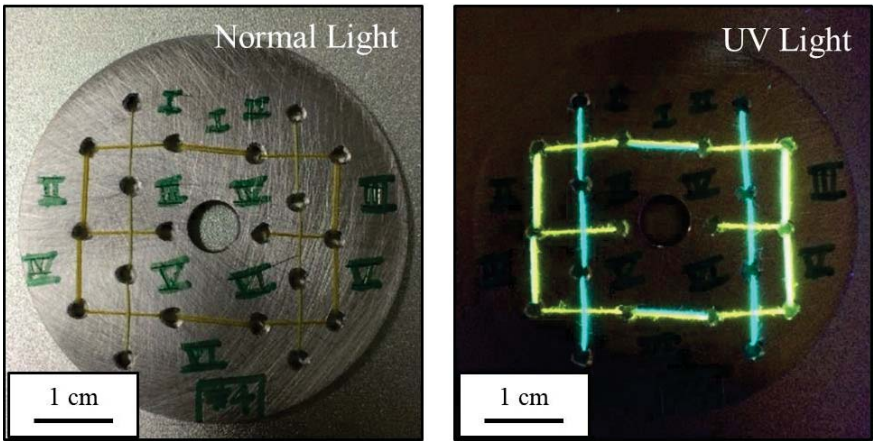

Figure 9. Experimental setup used to test the welding ability of various ILs on a single experimental plate.

6.2.4 Treatment of plates with ionic liquid

After fixing the fluorescently dyed yarns on the aluminum plate, NFW treatment using IL was performed in a N_2-filled drybox (H_2O < 1 ppm) to prevent contamination of the IL with atmospheric water. The IL application was conducted at either 60 °C (EMIAc, EMPyrAc, AMIAc, AMPyrAc, MVIAc, and EVIAc) or at 100 °C (EVICl). Temperature control was achieved using two heating blocks surrounding the treatment plate. Each of the 12 positions on the plate were labelled I-VI (see Figure 9) for both parallel and crossed yarns. This scheme allowed the treatment time of IL to be varied systematically. For a given plate, 2 µL of IL was applied to each position at a specified time to determine the effects of time on the NFW process for a given IL. The treatment time of each position on the plate is described in Table 1.

Table 1. IL Treatment and Application Times

Position Identifier	IL Treatment Time (min)	IL Application time (min)
I	60	0
II	30	30
III	15	45
IV	10	50
V	5	55
VI	0	Not Applied

Following application of IL to each spot on the plate for the specified amount of time, the whole plate was transferred into a methanol solution to quench the NFW process (as illustrated using water in Figure 3c). Following the methanol rinse, the plate was transferred to distilled water for further IL removal. After rinsing in stirred water for at least 24 h, the plate was transferred to a 60 °C oven to dry for 24 h before further analysis.

6.2.5 Polymerizing the poly-ILs

Each of the poly-ILs was evaluated for its ability to polymerize in the absence of a biopolymer material. For this process, polymerization was attempted using both a thermal initiator, AIBN, and a photoinitiator, HMPP. Based on procedures in the literature,[13, 15, 16, 18] AMICl, MVII, MVIAc, EVIAc, EVIBr, and EVICl were each exposed to these radical initiators, both neat and in solution with molecular co-solvents such as ACN.

In evaluating the polymerization ability of the ILs that were liquid at room temperature, a homogeneous solution of IL and initiator was generated with stirring alone. ILs that were not liquid at room temperature (Table 2) required an additional heating step prior to mixing (80°C for AMICl and 100°C for EVICl). The compositions of IL and initiator mixtures listed in Table 3 were determined based on previous work in the literature and results from our own experiments.[13, 18]

Table 2. Measured Melting Points (MP) of Select ILs

IL	MP (°C)
AMICl	~59
MVII	66.4-68.9
EVIBr	99.7
EVICl	79.6-81.2

Polymerization tests were conducted on ILs in solution to determine solvent effects on the process and to confirm the acetate inhibition effect. Each solution composition tested is described in Table 3. In preparing these solutions, the IL and initiator were added (by mass) to a 20 mL scintillation vial to achieve the desired composition. To this, the desired amount of solvent was added by volume using a disposable pipet.

Table 3. Target IL solution compositions

IL	Solvent	Solvent Volume (mL)	Initiator	Additions	Initiator/IL (mol%)	Polymerized
AMICl	None*	0	AIBN		1	No
AMICl	None*	0	HMPP		1	No
EVIBr	Chloroform	15	AIBN		3	Yes
	Acetonitrile	5	HMPP		5	Yes
	Acetonitrile	1	HMPP		5	Yes
	Acetonitrile	5	HMPP	Acetic Acid	5	Yes
EVIAc	Chloroform	15	AIBN		3	No
	Acetonitrile	15	AIBN		3	No
	Acetonitrile	5	HMPP		5	No
	Acetonitrile	1	HMPP	MCC	1	No
	None	0	HMPP		10	No
MVII	Acetonitrile	5	HMPP		5	Yes
EVICl	Acetonitrile	1	AIBN		1	Yes
	Acetonitrile	1	HMPP		1	Yes
	Acetonitrile	1	HMPP		5	Yes
	Acetonitrile	1	HMPP	MCC	1	Yes
	Water	1	HMPP		1	Yes
	Water	2	HMPP	Potassium Acetate	1	No[#]
	DMSO	1	HMPP		3	Yes
	None*	0	HMPP		1	Yes

**Required heating to melt the IL and mix in the photoinitiator*

[#]While the product was still liquid, a small portion of the monomer had polymerized

The generated polymerized IL products were analyzed using both NMR and attenuated total reflectance Fourier transform infrared (ATR-FTIR) spectroscopies (Appendix Figures A-10, A-11, A-27, A-28).

6.2.6 Generating poly-IL biocomposites

The first method used to generate a poly-IL biocomposite involved dissolving MCC in EVICl. In this approach, 3 wt% of MCC was dissolved in a solution containing a 1:1 mole fraction EVICl:ACN and 1 mol% of HMPP (with respect to the IL). This solution was exposed to a 120V 100W mercury vapor lamp (Evergreen Pet Supplies) for 3 min to polymerize the EVICl and was evaluated using scanning electron microscopy.

Second, bulk welding and polymerization of EVICl was conducted using both Aida Cloth (for preliminary experiments) and a jig apparatus with a hollow backing. In initial tests, Aida

Cloth was soaked with EVICl and welded for 1 h at 100 °C. After this time, the cloth was exposed to the mercury vapor lamp for 3 min on each side. This sample was tested by simple swelling tests with water.

The hollow-backed jig setup used to generate biocomposites was similar to the parallel yarn junctions shown in Figure 9, but with the added feature of twisting the yarns to ensure contact was maintained throughout the welding process. In this setup, dyed cotton yarns were suspended on the jig and treated with excess EVICl to thoroughly coat the material. This was heated at 100 °C for 3 h to allow for welding before the plate was exposed to the mercury vapor lamp for 3 min on each side. During and after wetting with water, the polymerized IL biocomposite materials were evaluated using CFM and ATR-FTIR.

6.3 Instrumental Methods

6.3.1 Visualization of dyed yarns using confocal fluorescence microscopy (CFM)

The dyed yarns were imaged using a CFM instrument (Nikon C2si) and associated analysis software (NIS-Elements) to verify the presence of bound fluorescent dye molecules and analyze the IL-treated yarns. The 408 nm and 488 nm lasers were used to capture the unique fluorescence wavelengths of DCCH and FTSC.

This CFM process was used to analyze the plates containing IL-treated, fluorescently-labelled yarns as well as the generated polyionic biocomposites. Criteria used to evaluate the modified biomaterials using CFM included the number of stray fibers, the apparent movement of fluorescently-labeled polymer, the dimensional changes of the yarns, and the general appearance of the welded material.

6.3.2 Imaging of modified biomaterials using scanning electron microscopy (SEM)

After examining the welded yarns using CFM, the welded yarn samples were further visualized using SEM (Tescan MIRA3). Prior to imaging, samples were sputter coated with a layer of gold (Hummer 6.2). SEM (10 kV) was able to provide more detailed information about the materials' surface morphology than CFM alone. SEM was also used to provide elemental analysis of the polymerized EVICl-MCC biocomposite. This sample was prepared for SEM analysis by sectioning with a razor blade and coating in conductive carbon using a high vacuum carbon evaporator (Cressington 208C).

6.3.3 Mechanical properties measurement using atomic force microscopy (AFM)

After imaging the welded samples using SEM, the parallel yarn junctions were analyzed using AFM. AFM provides imaging complementary to CFM and SEM, but can also measure the nanomechanical properties (stiffness, toughness, elasticity, adhesion) of the welded material. The welded samples were prepared for AFM analysis by first potting the parallel yarn junctions in an epoxy mixture in a custom-made silicone mold to suspend the yarns. This epoxy mixture was prepared according to the procedure in the PELCO epoxy kit for a 'hard' solution. Potted samples were cross-sectioned on an RMC PowerTome PC instrument (cutting speed 1.4 mm/sec) using a diamond knife. The exposed cross-sections were analyzed using a Bruker Multimode 8 AFM in PeakForce Quantitative Nanoscale Mechanical (QNM) characterization mode with Sanasyst Air cantilevers.

6.3.4 Ionic conductivity measurements of the polymerized IL

In order to determine the ionic conductivity of the polymerized IL, broadband dielectric spectroscopy measurements were made in the frequency range of $0.1 – 10^7$ Hz using a Novocontrol Alpha Analyzer with a QUATRO liquid nitrogen temperature control system with temperature stability ±0.1 K. Samples were measured in a parallel plate capacitor geometry with 10 mm diameter stainless steel electrodes. A sample thickness of 0.1 mm was maintained using silica rod spacers.

The only poly-IL analyzed using dielectric spectroscopy was polymerized EVICl. To prepare it for evaluation using dielectric spectroscopy, a solution containing 1 mol% photoinitiatior (HMPP) and the IL was initiated for 3 min under the mercury lamp, subsequently placed in the parallel plate capacitor and held at 410 K for 48 h. Afterwards, the capacitor and sample were loaded into the dielectric spectrometer and annealed at 450 K for 24 h to erase any thermal history prior to making the conductivity measurement.

7. Results and Discussion

7.1 Novel ILs' potential as NFW solvents

In this project, we successfully synthesized nine ILs – EMIAc, EMPyrAc, AMIAc, AMPyrAc, MVII, MVIAc, EVIBr, EVICl, and EVIAc (Figure 10). Seven of these ILs were evaluated in the NFW process, five were evaluated for their polymerization ability, and one was evaluated for its ability to generate a polyionic biocomposite. The preparation of these ILs is supported by NMR peak assignments included with the description of the synthesis of each respective IL and their associated NMR spectrum included in Appendix Figures A-1 to A-11. These are complemented by data from ATR-FTIR, which are included in Appendix Figures A-18 to A-28.

The first part of this study was a systematic evaluation of welding ability of ILs containing sequential changes in structure (Figure 10). The welding ability of EMIAc had been demonstrated in the past and served as a 'control' IL in this project.[10, 24] Each IL was selected for its unique character, relative to this classic NFW solvent. In short, EMPyrAc was chosen because its cation possessed a non-aromatic ring structure. AMIAc was the first poly-IL synthesized and only differed from the EMIAc by one functional group (allyl vice ethyl). AMPyrAc, similarly, differed from EMPyrAc by one allyl functional group. MVIAc allowed for the evaluation of the welding capabilities of an IL with a vinyl group. EVIAc was generated to reduce the practical (viscosity) limitations of MVIAc in the NFW process. EVICl was explored because it was suspected to be an effective welding solvent that could also be successfully polymerized.

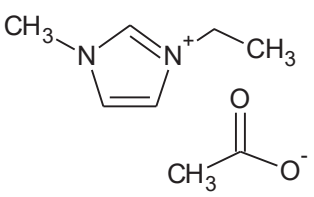

1-ethyl-3-methylimidazolium acetate (EMIAc)

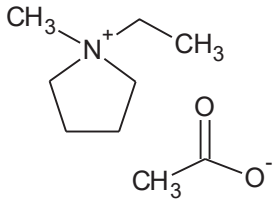

1-ethyl-1-methylpyrrolidinium acetate (EMPyrAc)

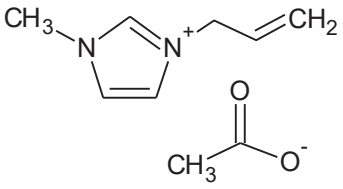

1-allyl-3-methylimidazolium acetate (AMIAc)

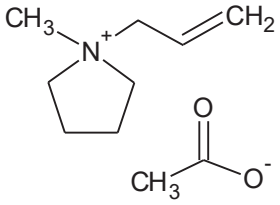

1-allyl-1-methylpyrrolidinium acetate (AMPyrAc)

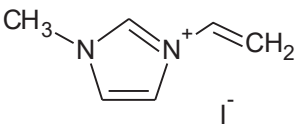

1-methyl-3-vinylimidazolium iodide (MVII)

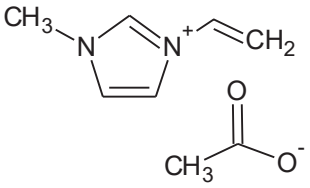

1-methyl-3-vinylimidazolium acetate (MVIAc)

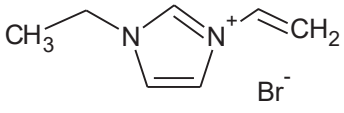

1-ethyl-1-vinylimidazolium bromide (EVIBr)

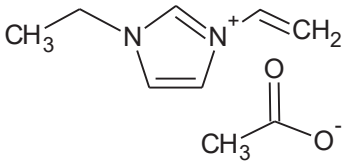

1-ethyl-1-vinylimidazolium acetate (EVIAc)

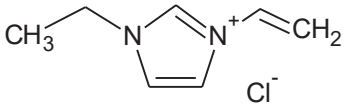

1-ethyl-1-vinylimidazolium chloride (EVICl)

Figure 10. The nine ILs synthesized in this project.

Fluorescently labelling the cotton yarns employed in the welding process allowed the use of CFM to monitor the mobilization of polymers from the yarns at various stages in the welding process. Several meters of yarn were dyed with either DCCH or FTSC. Visual inspection showed that apart from the dye color, the dyed yarns had no differences in physical features from the non-dyed yarns. The DCCH-dyed yarns appeared yellow-green in the CFM imaging while the FTSC-dyed yarns appeared medium blue-green (Figures 11 and 12).

These dyed yarns were used in NFW experiments to evaluate how IL cation and anion structure impacted the IL's welding effectiveness and determine how a polymerizable functional group affects a given IL's welding ability. This provided useful information that will direct future work to better pursue the goal of novel, functional biopolymer materials.

The welded products were comprehensively examined using CFM and SEM to monitor the polymer movement that occurs in NFW (selected images shown in Figures 11 and 12, complete images can be found in Appendix Figures A-12 to A-17, EVIAc not shown). Both imaging techniques offered valuable insight into the welding capabilities of the five ILs, and allowed (1) the confirmation of the welding capability of the pure EMIAc and (2) the discovery of five novel ILs were effective welding solvents. Before discussing the results of the five novel ILs synthesized and evaluated in NFW, the welding process is discussed using the results obtained with EMIAc (Figure 11).

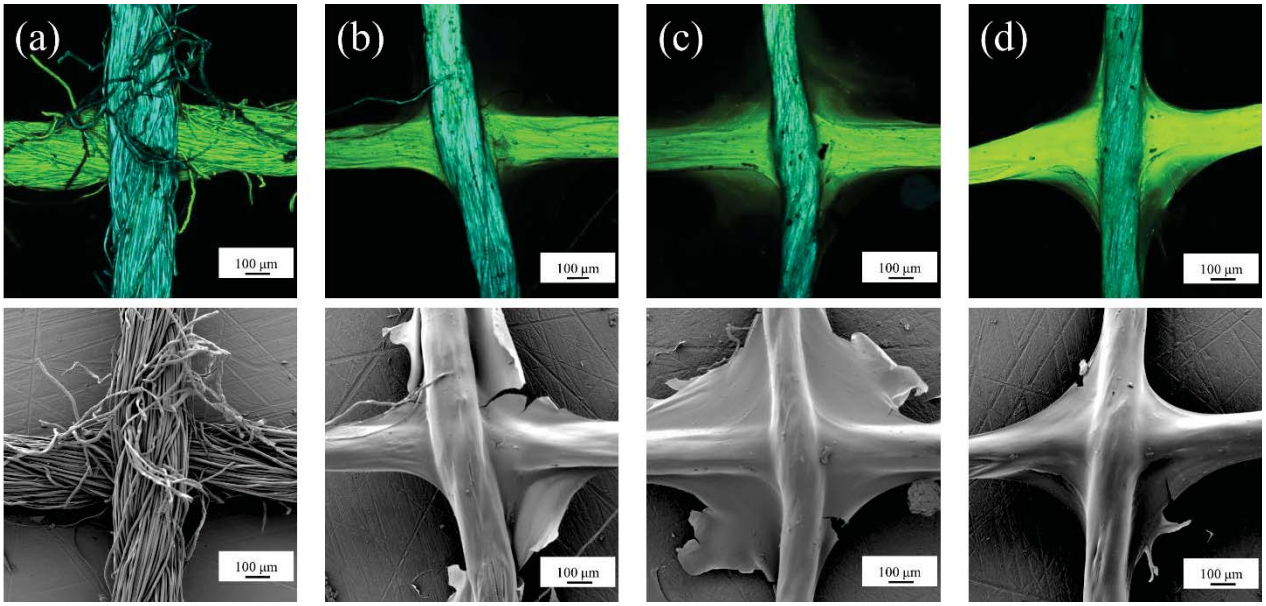

Figure 11. Confocal Microscopy (CFM) (top, colored) and Scanning Electron Microscopy (SEM) (bottom, grayscale) of (a) an untreated cotton yarn junction, and junctions treated with EMIAc at 60 °C for (b) 15 min, (c) 30 min, and (d) 60 min. Samples were gold-sputtered prior to imaging in the SEM (10 kV).

As shown in Figure 9 in the procedures section, each experimental setup had the ability to evaluate welding at 12 replicate yarn junctions. The images shown in Figure 11 represent four junctions treated with EMIAc for different amounts of time (the full set of images collected for EMIAc are included in Figure A-12). These data illustrate how time effects the welding process.

As the yarns were treated with IL for increasing amounts of time, it became more difficult to distinguish individual fibers within the yarns. Additionally, the surface of the junction became smoother with increasing treatment time, indicating the IL was able to mobilize the fibers to a higher degree and redistribute them more evenly on the surface of the material. A final sign that indicates the presence of welding is the formation of a fluorescent 'webbing' between yarns in the crossed yarn junctions (shown in Figure 11) caused by excess IL flowing across the yarn material and mobilizing some of the fluorescently-labeled biopolymer. It can be noted in the CFM images that this webbing is the same color as the bottom (furthest from the viewer) yarn. This does not indicate that only the bottom yarn was mobilized; this is a result of the experimental setup, with the yellow-green colored yarn being placed on the bottom and in contact with the plate below it. In the parallel yarn images shown in Appendix Figure A-12, both yarns appear to be equally mobilized. These characteristics were useful in understanding the appearance of welded materials, enabling our analysis of the welding abilities of five other, novel ILs.

Figure 12 shows a selection of the images that were collected from the yarns welded for 60 min with five of the six synthesized ILs used in NFW experiments (EMIAc, EMPyrAc, AMIAc, AMPyrAc, MVIAc).

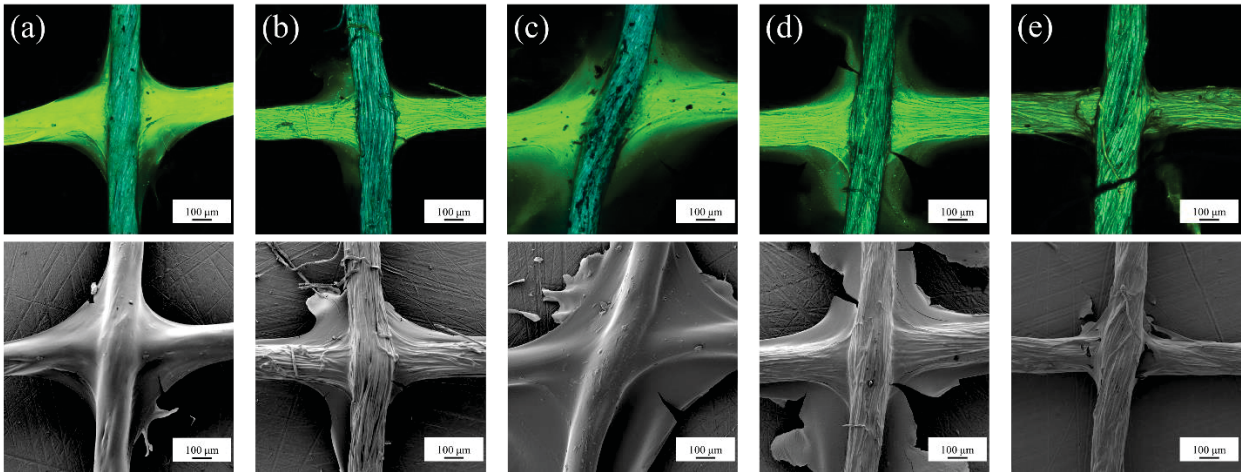

Figure 12. Confocal Microscopy (CFM) (top, colored) and Scanning Electron Microscopy (SEM) (bottom, grayscale) of cotton yarns treated for 60 min at 60 °C with (a) EMIAc, (b) EMPyrAc, (c) AMIAc, (d) AMPyrAc, and (e) MVIAc. Samples were gold-sputtered prior to imaging in the SEM (10 kV).

This work shows a new class of ILs containing the non-aromatic pyrrolidinium cation (EMPyrAc and AMPyrAc) are capable NFW solvents, in spite of the fact that the pyrrolidinium cation is not capable of hydrogen bonding, and simulation studies have predicted that EMPyrAc cannot dissolve cellulose.[25] However, this work shows that EMPyrAc and AMPyrAc can be used to weld, albeit to a lesser degree than EMIAc (the number of discernible fibers is higher for EMPyrAc and AMPyrAc than for EMIAc as seen in the SEM images). The presence of the fluorescent 'webbing' provides a significant indication of the mobilization of biopolymer fibers, and confirms that fiber-welding did occur. Earlier NFW studies in our laboratory had been based on the assumption that only ILs with the ability to fully dissolve biopolymer materials could be used in NFW. These exciting new results represent an important and significant discovery in this field. Clearly, ILs do not have to be able to fully dissolve a biopolymer material in order to be a

capable NFW solvent. This result opens the door to a wide range of novel ILs that can be considered in the NFW process.

Chemically, AMIAc is much like EMIAc in that they both have an acetate anion and the cation has the imidazolium ring functional group. However, AMIAc has an allyl group that classifies it as a poly-IL. Despite the presence of this additional functional group, the AMIAc was still clearly able to fiber-weld the cotton yarn. After 60 min of treatment with AMIAc, the cotton appeared much like the cotton treated with EMIAc for the same amount of time (compare Figure 12a and Figure 12c). The lack of stray fibers, lack of discernible strands, and the 'webbing' were very similar to the characteristics of the EMIAc-welded material.

The AMPyrAc combined the two alterations to EMPyrAc and AMIAc that distinguished them from EMIAc. Because of the addition of the allyl group, this was also a novel poly-IL. The images shown in Figure 12d indicate the welding ability of this solvent was similar to the other pyrrolidinium IL tested (EMPyrAc, Figure 12b).

Allyl and vinyl groups are both effective polymerizable functional groups because the double bond they possess can undergo a polymerization reaction using a radical initiator. However, allyl functional groups have a lower reactivity than vinyl groups,[14] leading us to seek to evaluate whether ILs with the vinyl functional group could also be used in the NFW process, with the future goal of combining the welding and polymerization process. This drove the need to evaluate the MVIAc IL (Figure 12e). The CFM and SEM results from the EMIAc and AMIAc treated yarns seemed to indicate that imidazolium-based ILs had similar welding capabilities, but the MVIAc results indicated otherwise. The degree of welding did not progress as far with the MVIAc, with individual fibers still clearly discernible after 60 min of treatment. This result seems to be due to an ion mobility effect, as this IL was significantly more viscous than any of the allyl ILs, likely as a result of the small size of the methyl group, but also possibly due to IL purity. This viscosity effect seemed to be a significant factor in this IL's welding ability. Despite this result, we showed that this IL with a vinyl functional group is still capable of being used in the NFW process.

The final IL that we investigated for its welding ability was EVICl. This IL was chosen because it would remove some of the polymerization issues discussed in the next section, while also keeping an anion that has a demonstrable ability to manipulate biopolymer materials, the chloride anion.[12] Despite the previously demonstrated ability in solubilizing cellulose, EVICl did not demonstrate any significant amount of welding after 60 min, so the images obtained using the same procedure used for the other ILs were not noteworthy (CFM and SEM images are included in Figure A-17). However, after a significantly longer treatment time (11 h) and higher treatment temperature (100 °C) than the other ILs evaluated, EVICl did demonstrate an appreciable amount of welding (Figure 13).

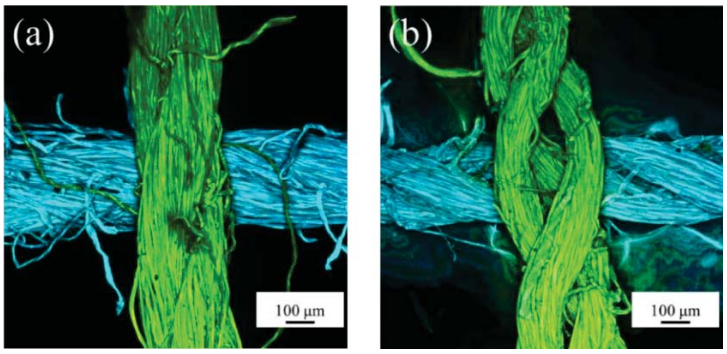

Figure 13. Confocal Microscopy (CFM) of cotton yarn junction (a) before treatment and (b) after treatment with EVICl at 100 °C for 11 h.

Figure 13 shows the same yarn junction of fluorescently labeled yarns before treatment with EVICl, and after 11 h of treatment in the welding process. This test demonstrated that the EVICl is able to mobilize biopolymer materials, given appropriate welding time. There is clear condensation of the yarn strands' diameters and mobilization of fluorescent biopolymer material can be seen in the background, both of which are indicative of biopolymer mobilization and welding.

One criterion used to evaluate the welding ability of each ILs in this study was changes in yarn diameter after welding. These changes were measured using the CFM software. Measurements were conducted at regions near the center of the welded yarns, providing a repeatable method to determine 'degree of welding'. This process was only used for the crossed yarn systems, and assumed that the yarns were perfectly cylindrical. Figure 14 shows an example of how these diameter measurements were made. Using this method, dimensions for the ILs evaluated were recorded and are included in Figure 15.

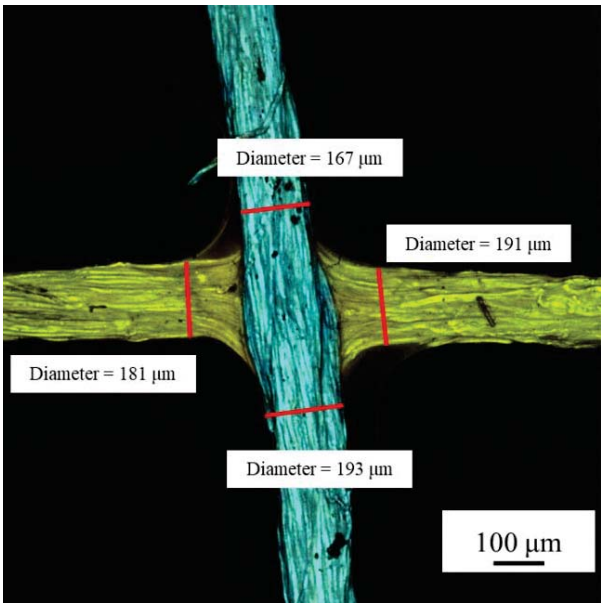

Figure 14. Confocal Microscopy (CFM) of cotton yarns fiber-welded with EMIAc for 5 min. Sample diameter measurements are superimposed in red.

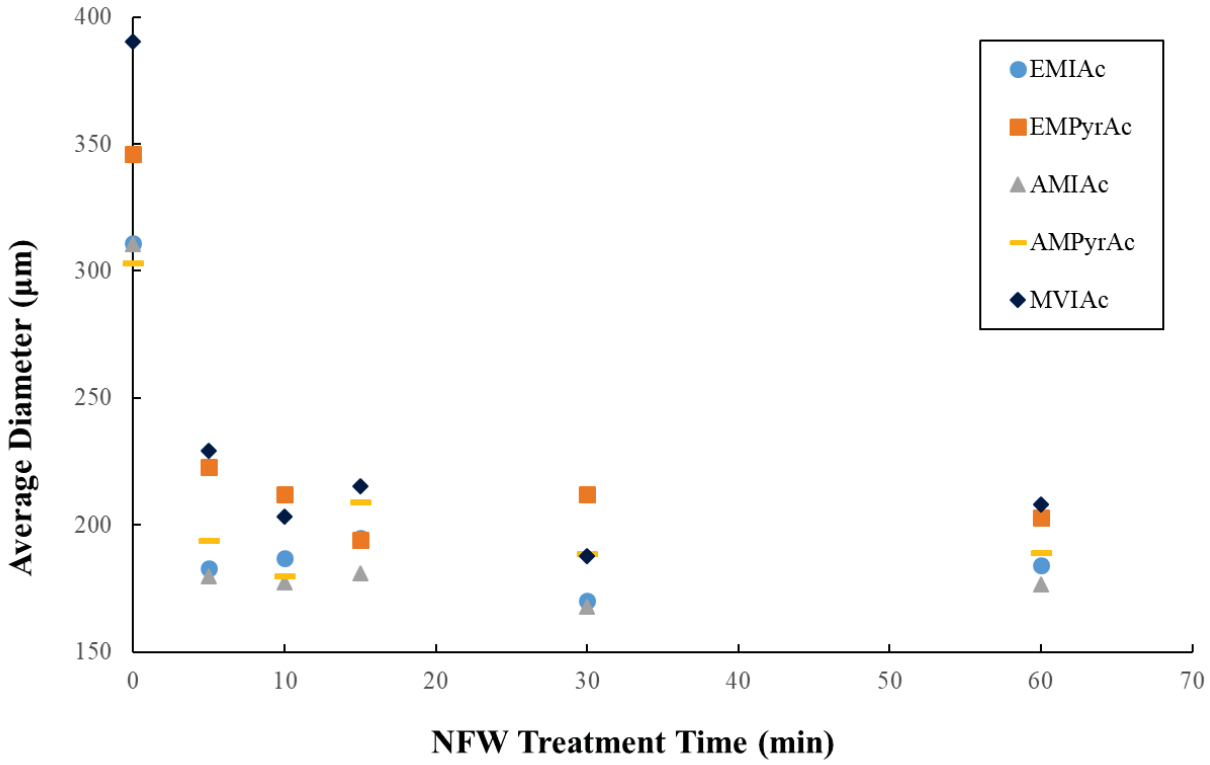

Figure 15. Plot of the cotton yarn diameter changes after fiber-welding with each of the five ILs evaluated in this study.

Our data show that the yarn diameter changes were consistent among the five ILs, as seen in the trends for the graph. Resources only allowed one set of data to be obtained for each IL system, limiting the statistical significance of this data. Considering this, it cannot be ignored that the average change in diameter at each treatment time was quite similar, and more surprisingly, did not change significantly for each of the five ILs evaluated. While this method to evaluate the degree of welding criteria is semi-quantitative at best, it does suggest that there is a limit to how much the NFW process will change the diameter of the cotton yarn. This observation may also be a result of the quenching process used to remove the IL from the cellulose matrix; the addition of IL in NFW mobilizes the external fibers of the cellulose yarn so that the yarn develops voids that the IL fills. Upon immediate removal of IL during the quenching process, the individual fibers of the yarn have less interactions to make with the surrounding environment, so the hydrogen bonds that held them to the IL become free to interact with each other and consolidate the structure. Because this quenching process was repeated among the various trials conducted, this may also explain the observations of similar diameter size. It would be useful to conduct more experiments that treat the junction with smaller time intervals to see how this parameter affects yarn diameter. Furthermore, in this experiment the quenching process removed the IL from the fiber immediately, so a future experiment could involve varying the removal process to determine whether this is a factor.

Although previous studies have indicated that EMPyrAc may not be able to solubilize cellulose,[25] our work has shown that this is not a requirement for it to be a good NFW solvent. This discovery made it more likely for us to believe that the poly-ILs, AMIAc and AMPyrAc,

could be effective in NFW. After synthesizing and welding with AMIAc and AMPyrAc, we discovered two more novel NFW solvents whose welding effectiveness were comparable to their non-polymerizable analogs. As shown in Figure 12 and Figure 15, the AMIAc and the EMIAc welded to similar degrees, with no significant differences between the number of distinguishable fibers and apparent smoothness of the welded material. Similar results were observed between the AMPyrAc and EMPyrAc-welded materials. The evaluation of MVIAc and EVICl shows that ILs with the vinyl functional group are still able to weld, but further work is needed to determine whether the vinyl group plays a specific role in hampering the welding ability or whether this phenomenon is a result of kinetics effects due to viscosity. Despite this, it is concluded that the addition of the polymerizable allylic and vinylic functional groups does not hinder the welding process in a significant way.

7.2 AFM of welded materials

While CFM and SEM provide useful information about the external features of the welded material, the AFM technique developed in this study has shown the potential for this method to further elucidate the effects of the welding process on the interior portions of the biomaterial. This process involves the potting and cross-sectioning of the material, which allows analysis of the nanomechanical properties of the welded yarn junctions. Figure 16 shows the modulus map for a sample of EMIAc-treated cotton yarns.

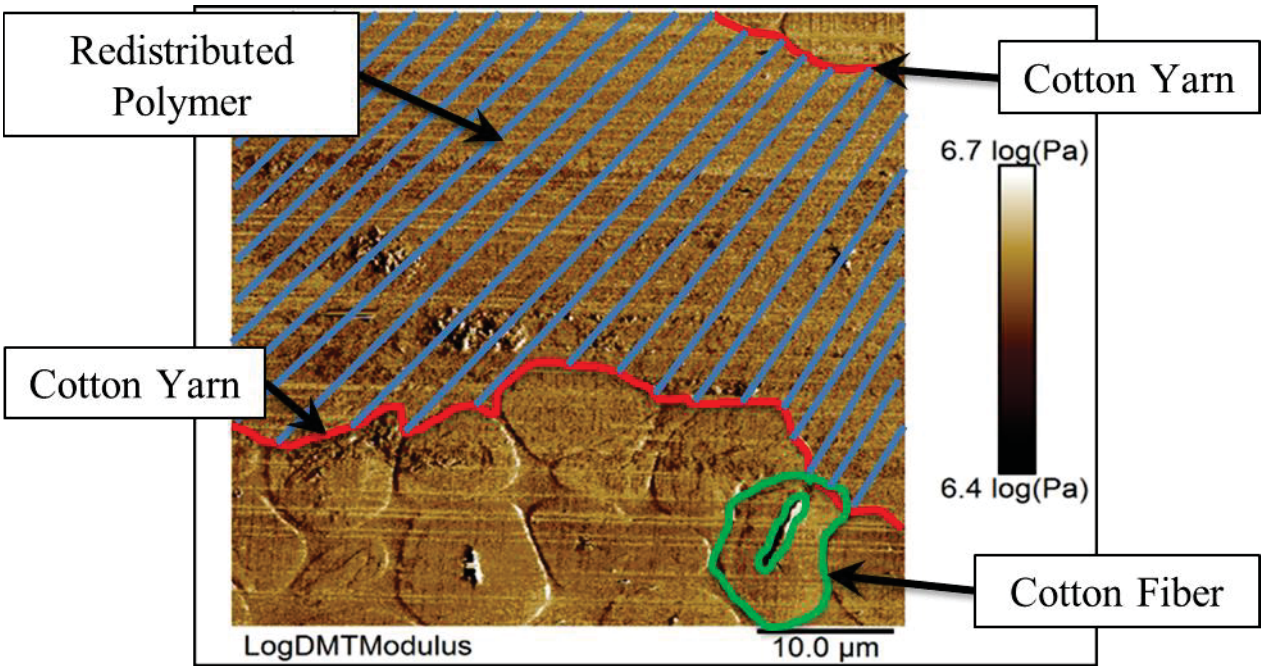

Figure 16. Atomic force microscopy (AFM) modulus mapping of the EMIAc-treated cotton yarn junction with key regions highlighted and labelled.

This image shows how the measured modulus changes across the cross-section of the welded material, with regions of lighter coloration representing stiffer regions in the yarn. In general, Figure 16 shows that the individual fibers within the yarns are still distinguishable from one another after the welding process. AFM allows evaluation of the mechanical properties of the interface between yarns, providing information about the mechanical properties of the mobilized

material as well as further confirming the welding process. This technique is a powerful tool to evaluate welded materials and is well suited to evaluate future welded biocomposites.

Additionally, AFM revealed new insight into the structure of the welded biopolymer materials. In particular, our data indicate the potting process did not cause epoxy to permeate through the welded material. From this, it was determined that in Figure 16, the region between the cotton yarns (outlined in red) was the redistributed biopolymer material (highlighted in blue). An example of a distinguishable fiber within the cotton yarn is highlighted in green for reference. The nanomechanical properties of this interface is of high interest because it is the junction where the native structure of the cotton yarn has been modified the most, and would have properties that differ significantly from the non-welded material. Obtaining more information about this region would provide a better understanding of the redistribution process inherent in NFW.

As seen in Figure 16, there was a significant amount of 'chatter' in the AFM analysis of the cross-sections, which manifested as the horizontal lines across the entire modulus map. This was a result of the process used to cross-section the potted yarns. Attempts to reduce this by switching from a glass knife, which may have had some imperfections in the blade, to a diamond knife have not removed this issue. Future work will consider altering the epoxy formulations as well as examining the effects of the microtoming technique used to adjust the angle of the blade, cutting speed, and formulations of the epoxy mixture.

7.3 Characterizing the polymerized IL

As shown in Table 3, several combinations of the polymerizable ILs, initiator molecules, solvent, and additional chemicals were evaluated for their ability to produce polymerized IL. The determination of whether polymerization occurred was made using several factors: physical changes in the IL, spectral analysis using ATR-FTIR, and spectral analysis using NMR.

In the process of forming a polymerized IL, the relatively small monomer molecules chemically bond to one another to form a polymer (Figure 4). Because these polymer molecules are much larger than the starting material, they are much less mobile and effectively form a rigid structure. The formation of a rigid and clear solid gave the most direct indication of polymerization. Beyond this physical property, the solid, polymerized ILs were able to absorb a significant amount of water, swelling to several times their original size. Without any crosslinking agents in these polymerized ILs, the network of polymerized product could easily incorporate water molecules that interact with the charges of the polymerized ILs. These observations provided a preliminary indication of whether polymerization had occurred. Subsequent analysis using ATR-FTIR and NMR spectroscopies provided more rigorous evidence of polymerization.

ATR-FTIR spectroscopy provides chemical information based on the energy of infrared radiation that the chemical absorbs. This is a result of various functional groups absorbing radiation at wavelengths specific to the molecule's chemical structure. ATR-FTIR provided a useful analysis of the polymerized ILs because it could identify the reduction of certain chemical groups found in the poly-ILs. The overlaid ATR-FTIR spectra in Figure 17 shows the reduction of peaks due to the loss of the vinyl group in the polymerization process of EVICl.

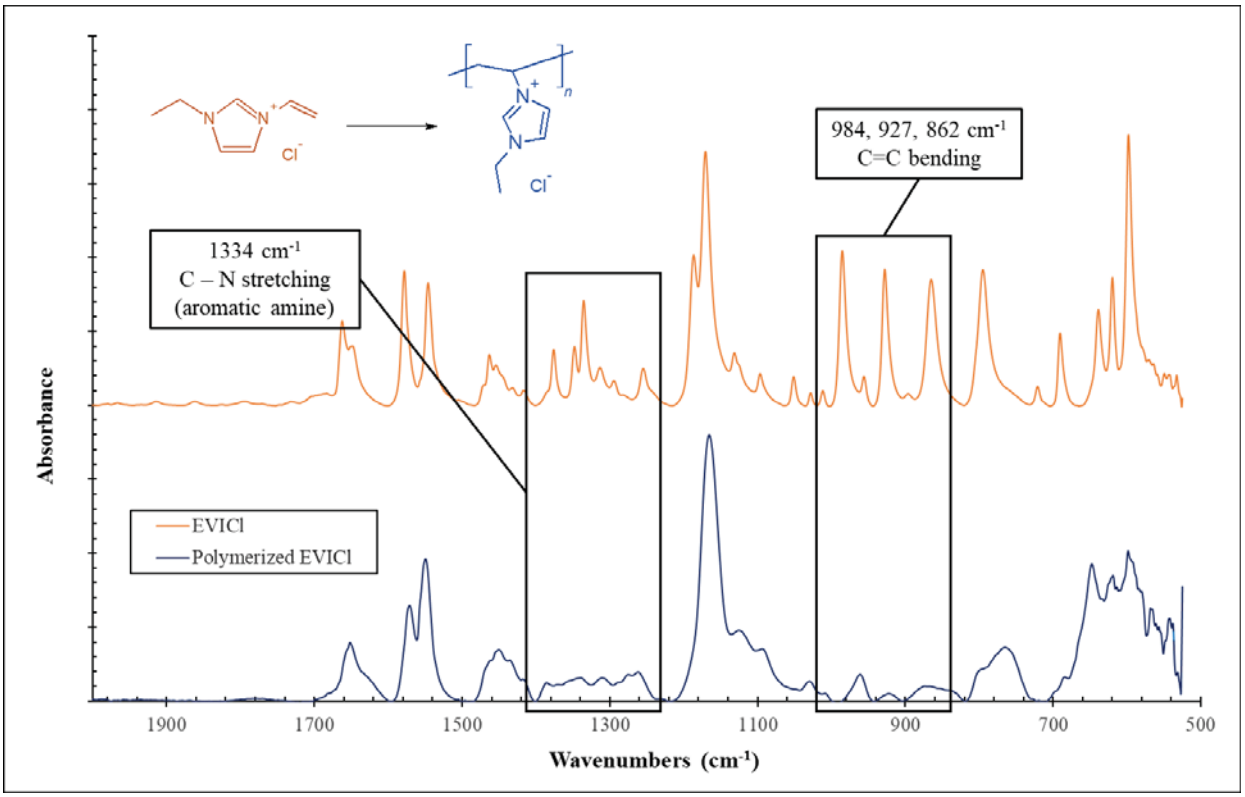

Figure 17. Normalized ATR-FTIR spectra of EVICl monomer (orange) and polymerized product (blue).

The ATR-FTIR spectra shown in Figure 17 were collected from both the non-polymerized EVICl monomer (orange) and the polymerized product (blue). These spectra were normalized for the alkyl C–H stretch at 2980 cm^{-1}. The peak assignments highlighted in the figure illustrate the expected reduction in absorption due to the loss of the vinyl group during the polymerization process. In summary, the absorption peaks associated with the C–N stretching mode that appeared at 1334 cm^{-1} as well as the C=C bending modes that appeared at 984 cm^{-1}, 927 cm^{-1}, and 862 cm^{-1} were reduced after the polymerization reaction, providing clear evidence that EVICl was polymerized successfully. These assignments were made according to standard IR spectroscopy absorptions.[26]

^{1}H-NMR spectroscopy provides similar chemical evidence for the results of polymerization. Figure 18 shows the NMR spectra of both the EVICl monomer (Figure 18a) and the polymerized product (Figure 18b). The peak assignments shown in Figure 18 follow those listed in the Appendix.

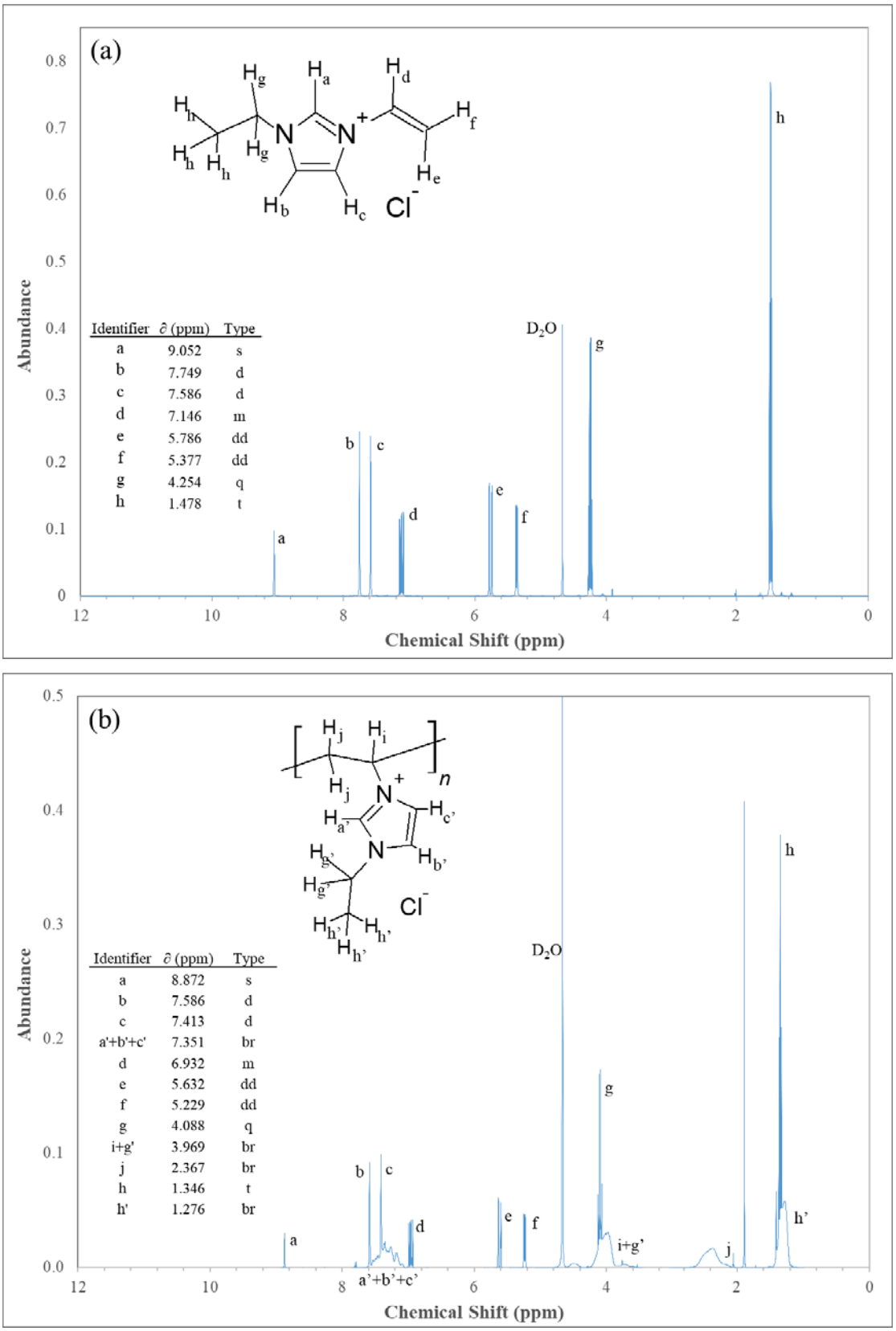

Figure 18. NMR spectra comparing the (a) EVICl monomer and (b) the polymerized product.

The peak assignments indicated in the figure show that the peaks for the monomer (Figure 18a) are still present in the polymerized product (Figure 18b), but they appear at a lower abundance than the solvent peak at 4.667 ppm in Figure 18a and 4.501 ppm in Figure 18b. Additionally, these were accompanied by broad peaks at 7.413 ppm, 3.969 ppm, 2.367 ppm, and 1.276 ppm, which are all indicative of polymerized product. These were associated with the polymerized product because (1) the polymerization process will inherently generate a wide range of polymer chain lengths with slightly different chemical shifts and (2) the polymerized product will exhibit hindered molecular tumbling as a more sterically constrained molecule. The hydrogens labeled 'i' and 'j' on the sp^3 hybridized carbons in Figure 18b provide a clear indication of polymerization because their ^{1}H-NMR chemical shifts are in the range of chemical shifts where they would be expected from the structure of the predicted product. These peak assignments are consistent with those made in 2008 by Zhao, *et al.*[15]

These ATR-FTIR and NMR data complemented the observations made on the polymerized EVICl, providing confirmation that this IL could be successfully polymerized as a neat IL/initiator mixture. Using a combination of these three techniques on the mixtures made according to Table 3, we were able to determine the polymerization ability of several of the generated poly-ILs in various polymerization mixture compositions. These results are summarized in the last column of Table 3.

Attempts to polymerize EVIAc (and MVIAc) in order to determine whether the preferred (acetate-based) welding solvents proved unsuccessful. To troubleshoot why these imidazolium-based acetate ILs could not polymerize, EVICl was polymerized in ACN, dimethyl sulfoxide, and water; none of these co-solvents inhibited IL polymerization. These results indicate that this inhibition is not likely due to a solvent effect. Dissolving MCC into EVICl did not prevent the IL monomer from polymerizing, and did not allow the EVIAc to polymerize when dissolved in that IL. This test was to simulate the conditions that would be found in polymerizing the poly-ILs within a biopolymer material after undergoing the mobilization step in the NFW process (Figure 3b). The hypothesis was that even though the EVIAc would not polymerize alone, it might be polymerized in a solution with biopolymer material. This was not the case. After eliminating these other potential influences, it was hypothesized and later confirmed that the acetate anion inhibits polymerization. This result was confirmed by attempting (and failing) to polymerize EVICl in a potassium acetate solution in water. While EVICl will readily polymerize in water without potassium acetate, adding the salt prevented the widespread polymerization seen for all other polymerizable mixtures.

7.4 Evaluating polymerized biocomposite

Although the acetate ILs were able to offer the most useful solvents for NFW, they hampered the polymerization process required to generate polyionic biocomposites. Despite this obstacle, EVICl has been demonstrated as a capable NFW solvent, so this was used to generate biocomposite materials (Figure 19 and 20).

One biocomposite was generated by dissolving MCC in an EVICl/ACN solution with HMPP. This was polymerized through exposure to UV light. As a control, the same EVICl/ACN solution with HMPP was polymerized without any MCC. After polymerization, these samples were carbon coated and analyzed using SEM (Figure 19).

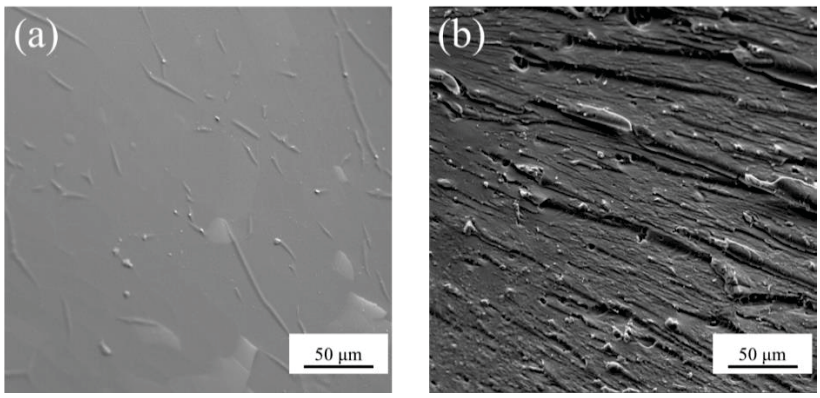

Figure 19. Scanning Electron Microscopy (SEM) of (a) polymerized EVICl/ACN solution and (b) polymerized EVICl/ACN solution containing 3 wt % MCC.

Figure 19a shows the polymerized EVICl surface is completely smooth. However, the surface morphology of the polymerized EVICl-MCC composite was much rougher (see Figure 19b), and showed that MCC and EVICl were both uniformly distributed throughout the polymer composite matrix. Energy dispersive X-ray spectroscopy (EDS) maps of the EVICl-MCC biocomposites (data not presented), showed chloride uniformly distributed across the surface and confirmed this conclusion. This observation may play a role in the analysis of the other generated composite materials.

Another biocomposite was generated using Aida Cloth treated with an EVICl/HMPP mixture applied at 100 °C for 1 h followed by polymerization. This biocomposite demonstrated that the polymerized IL can be robustly embedded within the cloth because after successive washing and drying, the gel of polymerized EVICl integrated within the cloth would stay embedded in biopolymer material. This observation directed continued work in this area, examining biocomposites generated from fluorescent yarns that can be monitored using CFM.

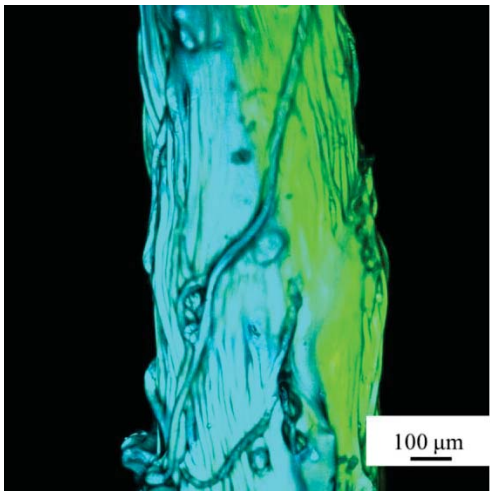

Figure 20. Confocal Microscopy (CFM) of twisted, fluorescently labelled yarns after welding at 100 °C for 3 h using EVICl that was subsequently polymerized in situ.

A biocomposite material was generated using the jig apparatus designed for polymerization. Figure 20 shows the CFM image of the biocomposite material generated after washing excess non-polymerized EVICl and short-chain polymerized product. This biocomposite material was prepared using two fluorescently dyed yarns, EVICl, and HMPP. After welding the twisted yarns for 3 h at 100 °C using a 1 mol% HMPP in EVICl solution, the polymerization of the IL was achieved via exposure to UV light. The biocomposite was wetted with 0.1 mL of water and dried to generate the product shown in Figure 20. CFM showed that the EVICl treatment and subsequent polymerization was able to mobilize the cotton fibers in the treated yarns and form an integrated polymerized IL/cotton network. This network formation is illustrated in Figure 21, which shows a collection of images of the biocomposite material swelling after exposure to water and the subsequent shrinking as the water dried.

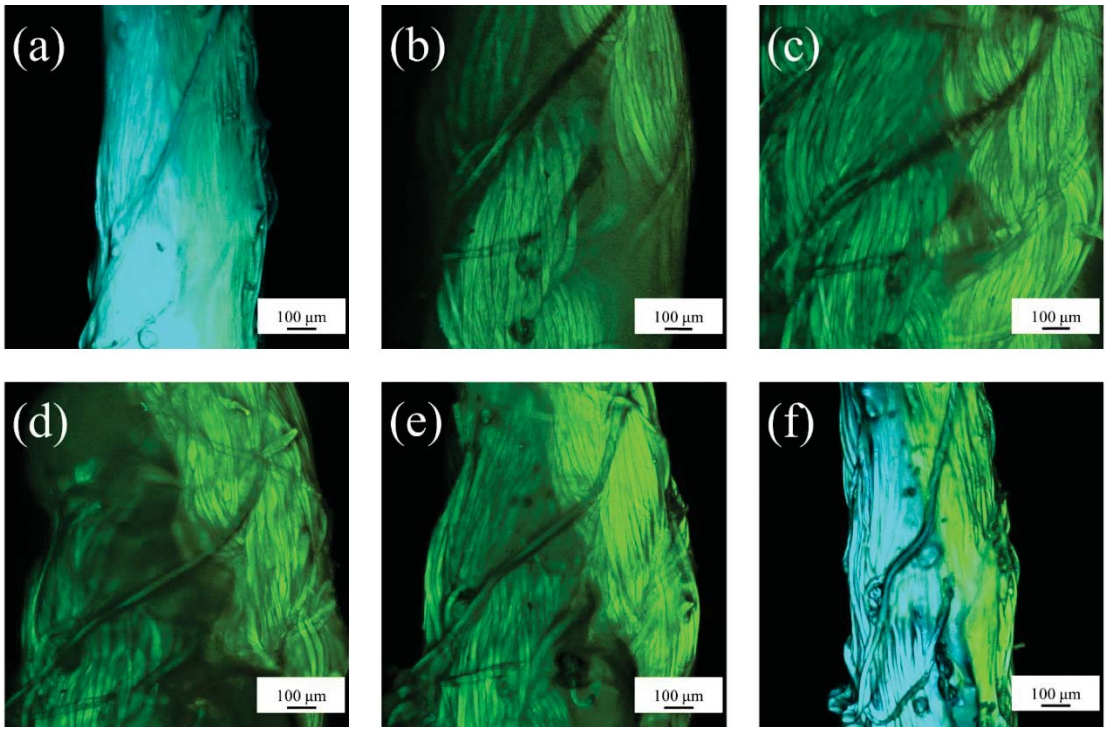

Figure 21. Confocal Microscopy (CFM) of polymerized EVICl-cotton biocomposite (a) before wetting and after (b) 4 min, (c) 9 min, (d) 26 min, (e) 36 min, and (f) 60 min of drying.

Figure 21 shows a series of images collected using CFM stationed on a single region of the polymerized IL within the cotton matrix over a period of 60 min. This shows the effect of adding ~0.1 mL of water to the biocomposite shortly after the image taken of the non-wetted biocomposite (Figure 21a). These images show that the biocomposite quickly swelled to more than twice its original diameter before slowly shrinking as it dried. The cross-sections of the yarns were measured and their diameters are plotted in Figure 22.

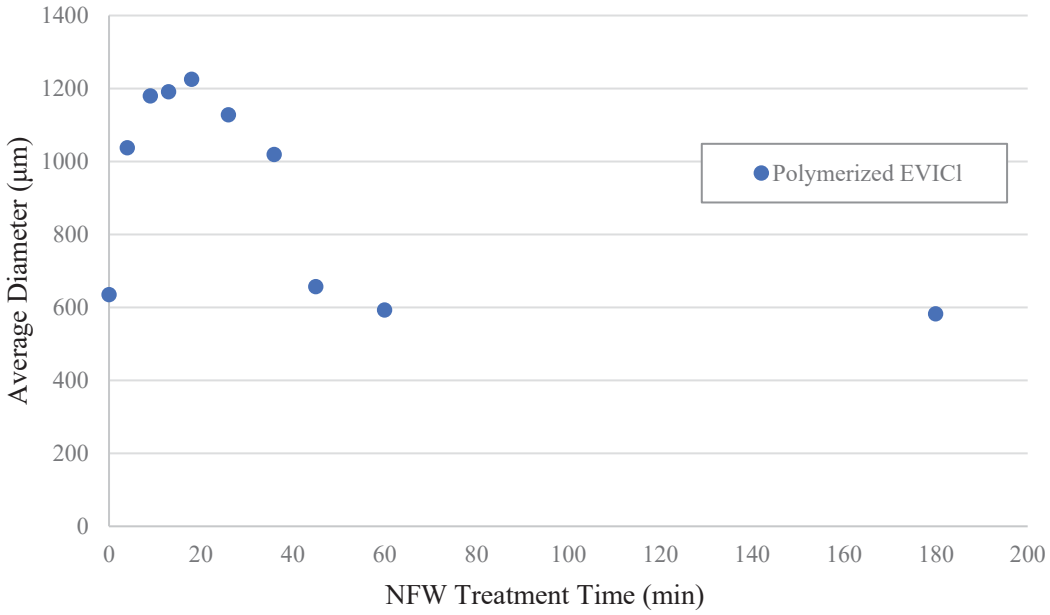

Figure 22. Measured diameters of the EVICl-cotton biocomposite during the water swelling process and subsequent drying at room temperature.

Figure 22 shows the change in diameter of the biocomposite after swelling with water. This swelling effect was not observed in untreated, fluorescently labeled yarns (not shown). These data provide convincing evidence that this polymerization process is effective at producing the polymerized product even between individual fibers. As the biocomposite swells, not only does the external layer of polymerized product grow, but the fibers it encases grow as well. This observation would only be seen if the polymerized product was integrated within the cotton backbone. Measurements of the biocomposite diameter taken show that the diameter nearly doubles after 18 min of soaking in water. The general shape of the curve in Figure 22 is a result of the biocomposite absorbing water until the 18 min mark after initial treatment with water. After this point, the diameter decreases as the water entrapped in the biocomposite evaporates, leaving behind the dried biocomposite shown in Figure 20.

Characterization of the polymerized biocomposite proved difficult because of the complicated nature of the material. As a combination of both a complex biopolymer and a polymerized IL with a broad distribution of molecular weights, ATR-FTIR analysis of the biocomposite did not result in any significant information. ATR-FTIR analysis of the material varied significantly with the region of the biocomposite being examined because the process used to generate the material could not provide a uniform coating. This difficulty was exacerbated by the high MP of the EVICl used to generate the composite, which required the welding portion of the biocomposite synthesis process to be conducted at a relatively high temperature (100 °C). In the future, this will be mitigated by synthesizing and using other ILs with non-acetate anions that will be useful in the welding process and can be manipulated at lower temperatures to facilitate a more controlled application.

7.5 Ionic conductivity of polymerized ILs

Using broadband dielectric spectroscopy, the ionic conductivity of the polymerized EVICl was measured in the conditions described in the procedure section. At room temperature, the ionic conductivity of the polymerized EVICl was measured to be 4×10^{-13} S/cm. This was about thirteen orders of magnitude lower than a comparable IL monomer. Figure 23 shows the variation of the ionic conductivity with respect to temperature.

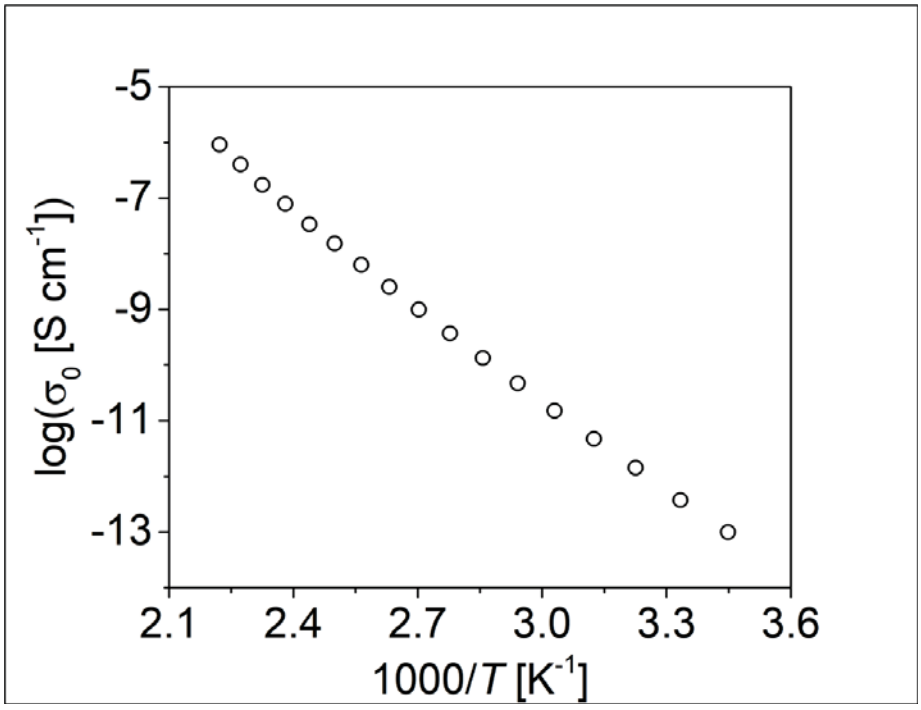

Figure 23. Temperature dependence of polymerized EVICl ionic conductivity.

This low ionic conductivity is likely a result of the polymerization process effectively locking the cation into a large, immobile chain, preventing this species from conducting charge as freely as an IL monomer. This ionic conductivity was also five orders of magnitude lower than other polymerized ILs reported in the literature,[27] but this follows from the general trends predicted for the glass transition temperate, T_g, described by Smith et al.[16] In summary, for a given polymerized cation, the T_g decreases with decreasing anion size. Because the single chloride ion of EVICl is one of the relatively small cations, the T_g of this polymerized IL is much higher than room temperature. The effect T_g has on ionic conductivity has to do with the kinetics involved; a polymer behaves more fluidly when its temperature is raised above its T_g. When it is more fluid, the ions within the polymerized IL can move more freely and conduct charge more effectively, raising its ionic conductivity. This information is being used to direct future work in synthesizing new poly-ILs for the NFW process.

8. Conclusion

Building on previous work, this project has demonstrated the viability of additional imidazolium and pyrrolidinium based ILs in the NFW process. These experiments have shown the possibilities of synthesizing EVICl, EVIBr, and MVII from the imidazole and halide precursors; and EMIAc, EMPyrAc, AMIAc, AMPyrAc, MVIAc, and EVIAc through a direct anion exchange process of their halide precursors. The synthesis of each of these ILs was confirmed using both NMR and ATR-FTIR spectroscopies. The dyeing process used to fluorescently label the cellulose yarns with FTSC and DCCH were able to consistently tag the yarns for visualization using CFM. These fluorescently-dyed yarns were used in an experimental setup created to systematically treat dyed yarns with the synthesized ILs. The resulting fiber-welded yarns were evaluated using CFM and their diameters were measured after varying IL treatment time and composition. To further characterize the welding process, a powerful, new method using AFM was developed to understand the mechanical properties at the welded yarn interface. CFM and SEM confirmed the welding abilities of all the ILs tested. This showed that the imidazolium-based ILs welded to similar degrees regardless of the presence of the allyl polymerizable functional group. This was also true for the pyrrolidinium-based ILs. The addition of the vinyl group also did not inhibit the ability to weld the biomaterials, but the viscosity of the IL seemed to play a role in its ability to mobilize biopolymers. It was found that the diameter of the welded yarns did not vary significantly between the different treatment times and the different ILs tested, suggesting that this may not be a particularly useful metric in determining degree of welding for comparing different NFW methods. However, a qualitative assessment can still be used to evaluate the degree of welding, based on insight of the mechanisms of this process developed in this project, and the AFM work shows great promise as a quantitative tool for evaluating NFW.

Polymerization experiments on five of the seven generated poly-ILs showed that the acetate anion, while useful in welding the biomaterials, inhibited the radical polymerization process. Despite this, the non-acetate ILs, namely EVIBr, EVICl, and MVII, were able to be polymerized ex-situ, and in solution, using either the AIBN thermal initiator or the HMPP photoinitiator. Of these three, EVICl was used in further evaluation and in developing the polyionic biocomposite. The polymerized EVICl was ionically conductive, but its conductivity value was low relative to other polymerized ILs in the literature.[17, 27] This material was examined using CFM, which showed that the polymerized product was robustly integrated within the biomaterial matrix.

Future work will improve the AFM analysis process, generate ILs with better handling characteristics, and develop poly-ILs with improved electrical properties. Preparing the samples for AFM identified the difficulties with obtaining a smooth cross-section of the welded material within the epoxy resin. Improving this technique will allow for more precise measurement of the mechanical properties of welded material and of the synthesized biocomposite. EVICl was difficult to work with because it needed to be kept at a relatively high temperature to weld the biopolymer material. Developing an IL that can both be polymerized and more easily used in the NFW process will be crucial to improving the properties of the synthesized product. This point is related to the issue of the poor ionic conductivity of the polymerized EVICl. Synthesizing an IL with a larger anion would also decrease the T_g of the polymerized product, leading to an improved ionic conductivity of the polymerized material.

9. Glossary

- **Alkenyl** – chemical group characterized by a double bond between two carbon atoms
- **Alkyl** – chemical group consisting of carbon and hydrogen atoms linked by only single bonds
- **Anion** – negatively charged ion species
- **Biocomposite** – composite material consisting in some part of a material generated from a living organism
- **Biopolymer** – polymer generated by a living organism
- **Biopolymer fiber** – individual strand composed of biopolymers held by intermolecular forces
- **Biopolymer material** – material generated by a living organism typically composed of biopolymer fibers (e.g. cotton, silk, chitin, wool) organized in an organism-specific structure
- **Bulk Modulus** – measure of a sample's volume response to pressure; a measure of elasticity
- **Cross-section** – image obtained by cutting a material, such as a yarn, perpendicular to its long axis
- **Dissolution** – process of dissolving a material in solution
- **Electrolyte** – material with ability to conduct electrical charge in the form of ions or electricity
- **Fluorescent** – property of a material to emit light in response to absorbing light
- **Fluorescently-label** – chemically bind a fluorescent molecule to a material
- **Halide** – negatively-charged ion from the 7th row of the periodic table (includes F^-, Br^-, Cl^-, I^-)
- **Ion** – charged chemical species (such as Na^+, K^+, Cl^-)
- **Ionic Compound** – general classification of a chemical consisting of ions
- **Imidazolium and Pyrrolidinium ILs** – general chemical class of ILs based on imidazole and pyrrolidine cation structure; used in previous SC495 work
- **In-situ Polymerization** – polymerization of PILs within a biopolymer material matrix
- **Morphology** – study of the form/structure of a material
- **NFW Solvent** – solvent capable of mobilizing biopolymers within a fiber
- **Polar** – possessing an electrical polarity (positive or negative charge)

- **Polyionic Biocomposite** – biocomposite material containing a number of charged chemical species bound in a polymer

- **Polymer** – chemical compound made of a long chain of monomer building blocks

- **Polymerizable** – property of a molecule to be able to be joined together and form a polymer

- **Quaternization Reaction** – chemical reaction that forms a chemical group with four electron groups

- **Radical Initiator** – a reactive molecule that can form a radical after being excited by light or thermal energy, used in this project to polymerize alkenyl groups

- **Reactant** – starting material for a chemical reaction

- **Substituent** – any one of a number of commonly-described chemical groups in a molecule

10. References

1. Hoff, G. P., Nylon as a textile fiber. *Ind. Eng. Chem.* **1940,** *32* (12), 1560-1564.
2. Byrom, D., *Biomaterials: Novel Materials from Biological Sources*. Stockton Press: New York, NY, 1991.
3. Swatloski, R. P.; Spear, S. K.; Holbrey, J. D.; Rogers, R. D., Dissolution of cellulose [correction of cellose] with ionic liquids. *JACS* **2002,** *124* (18), 4974-4975.
4. Haverhals, L. M.; Foley, M. P.; Brown, E. K.; Fox, D. M.; De Long, H. C.; Trulove, P. C., Natural fiber welding: ionic liquid facilitated biopolymer mobilization and reorganization. In *Ionic Liquids: Science and Applications*, American Chemical Society: 2012; Vol. 1117, pp 145-166.
5. Mahmood, H.; Moniruzzaman, M.; Yusup, S.; Welton, T., Ionic liquids assisted processing of renewable resources for the fabrication of biodegradable composite materials. *Green Chem.* **2017,** *19* (9), 2051-2075.
6. Haverhals, L. M.; Sulpizio, H. M.; Fayos, Z. A.; Trulove, M. A.; Reichert, W. M.; Foley, M. P.; De Long, H. C.; Trulove, P. C., Characterization of polymer movement in fiber welded cellulose composites. *Electrochem. Soc. Trans.* **2010,** *33* (7), 91-98.
7. Jost, K.; Durkin, D. P.; Haverhals, L. M.; Brown, E. K.; Langenstein, M.; De Long, H. C.; Trulove, P. C.; Gogotsi, Y.; Dion, G., Natural fiber welded electrode yarns for knittable textile supercapacitors. *Adv. Energy Mater.* **2015,** *5* (4), 1-8.
8. Durkin, D. P.; Ye, T.; Larson, E. G.; Haverhals, L. M.; Livi, K. J. T.; De Long, H. C.; Trulove, P. C.; Fairbrother, D. H.; Shuai, D., Lignocellulose fiber- and welded fiber- supports for palladium-based catalytic hydrogenation: a natural fiber welding application for water treatment. *ACS Sustain. Chem. Eng.* **2016,** *4* (10), 5511-5522.
9. Haverhals, L. M.; Sulpizio, H. M.;Fayos, Z. A.; Trulove, M. A.; Reichert, W. M.; Foley, M. P.; De Long, H. C.;Trulove, P. C., Process variables that control natural fiber welding: time, temperature, and amount of ionic liquid. *Cellulose* **2012,** *19* (1), 13-22.
10. Haverhals, L. M.; Reichert, W. M.; De Long, H. C.; Trulove, P. C., Natural fiber welding. *Macromol. Mater. Eng.* **2010,** *295* (5), 425-430.
11. Haverhals, L. M.; Sulpizio, H. M.; Fayos, Z. A.; Trulove, M. A.; Reichert, W. M.; Foley, M. P.; De Long, H. C.; Trulove, P. C., Process variables that control natural fiber welding. *Electrochem. Soc. Trans.* **2010,** *33* (7), 79-90.
12. Zhang, H.; Wu, J.; Zhang, J.; He, J., 1-allyl-3-methylimidazolium chloride room temperature ionic liquid: a new and powerful nonderivatizing solvent for cellulose. *Macromolecules* **2005,** *38* (20), 8272-8277.
13. Murakami, M.-a.; Kaneko, Y.; Kadokawa, J.-i., Preparation of cellulose-polymerized ionic liquid composite by in-situ polymerization of polymerizable ionic liquid in cellulose-dissolving solution. *Carbohydr. Polym.* **2007,** *69* (2), 378-381.
14. Brown, A. C. R.; James, D. G. L., A kinetic study of the metathetical and addition reactions characterisitic of allyl polymerization. *Can. J. Chem.* **1961,** *40*, 796-803.

15. Zhao, F.; Meng, Y.; Anderson, J. L., Polymeric ionic liquids as selective coatings for the extraction of esters using solid-phase microextraction. *J. Chromatogr. A* **2008,** *1208* (1-2), 1-9.

16. Smith, T. W.;Zhao, M.; Yang, F.; Smith, D.; Cebe, P., Imidazole polymers derived from ionic liquid 4-vinylimidazolium monomers: their synthesis and thermal and dielectric properties. *Macromolecules* **2013,** *46* (3), 1133-1143.

17. Lemus, J.; Eguizabal, A.; Pina, M., UV polymerization of room temperature ionic liquids for high temperature PEMs: Study of ionic moieties and crosslinking effects. *International Journal of Hydrogen Energy* **2015,** *40*, 5416-5424.

18. Ho, T. D.; Yu, H.; Cole, W. T. S.; Anderson, J. L., Ultraviolet photoinitiated on-fiber copolymerization of ionic liquid sorbent coatings for headspace and direct immersion solid-phase microextraction. *Anal. Chem.* **2012,** *84* (21), 9520-9528.

19. Thomson, C. I.; Lowe , R. M.; Ragauskas, A. J., Imaging cellulose fibre interfaces with fluorescence microscopy and resonance energy transfer. *Carbohydr. Polym.* **2007,** *69* (4), 799-804.

20. Alcade, E.; Dinares, I.; Ibanez, A.; Mesquida, N., A simple halide-to-anion exchange method for heteroaromatic salts and ionic liquids. *Molecules* **2012,** *17* (4), 4007-4027.

21. Fei, S.; Kuang, D.; Zhao, D.; Klein, C.; Ang, W.; S., Z.; Graltzel, M.; Dyson, P., A supercooled imidazolium iodide ionic liquid as a low-viscosity electrolyte for dye-sensitized solar cells. *Inorg. Chem. Commun.* **2006,** *45*, 10407-10409.

22. Maksym, P.; Tarnacka, M.; Dzienia, A.; Erfurt, K.; Chrobok, A.; Zieba, A.; Kaminski, K.; Paluch, M., Facile route to well-defined imidazolium-based poly(ionic liquid)s of enhanced conductivity via RAFT. *Polymer Chemistry* **2017,** (35).

23. Chung, R. T.; Park, S.; Yates, E. A.; Durkin, D. P.; De Long, H. C.; Trulove, P. C., Ionic liquid property effects on the natural fiber welding process. *Electrochem. Soc. Trans.* **2018,** *86* (14), 249-255.

24. Haverhals, L. M.; Nevin, L. M.; Foley, M. P.; Brown, E. K.; De Long, H. C.; Trulove, P. C., Fluorescence monitoring of ionic liquid-facilitated biopolymer mobilization and reorganization. *Chem. Commun.* **2012,** *48*, 6417-6419.

25. Li, Y.; Liu, X.; Zhang, Y.; Jiang, K.; Wang, J.; Zhang, S., Why only ionic liquids with unsaturated heterocyclic cations can dissolve cellulose: a simulation study. *ACS Sustain. Chem. Eng.* **2017,** *5* (4), 3417-3428.

26. Silverstein, R. M.; Bassler, G. C.; Terence, C. M., Infrared spectrometry. In *Spectrometric Identification of Organic Compounds*, 5th ed.; John Wiley & Sons: New York, 1991; pp 158-164.

27. Heres, M.; Cosby, T.; Mapesa, E. U.; Liu, H.; Berdzinski, S.; Strehmel, V.; Dadmun, M.; Paddison, S. J.; Sangoro, J., Ion transport in glassy polymerized ionic liquids: unraveling the impact of the molecular strucutre. *Macromolecules* **2019,** *52* (1), 88-95.

11. Appendix

11.1 ^{1}H-NMR spectra of IL monomers and polymers

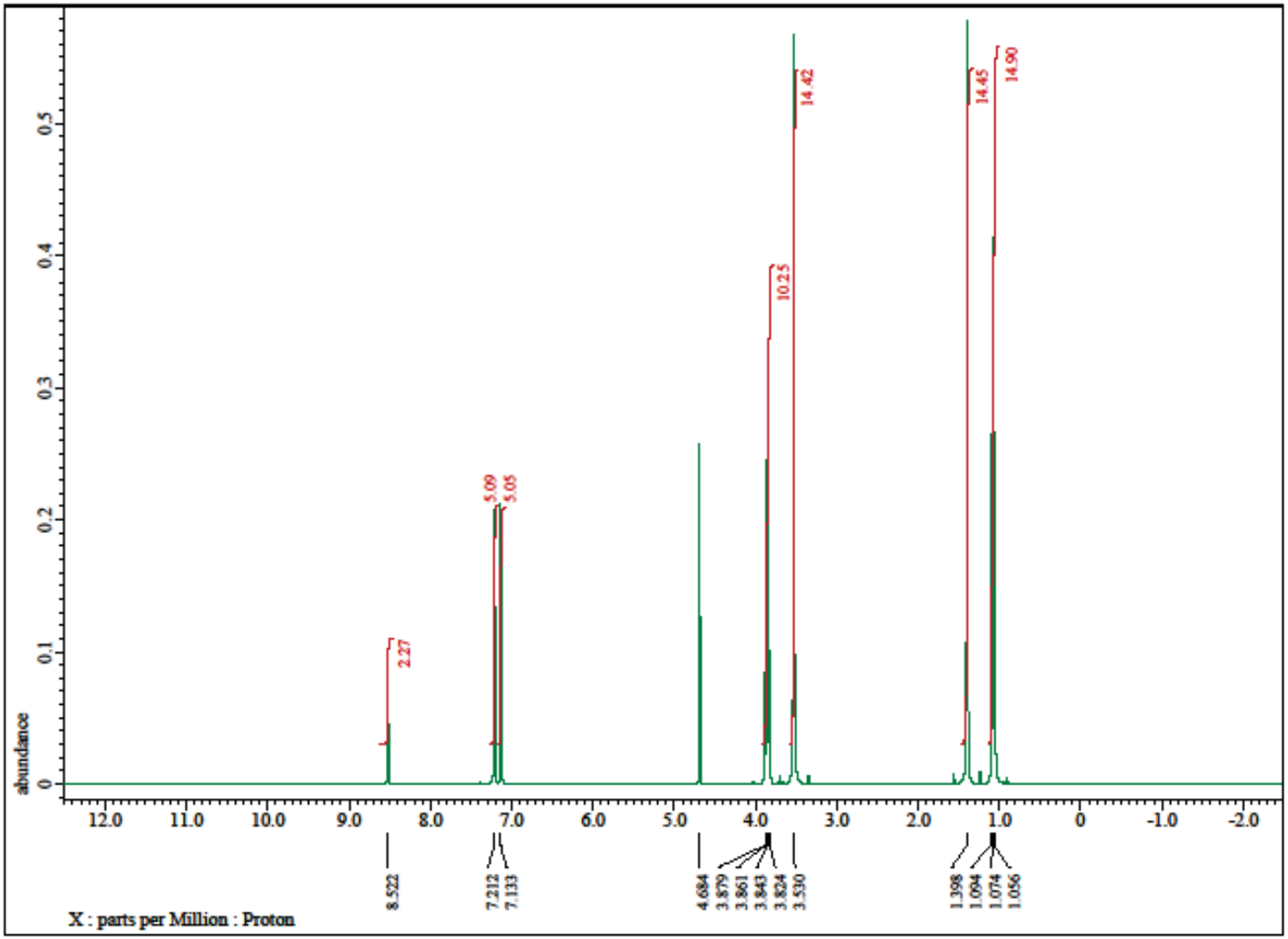

Figure A-1. ^{1}H-NMR of 1-ethyl-3-methylimidazolium acetate (400MHz, D_2O): 8.522 (1H, s, N^+–C**H**–N), 7.212 (1H, d, N^+–C**H**=CH), 7.133 (1H, d, CH=C**H**–N), 3.843 (2H, q, N^+–C**H$_2$**–CH_3), 3.530 (3H, s, C**H$_3$**–N), 1.398 (3H, s, C**H$_3$**–COO^-), 1.074 (3H, s, C**H$_3$**– CH_2).

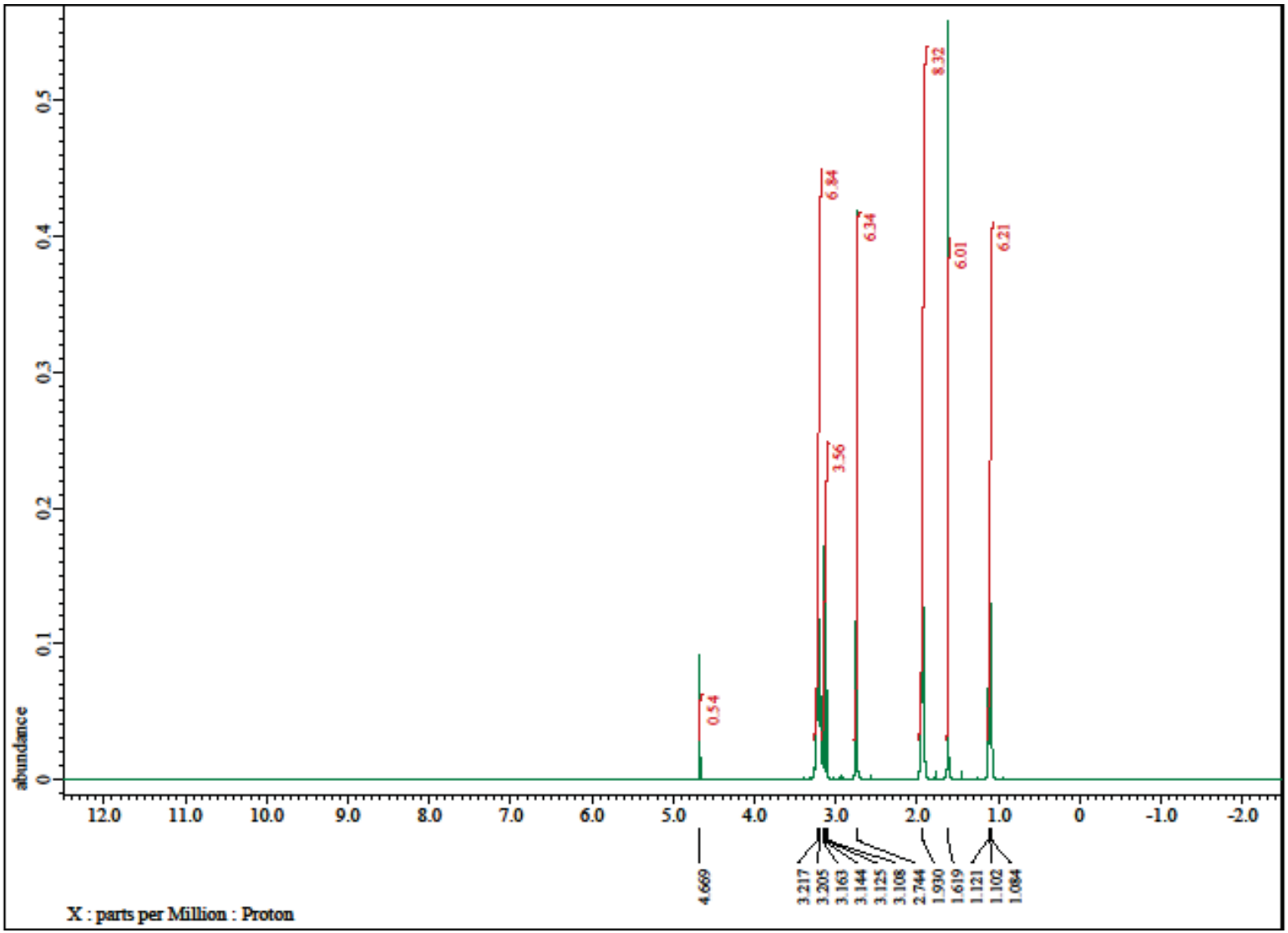

Figure A-2. ^{1}H-NMR of 1-ethyl-1-methylpyrrolidinium acetate (400MHz, D_2O): 3.217 (4H, m, N^+– C**H₂**–CH), 3.125 (2H, m, N^+–C**H₂**–CH_2), 2.744 (3H, s, C**H₃**–N^+), 1.930 (4H, br, CH_2–C**H₂**–C**H₂**–CH_2), 1.619 (3H, s, C**H₃**–COO^-), 1.102 (3H, tt, N^+– C**H₂**–CH_3).

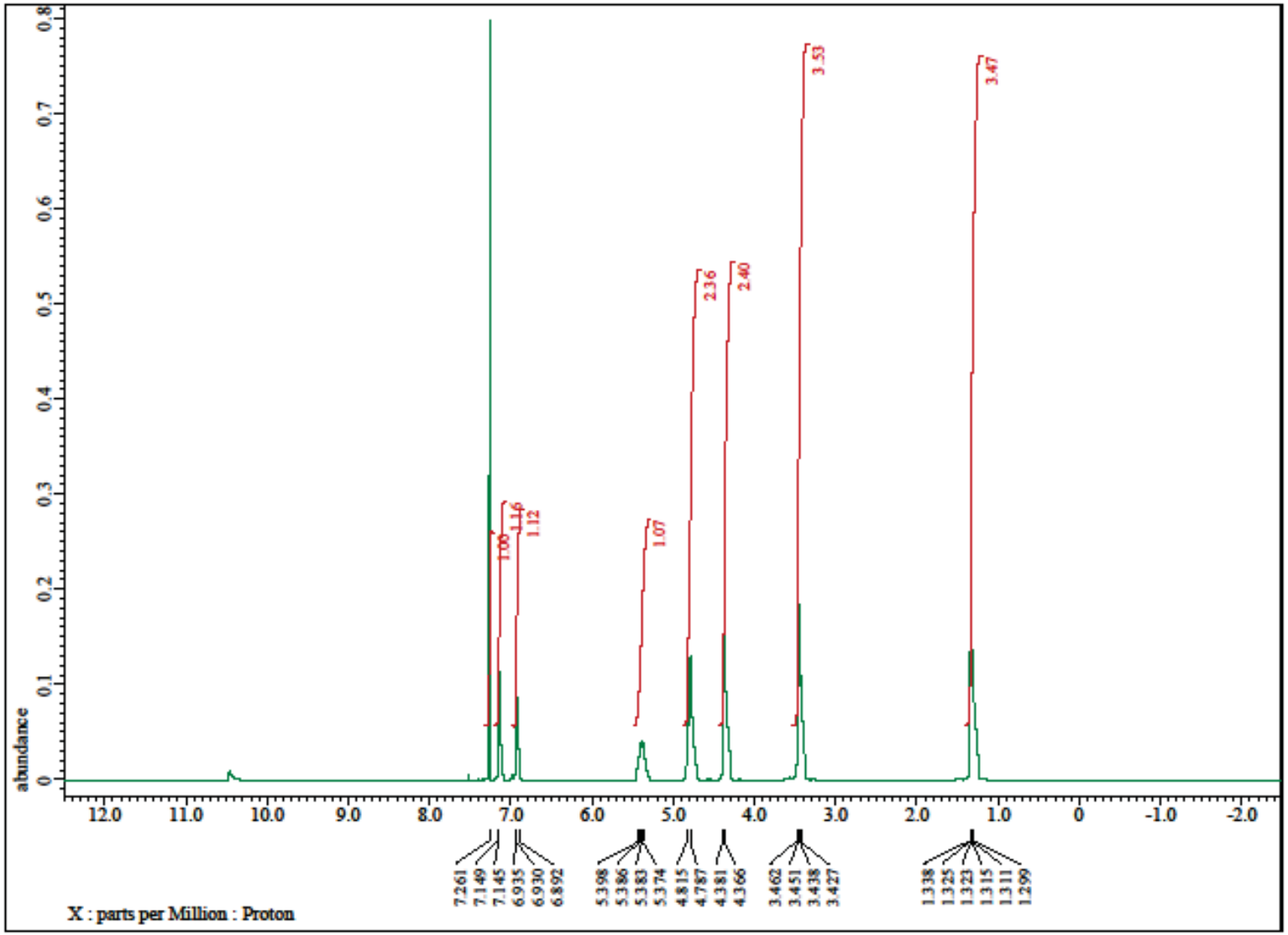

Figure A-3. ^{1}H-NMR of 1-allyl-3-methylimidazolium acetate (400MHz, $CDCl_3$): 10.461 (1H, s, N–C**H**–N), 7.147 (1H, d, N–C**H**=CH), 6.933 (1H, d, CH=C**H**–N), 5.385 (1H, m, CH_2–C**H**=CH_2), 4.787 (2H, d, C**H₂**=CH), 4.381 (2H, s, N–C**H₂**–CH), 3.462 (3H, s, C**H₃**–N), 1.338 (3H, s, C**H**-COO^-).

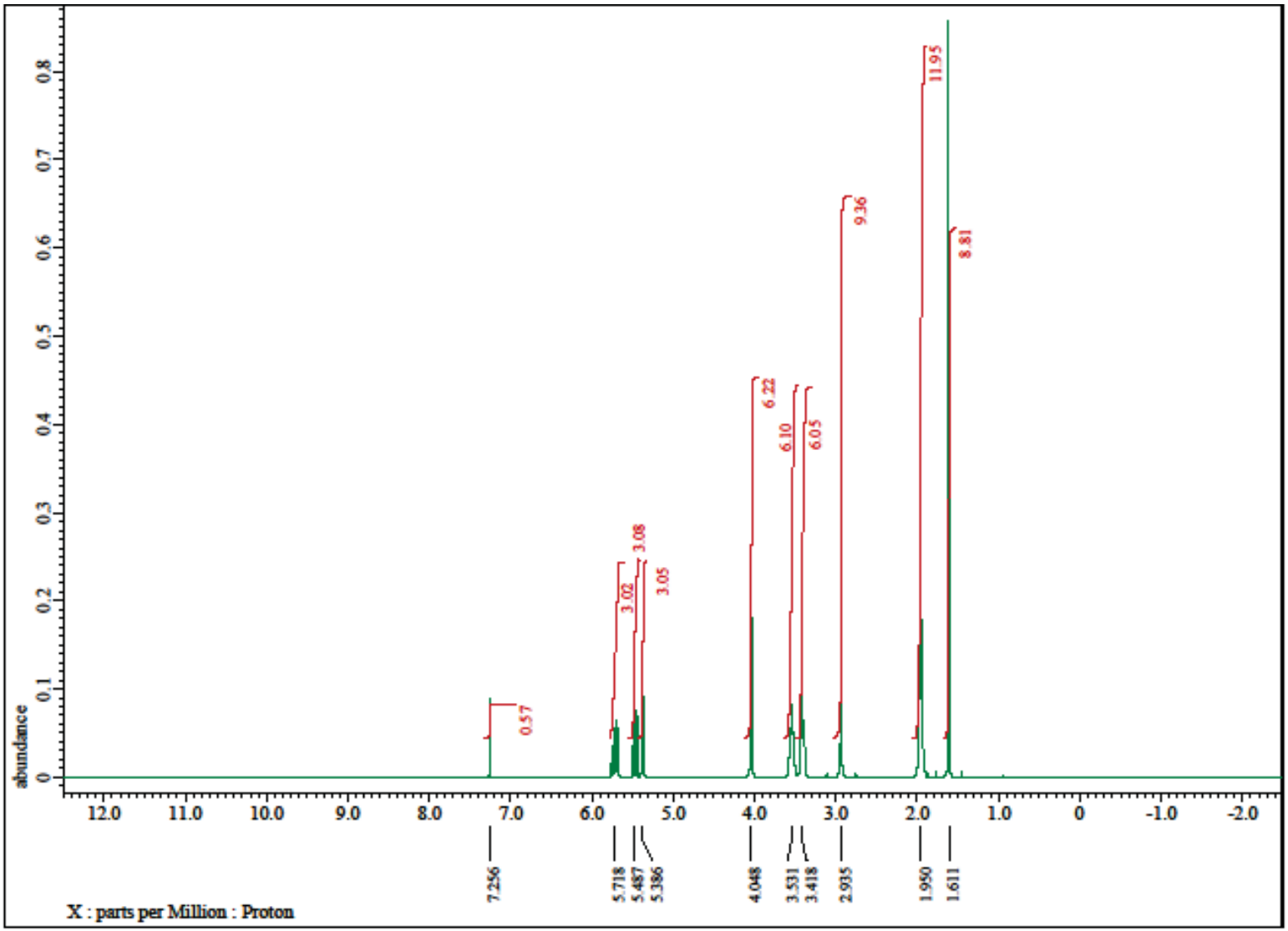

Figure A-4. ^{1}H-NMR of 1-allyl-1-methylpyrrolidinium acetate (400MHz, $CDCl_3$): 5.718 (1H, m, CH_2–C**H**=CH_2), 5.467 (1H, d, CH_2–CH=C**H**$_2$), 5.386 (1H, d, CH_2–CH=C**H**$_2$), 4.048 (2H, m, N^+–C**H**$_2$–CH), 3.531 (2H, m, N^+–C**H**$_2$–CH_2), 3.418 (2H, m, CH_2–C**H**$_2$–N^+), 2.935 (3H, s, C**H**$_3$–N^+), 1.950 (4H, br, CH_2–C**H**$_2$–C**H**$_2$–CH_2), 1.611 (3H, s, C**H**$_3$–COO^-).

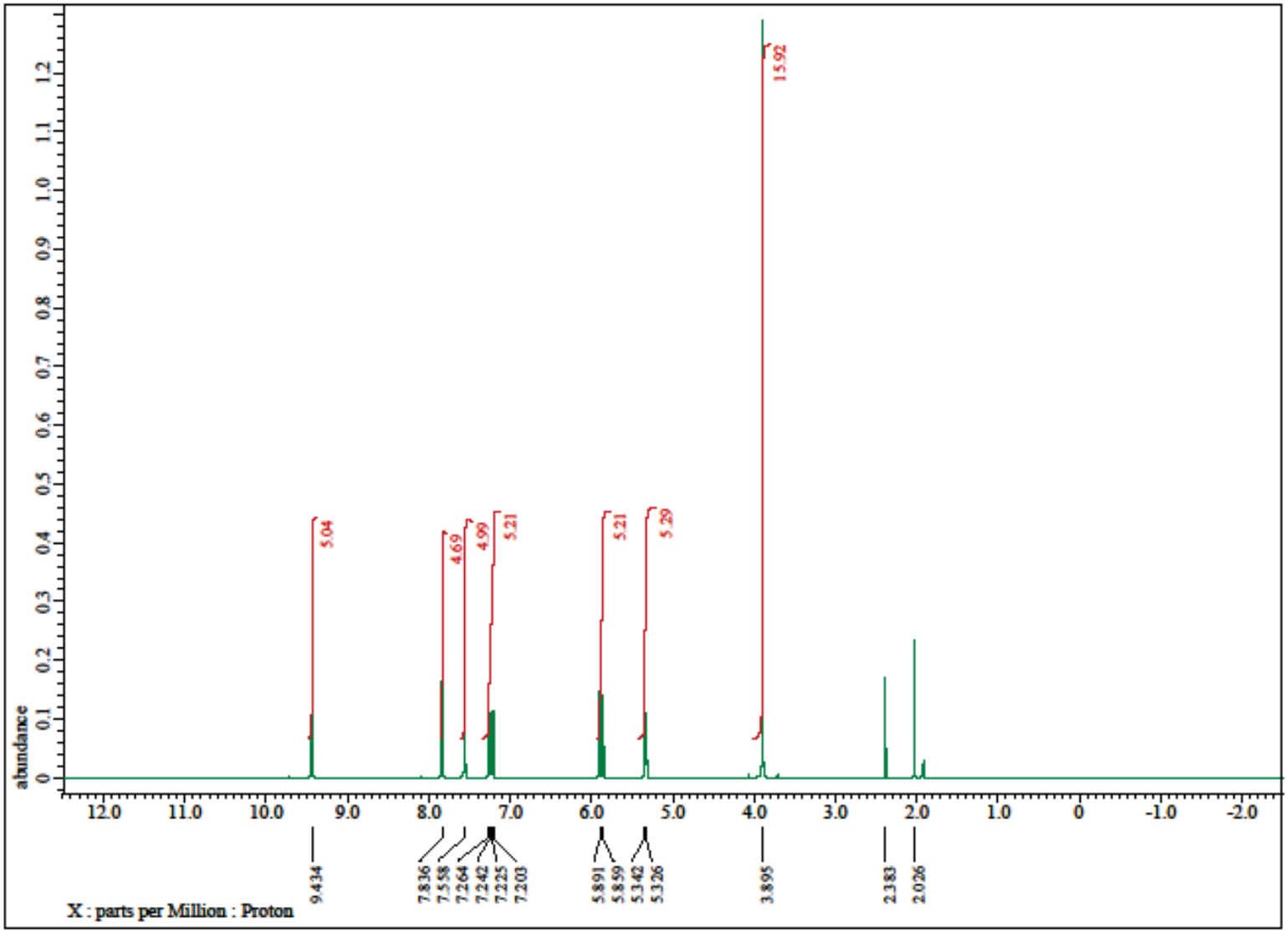

Figure A-5. ^{1}H-NMR of 1-methyl-3-vinylimidazolium iodide (400MHz, D_2O): 9.434 (1H, s, N^+=C**H**–N), 7.836 (1H, s, N^+–C**H**=CH), 7.558 (1H, s, CH=C**H**–N), 7.264 (1H, m, N–C**H**=CH_2), 5.891 (1H, d, CH=C$\mathbf{H}_2$), 5.342 (1H, d, CH=C$\mathbf{H}_2$), 3.895 (3H, s, N-C$\mathbf{H}_3$).

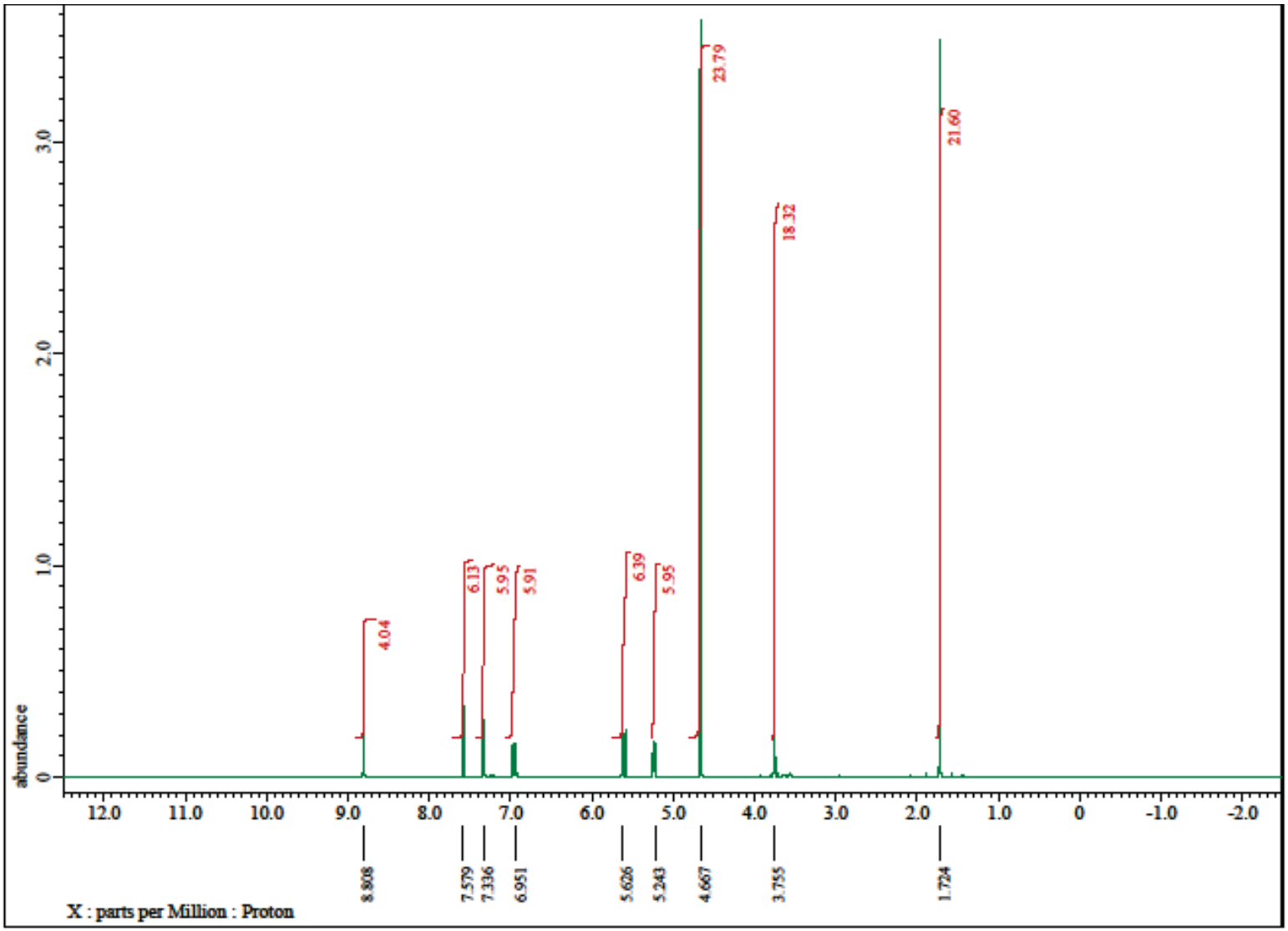

Figure A-6. ^{1}H-NMR of 1-methyl-3-vinylimidazolium acetate (400MHz, D_2O): 8.808 (1H, s, N^+=C**H**–N), 7.579 (1H, s, N^+–C**H**=CH), 7.336 (1H, s, CH=C**H**–N), 6.951 (1H, dd, N–C**H**=CH_2), 5.626 (1H, d, CH=C**H**$_2$), 5.243 (1H, d, CH=C**H**$_2$), 3.755 (3H, s, N-C**H**$_3$), 1.724 (3H, s, C**H**$_3$–COO^-).

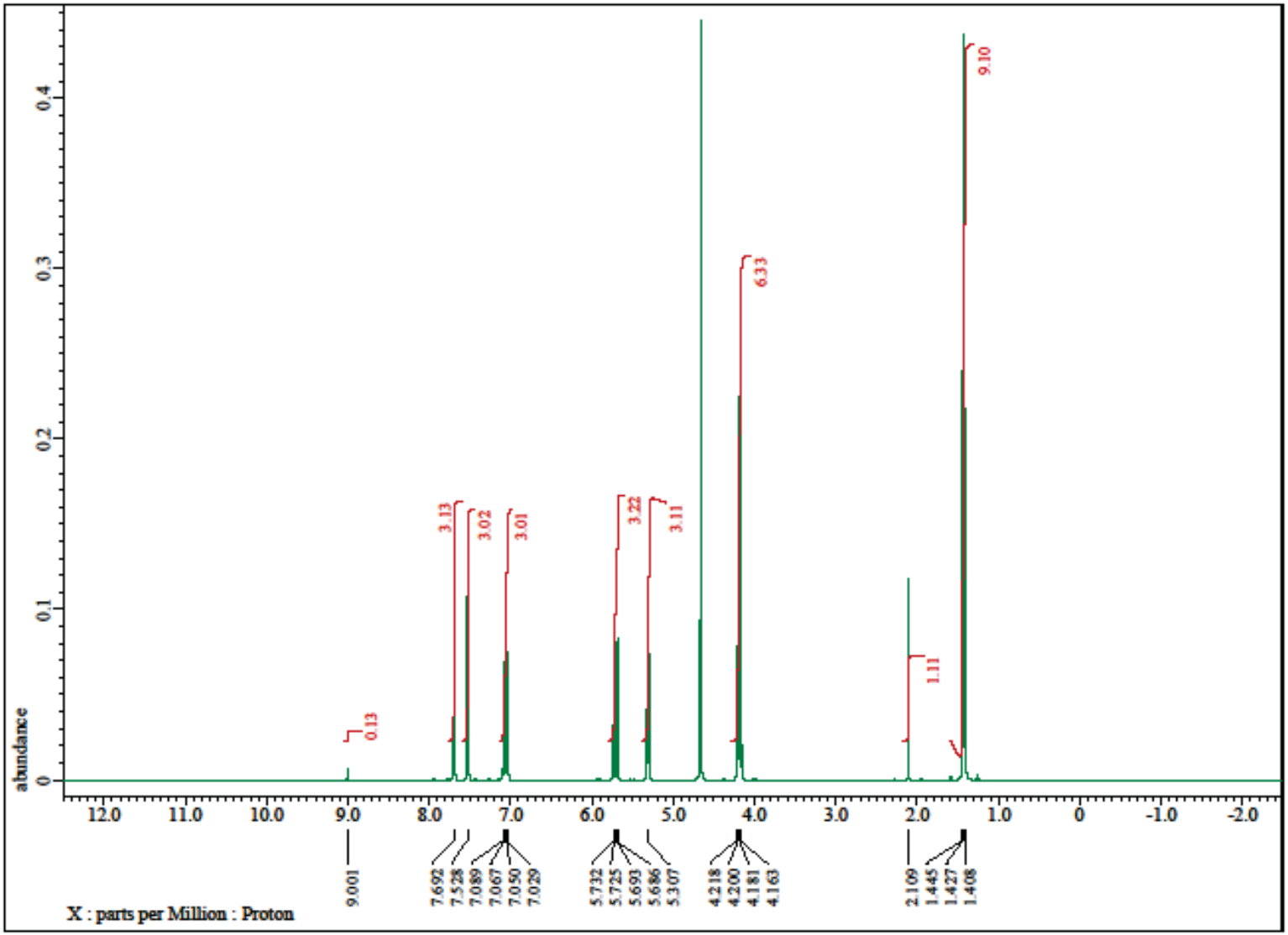

Figure A-7. ^{1}H-NMR of 1-ethyl-3-vinylimidazolium bromide (400MHz, D_2O): 9.001 (1H, s, N^+=C**H**–N), 7.692 (1H, d, N^+–C**H**=CH), 7.528 (1H, d, CH=C**H**–N), 7.059 (1H, m, N–C**H**=CH_2), 5.709 (1H, dd, CH=C**H**$_2$), 5.307 (1H, dd, CH=C**H**$_2$), 4.191 (2H , q, N–C**H**$_2$–CH_3), 1.427 (3H, t, CH_2–C**H**$_3$).

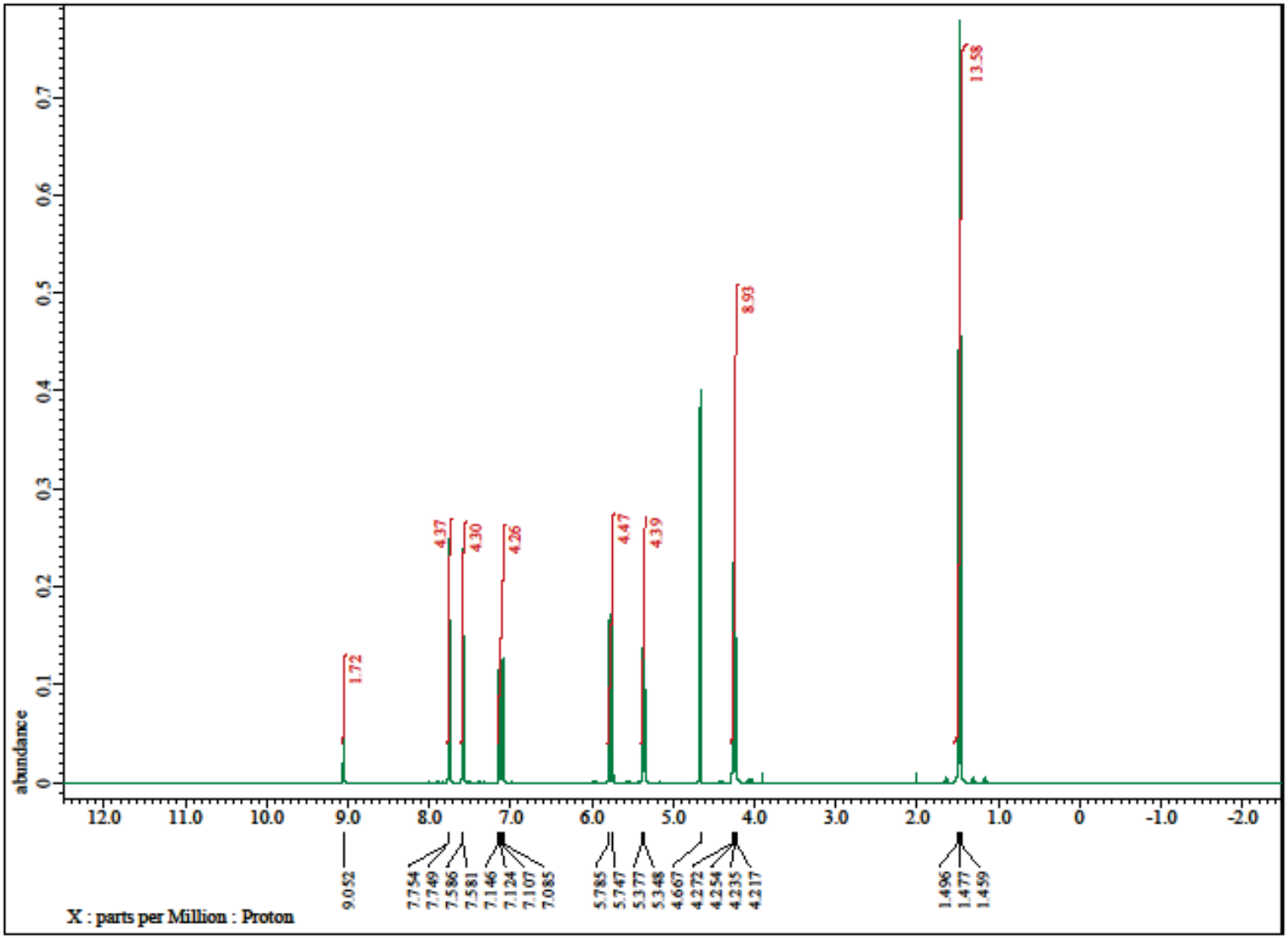

Figure A-8. ^{1}H-NMR of 1-ethyl-3-vinylimidazolium chloride (400MHz, D_2O): 9.052 (1H, s, N^+=C**H**–N), 7.752 (1H, d, N^+–C**H**=CH), 7.584 (1H, d, CH=C**H**–N), 7.116 (1H, m, N–C**H**=CH_2), 5.766 (1H, dd, CH=C**H**$_2$), 5.363 (1H, dd, CH=C**H**$_2$), 4.245 (2H , q, N–C**H**$_2$–CH_3), 1.477 (3H, t, CH_2–C**H**$_3$).

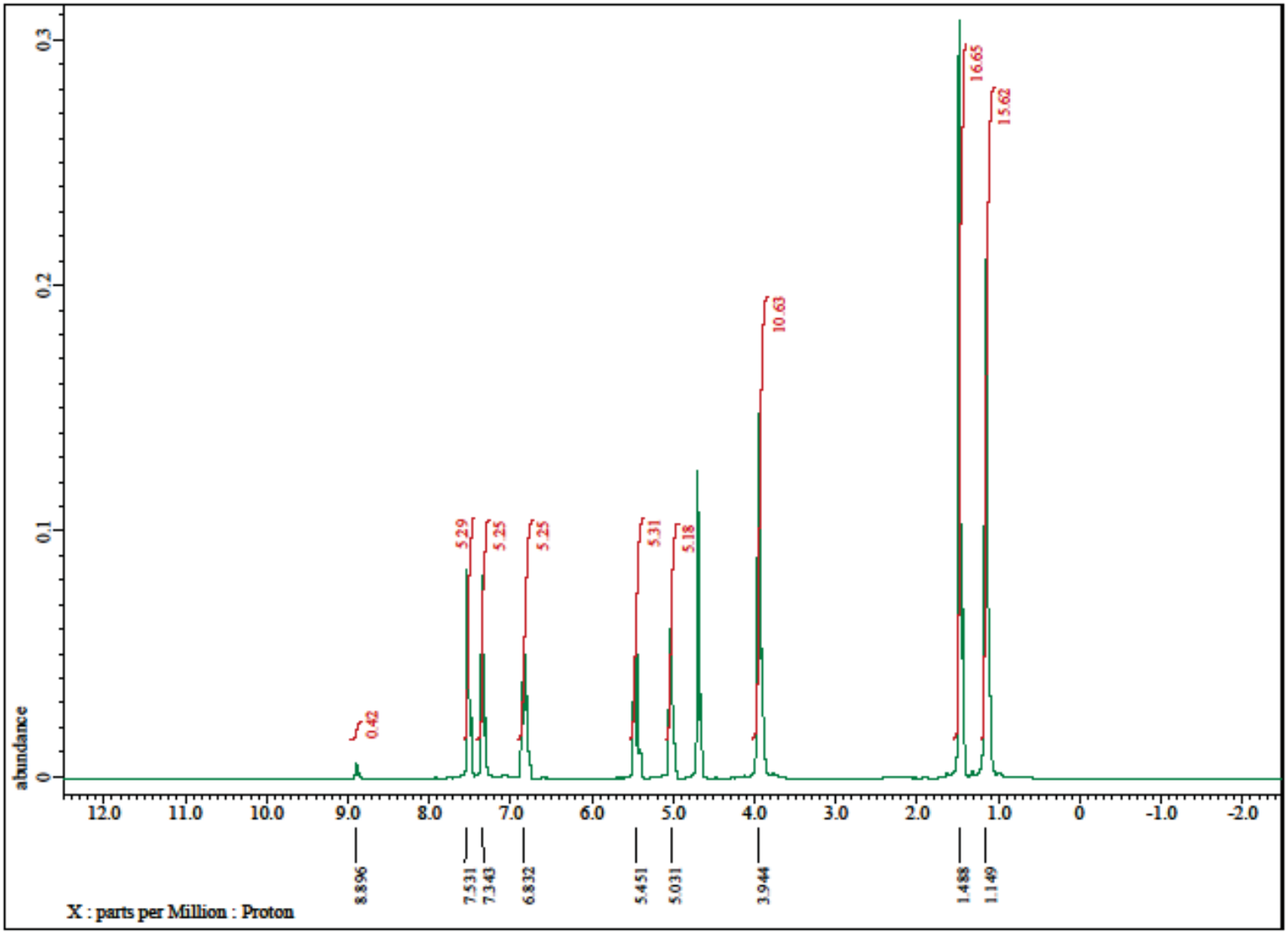

Figure A-9. ^{1}H-NMR of 1-ethyl-3-vinylimidazolium acetate, (400MHz, D_2O): 8.896 (1H, s, N^+=C**H**–N), 7.531 (1H, s, N^+–C**H**=CH), 7.343 (1H, s, CH=C**H**–N), 6.832 (1H, m, N–C**H**=CH_2), 5.451 (1H, d, CH=C$\mathbf{H}_2$), 5.031 (1H, d, CH=C$\mathbf{H}_2$), 3.944 (2H, m, N–C$\mathbf{H}_2$–CH_3), 1.488 (3H, m, CH_2–C$\mathbf{H}_3$), 1.149 (3H, s, C$\mathbf{H}_3$–COO^-).

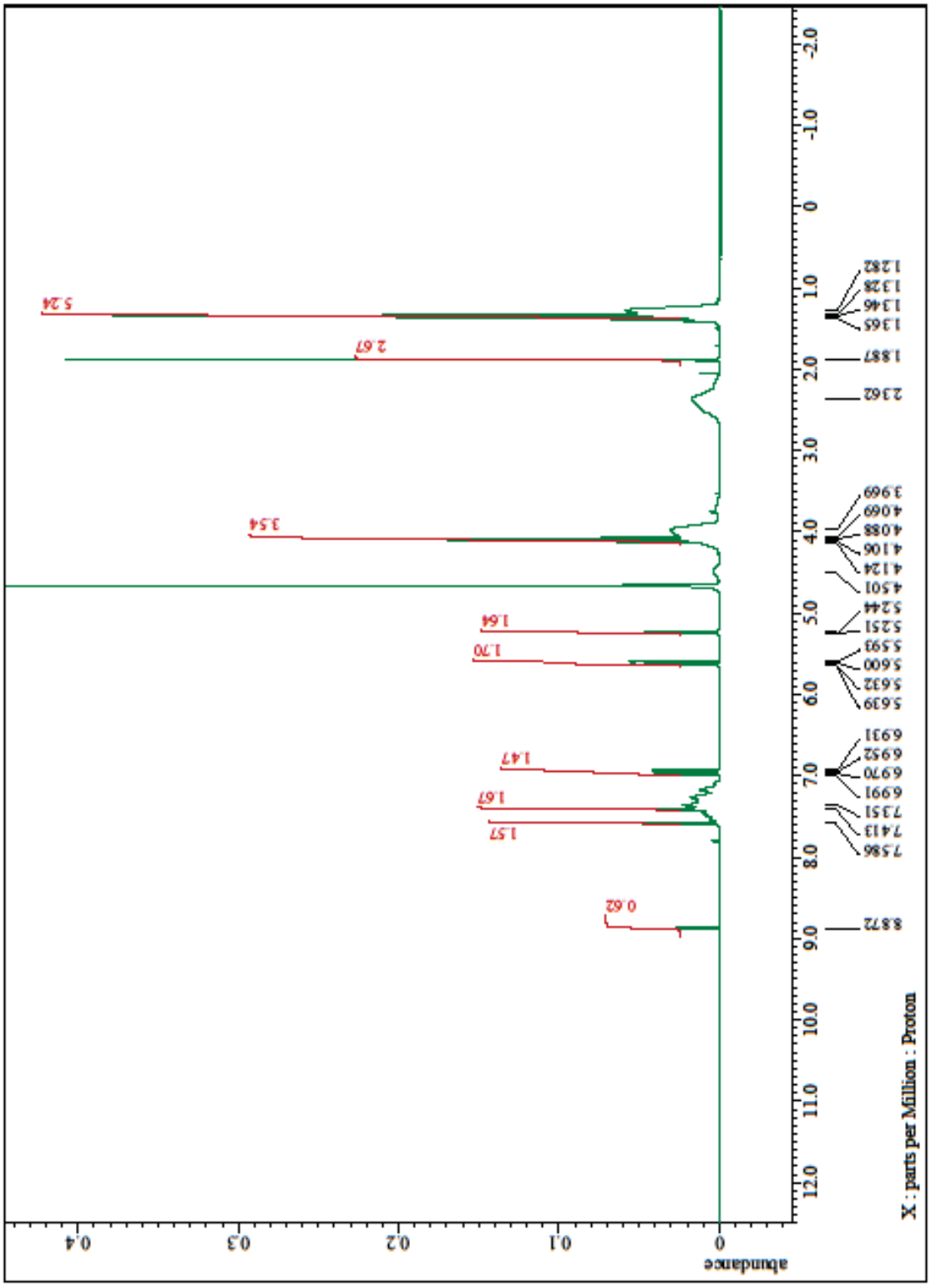

Figure A-10. ^{1}H-NMR of polymerized 1-ethyl-3-vinylimidazolium chloride (400MHz, D_2O).

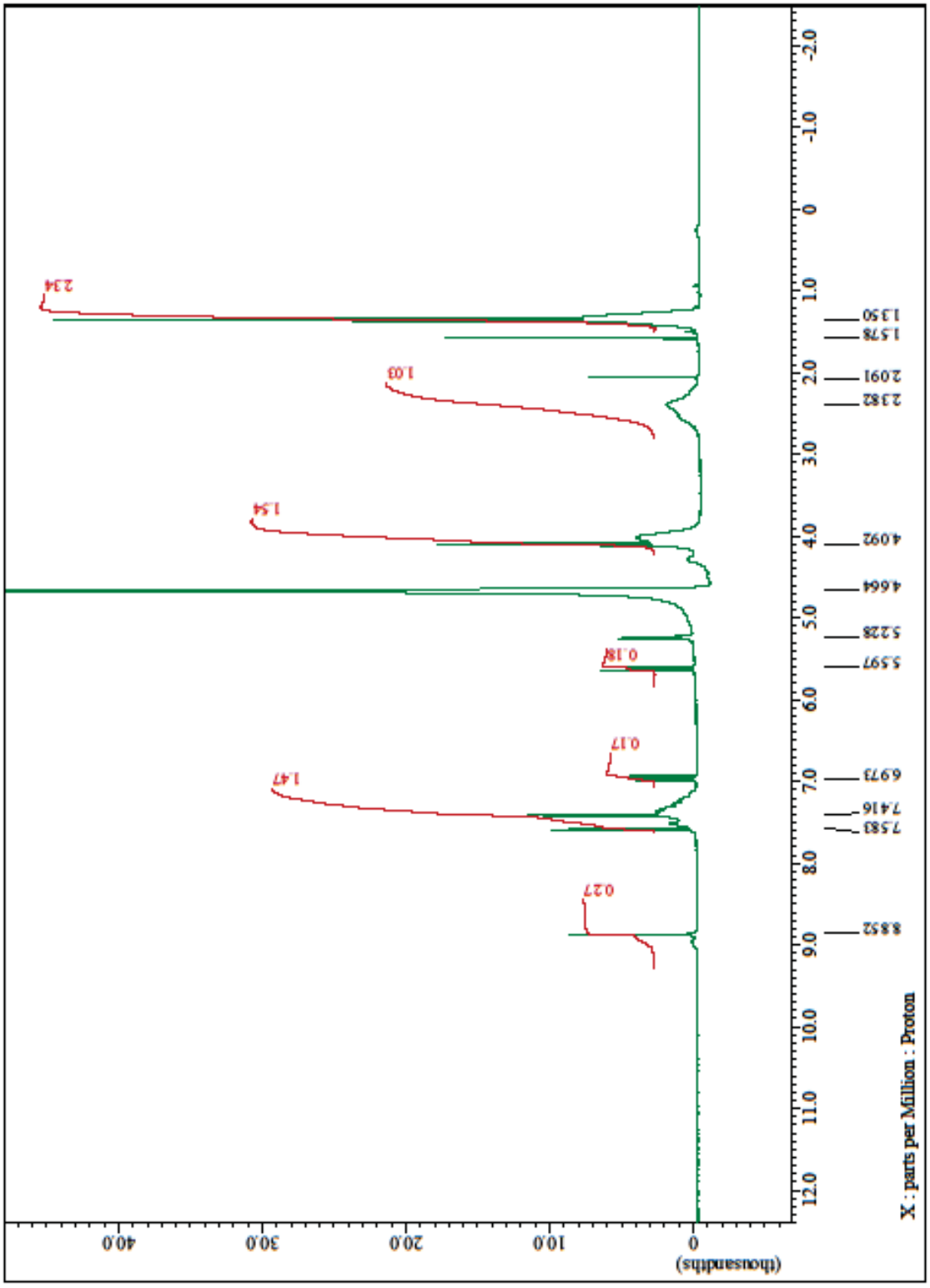

Figure A-11. ^{1}H-NMR of polymerized 1-ethyl-3-vinylimidazolium bromide (400MHz, D_2O).

11.2 Confocal fluorescence and scanning electron microscopy of welded yarns

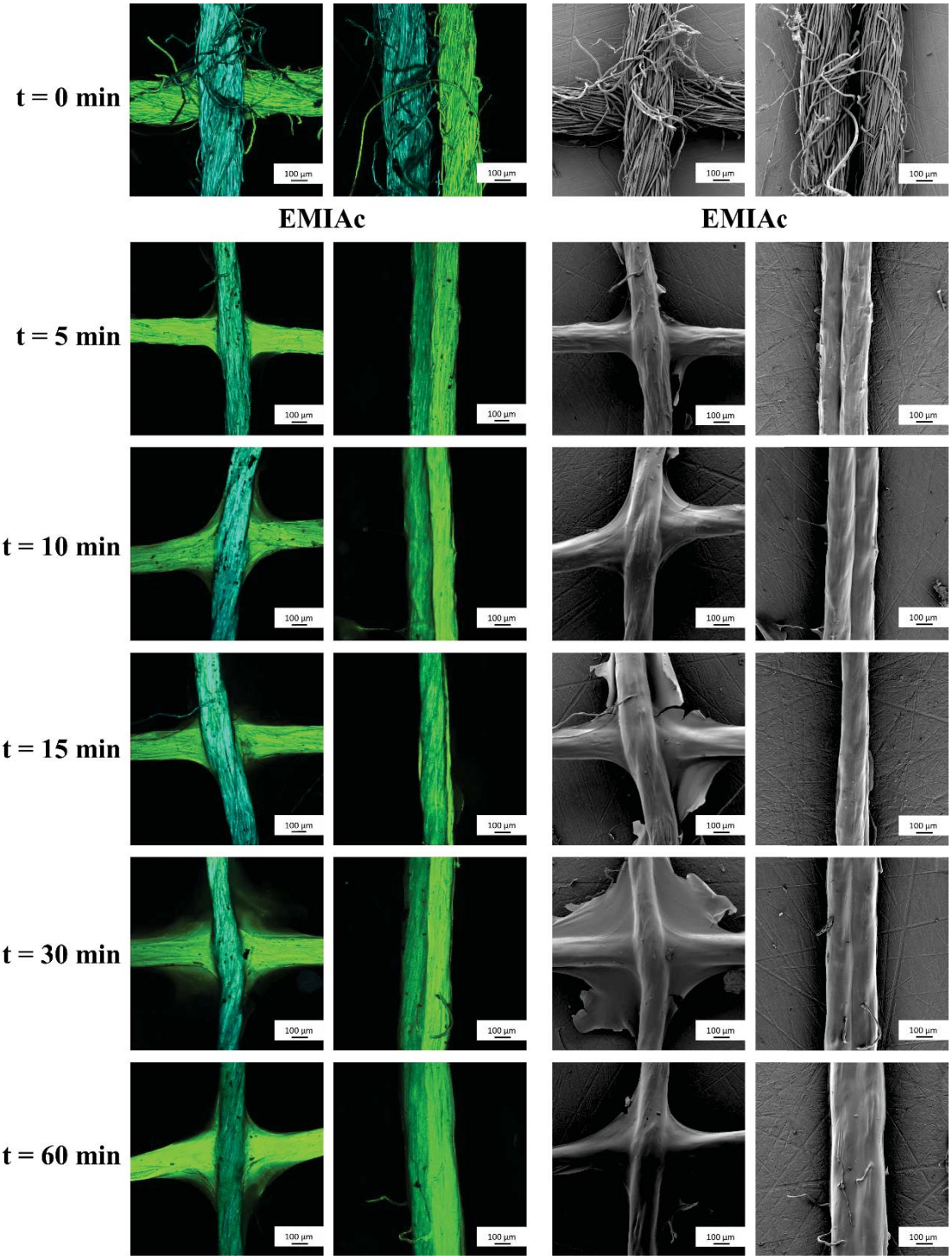

Figure A-12. Confocal microscopy (CFM) and Scanning Electron Microscopy (SEM) of yarns welded using 1-ethyl-3-methylimidazolium acetate (EMIAc) at 60 °C for various treatment times (top to bottom: untreated, 5 min, 10 min, 15, min, 30 min, 60 min). Samples were gold-sputtered prior to imaging in the SEM (10 kV).

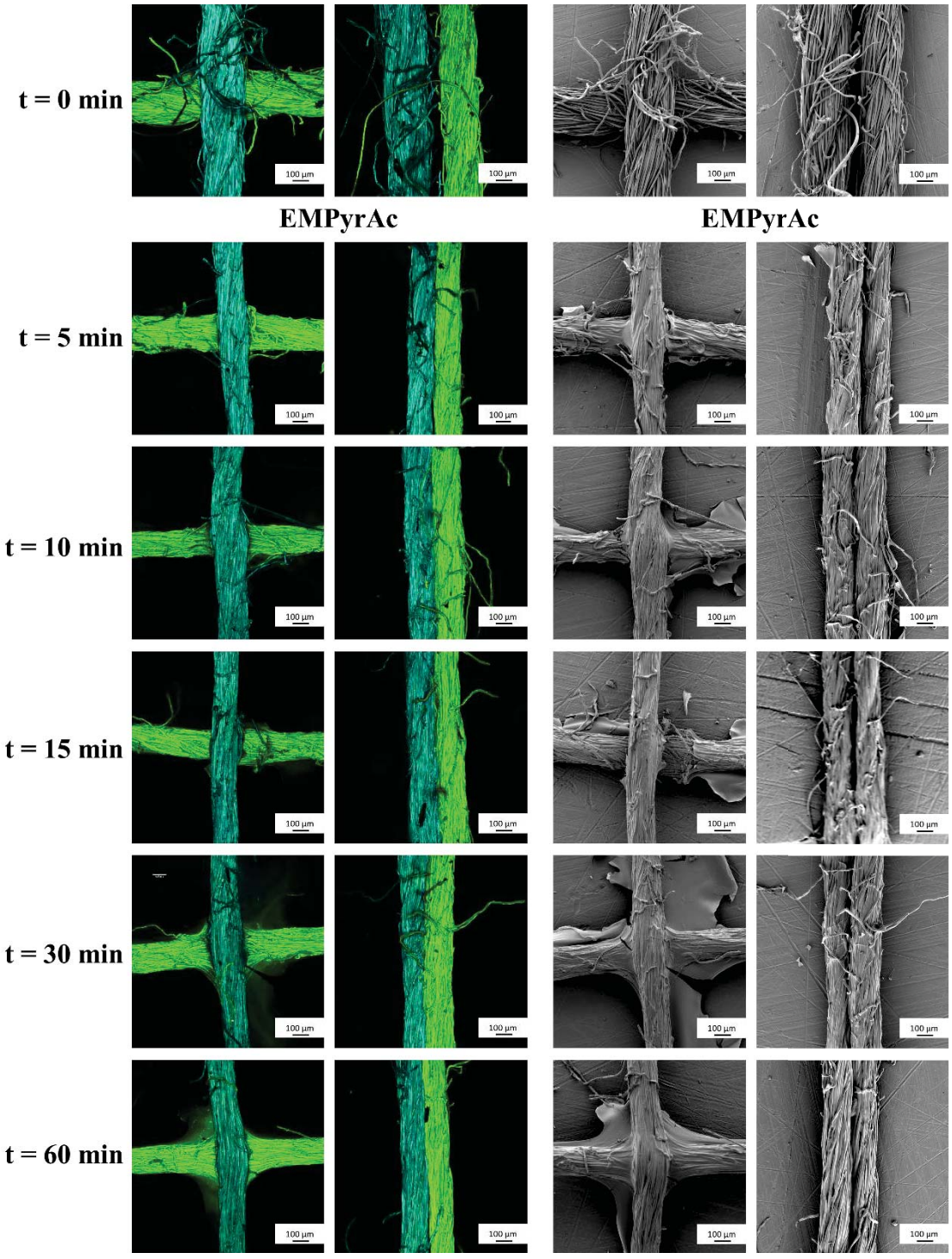

Figure A-13. Confocal microscopy (CFM) and Scanning Electron Microscopy (SEM) of yarns welded using 1-ethyl-1-methylpyrrolidinium acetate (EMPyrAc) at 60 °C for various treatment times (top to bottom: untreated, 5 min, 10 min, 15, min, 30 min, 60 min). Samples were gold-sputtered prior to imaging in the SEM (10 kV).

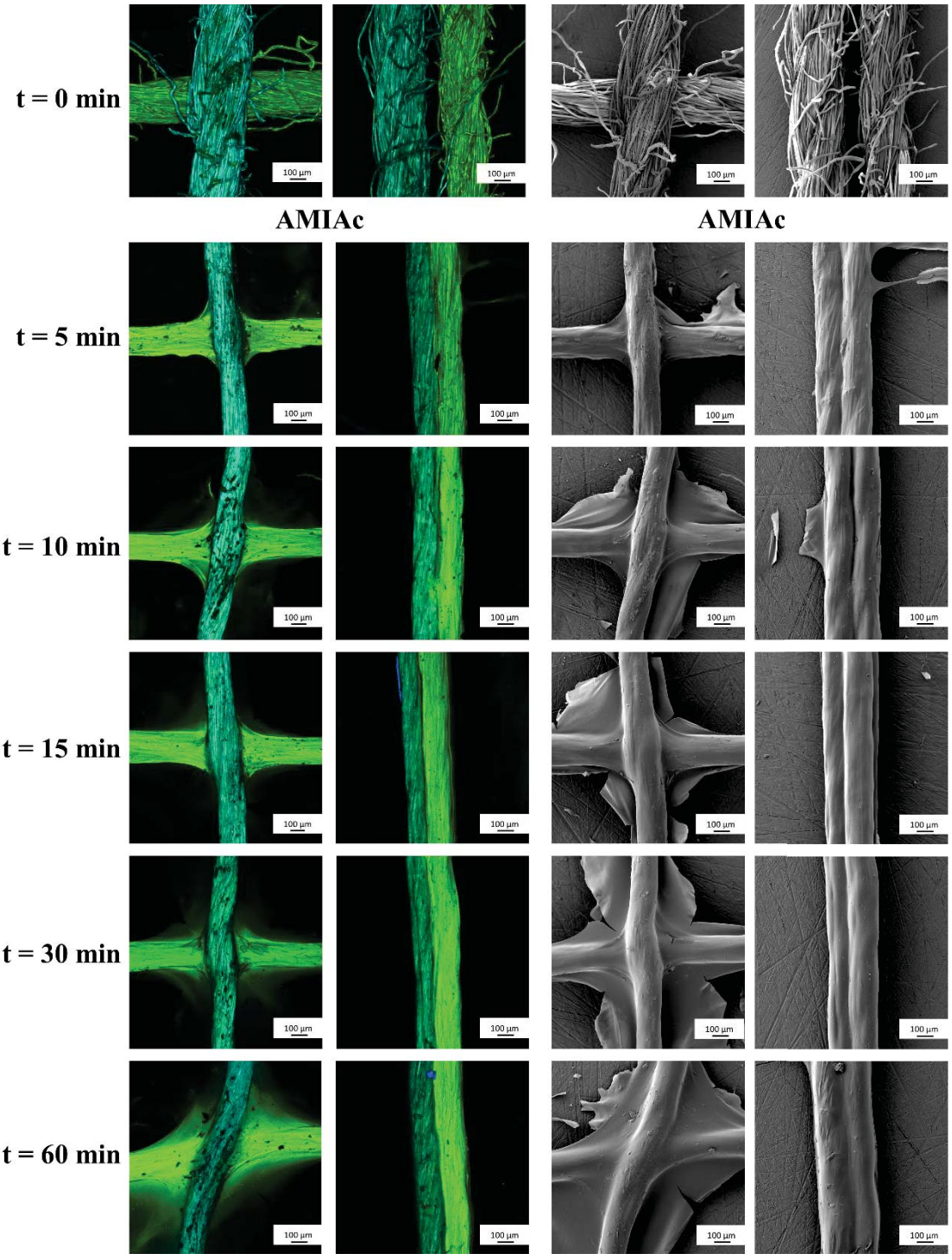

Figure A-14. Confocal microscopy (CFM) and Scanning Electron Microscopy (SEM) of yarns welded using 1-allyl-3-methylimidazolium acetate (AMIAc) at 60 °C for various treatment times (top to bottom: untreated, 5 min, 10 min, 15, min, 30 min, 60 min). Samples were gold-sputtered prior to imaging in the SEM (10 kV).

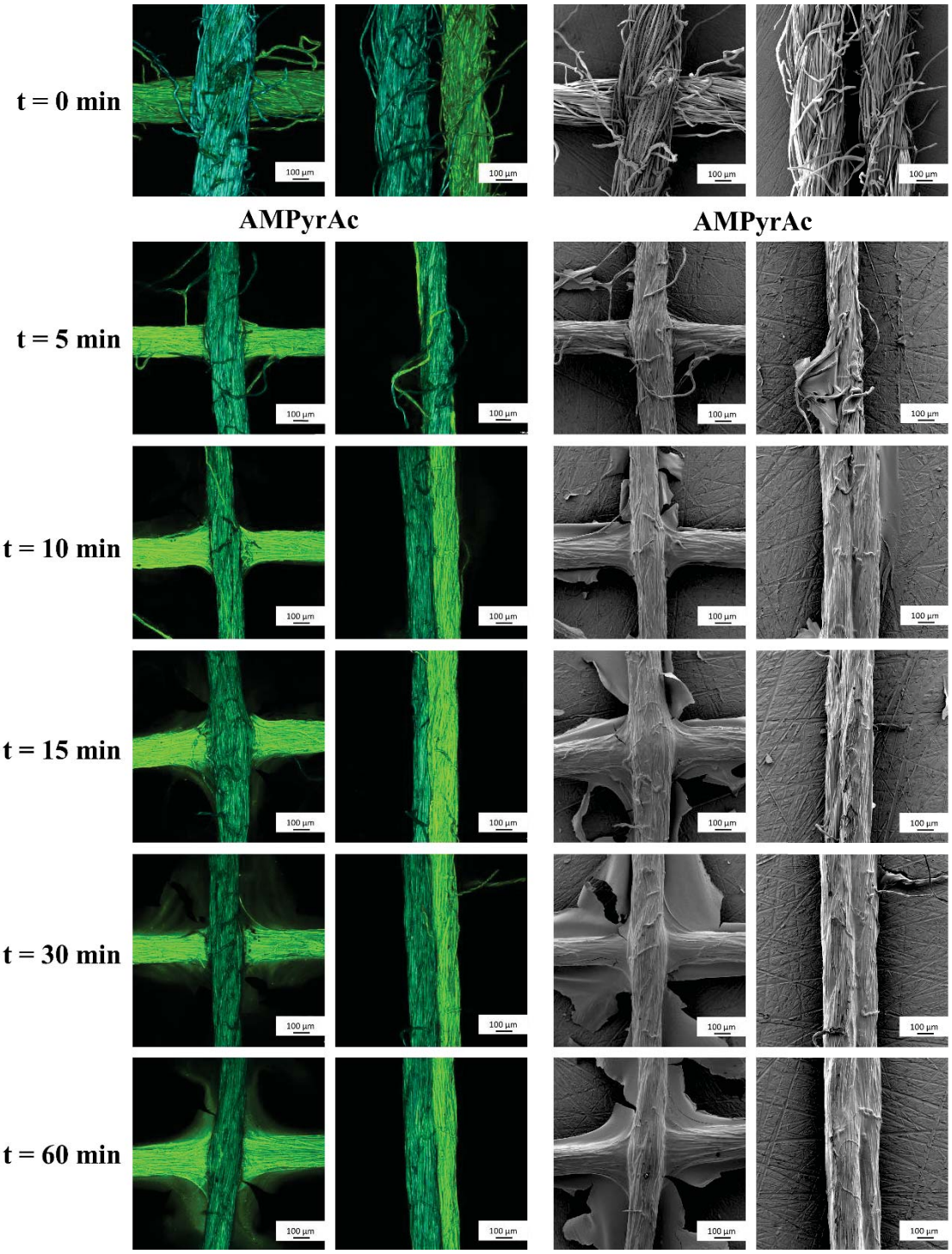

Figure A-15. Confocal microscopy (CFM) and Scanning Electron Microscopy (SEM) of yarns welded using 1-allyl-1-methylpyrrolidinium acetate (AMPyrAc) at 60 °C for various treatment times (top to bottom: untreated, 5 min, 10 min, 15, min, 30 min, 60 min). Samples were gold-sputtered prior to imaging in the SEM (10 kV).

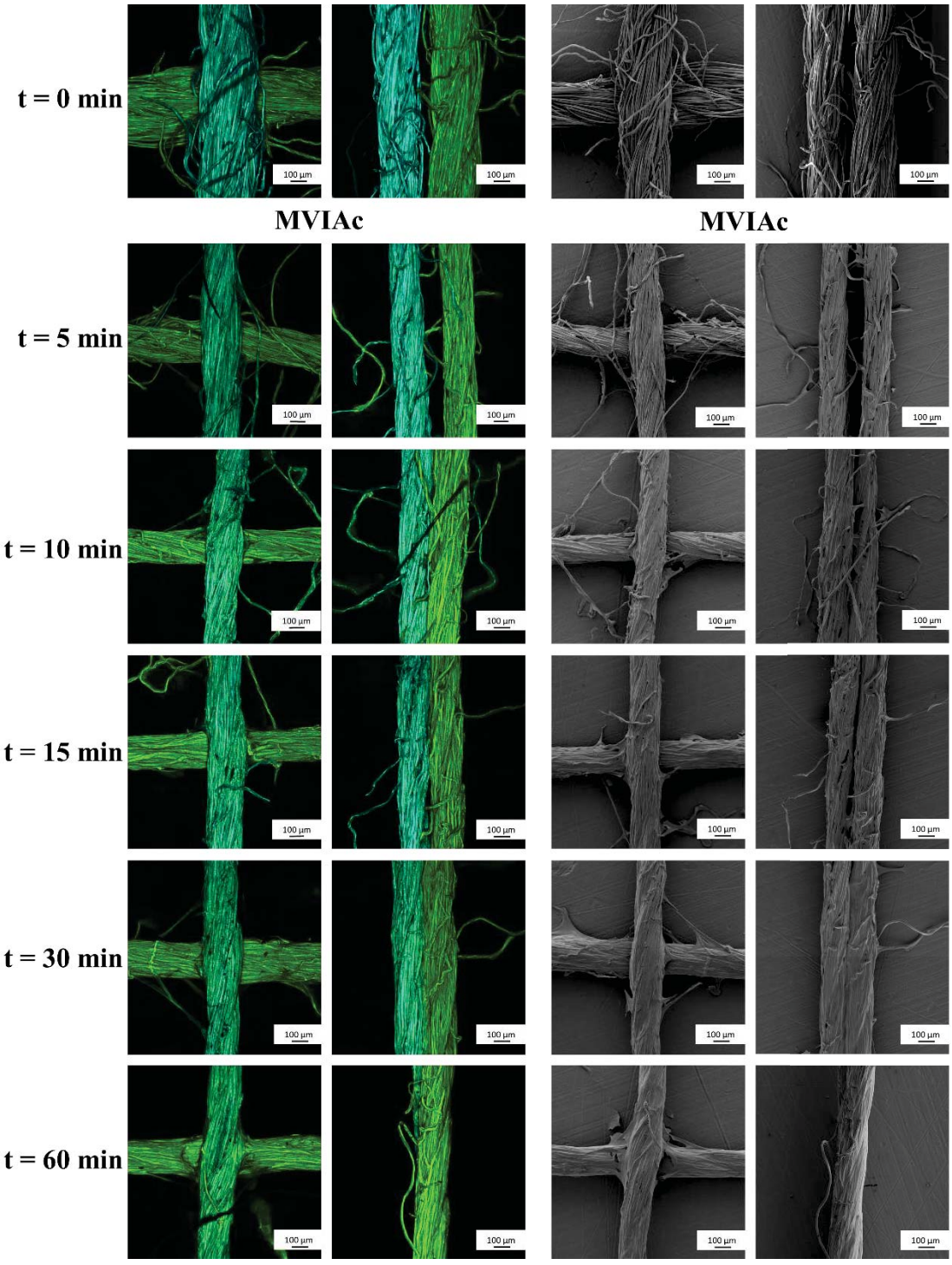

Figure A-16. Confocal microscopy (CFM) and Scanning Electron Microscopy (SEM) of yarns welded using 1-methyl-3-vinylimidazolium acetate (MVIAc) at 60 °C for various treatment times (top to bottom: untreated, 5 min, 10 min, 15, min, 30 min, 60 min). Samples were gold-sputtered prior to imaging in the SEM (10 kV).

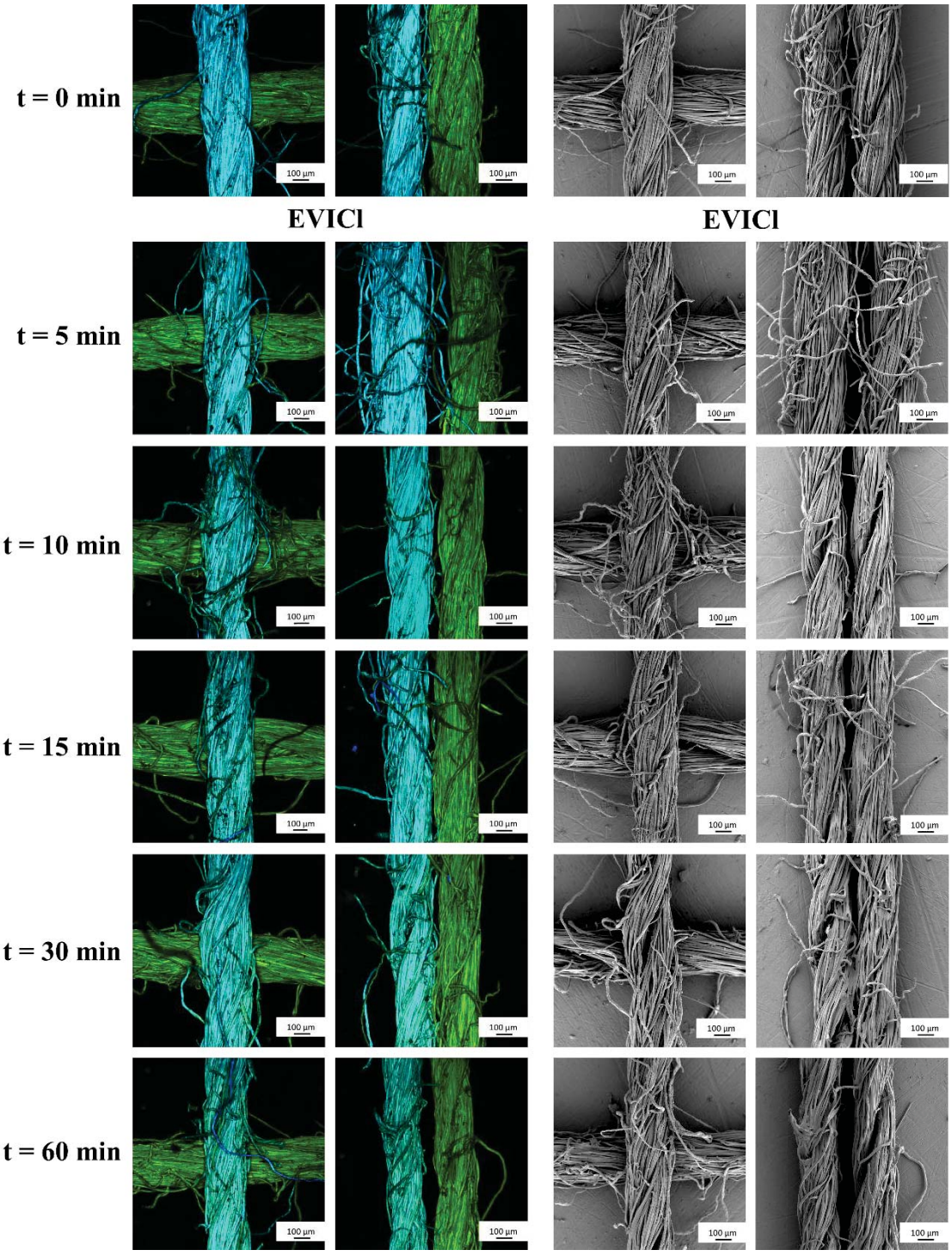

Figure A-17. Confocal microscopy (CFM) and Scanning Electron Microscopy (SEM) of yarns welded using 1-ethyl-3-vinylimidazolium chloride (EVICl) at 100 °C for various treatment times (top to bottom: untreated, 5 min, 10 min, 15, min, 30 min, 60 min). Samples were gold-sputtered prior to imaging in the SEM (10 kV).

11.3 ATR-FTIR Spectra of IL monomers and polymers

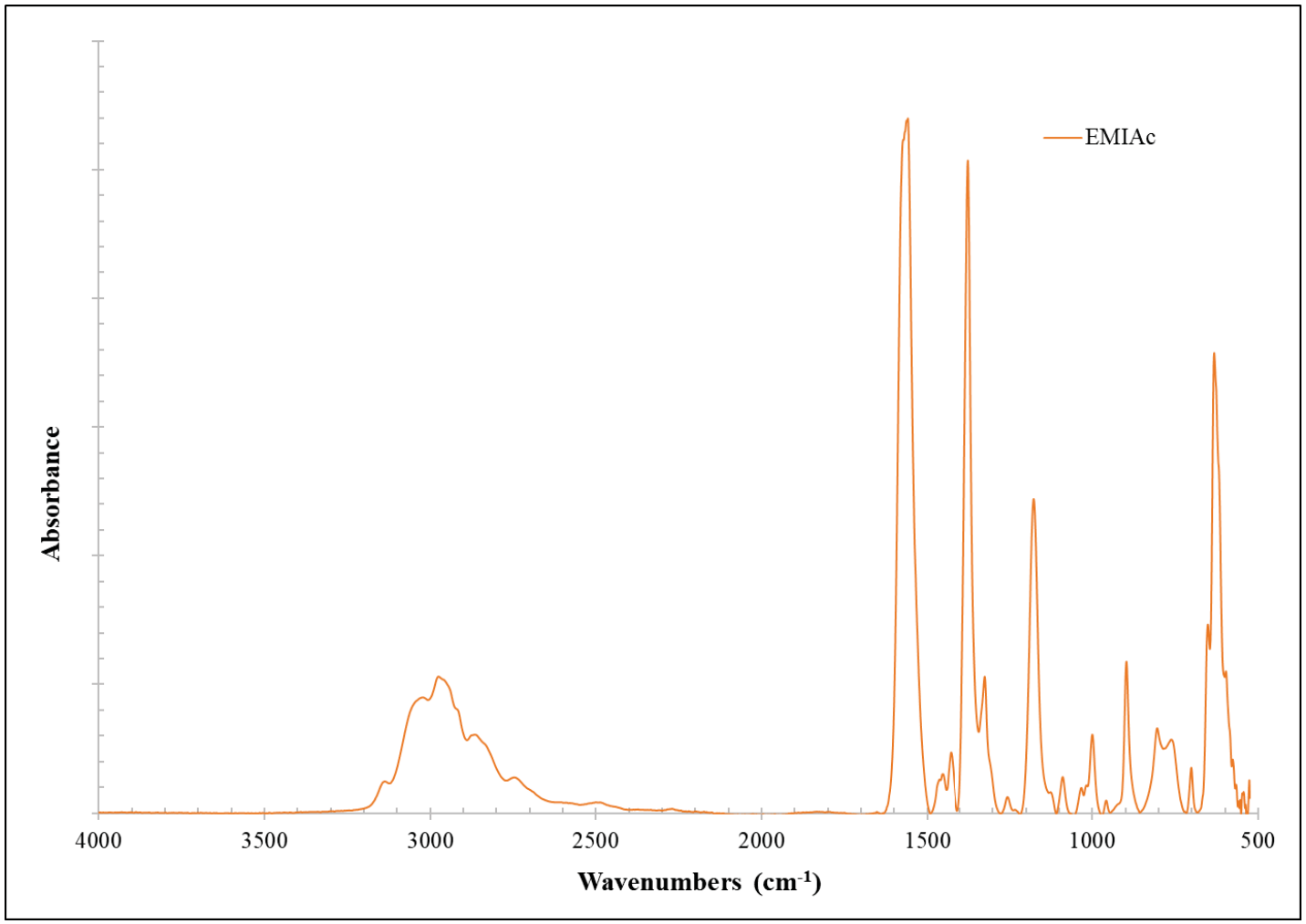

Figure A-18. Attenuated Total Reflectance-Fourier Transform Infrared Spectroscopy (ATR-FTIR) of of 1-ethyl-3-methylimidazolium acetate (EMIAc).

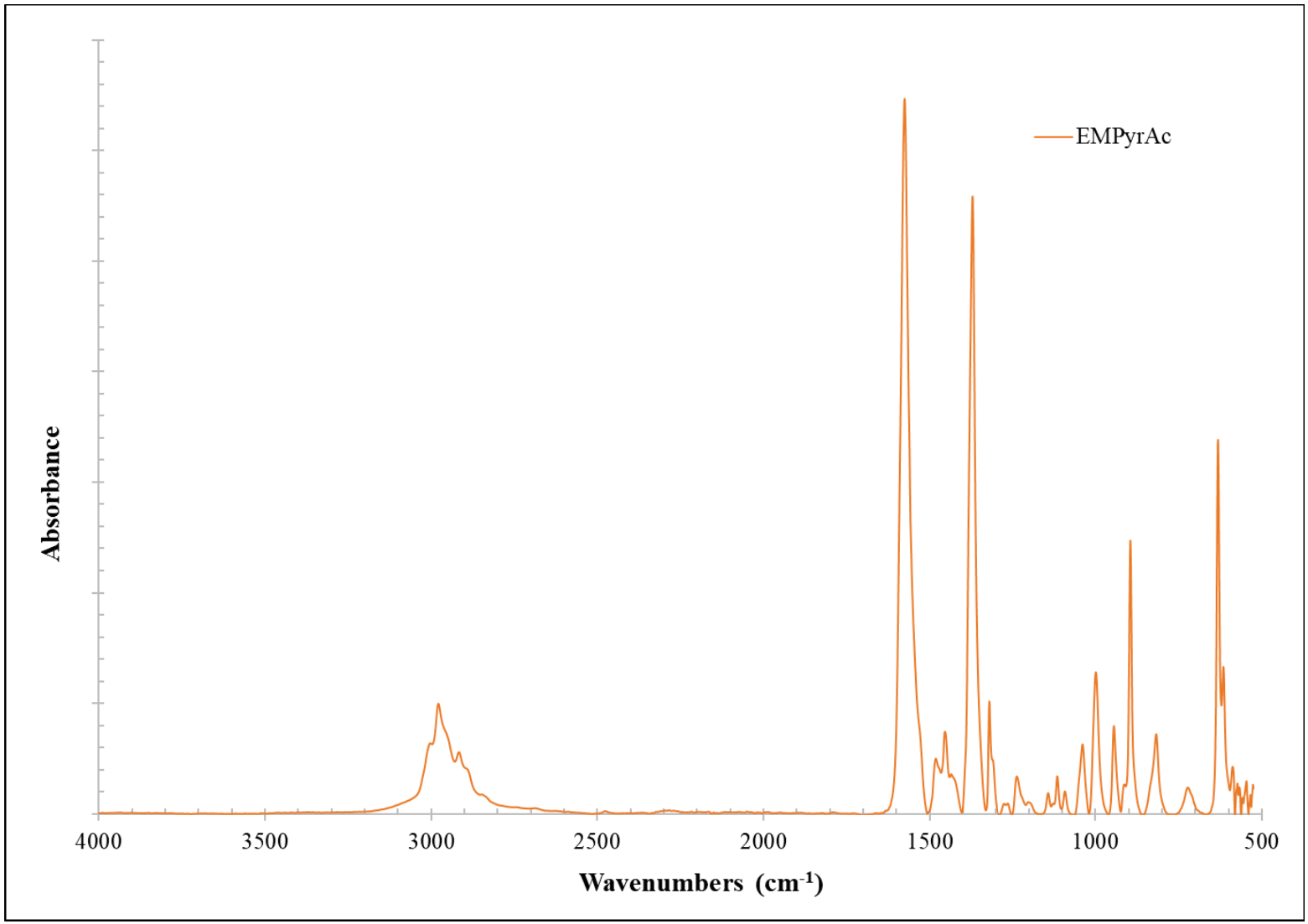

Figure A-19. Attenuated Total Reflectance-Fourier Transform Infrared Spectroscopy (ATR-FTIR) of of 1-ethyl-1-methylpyrrolidinium acetate (EMPyrAc).

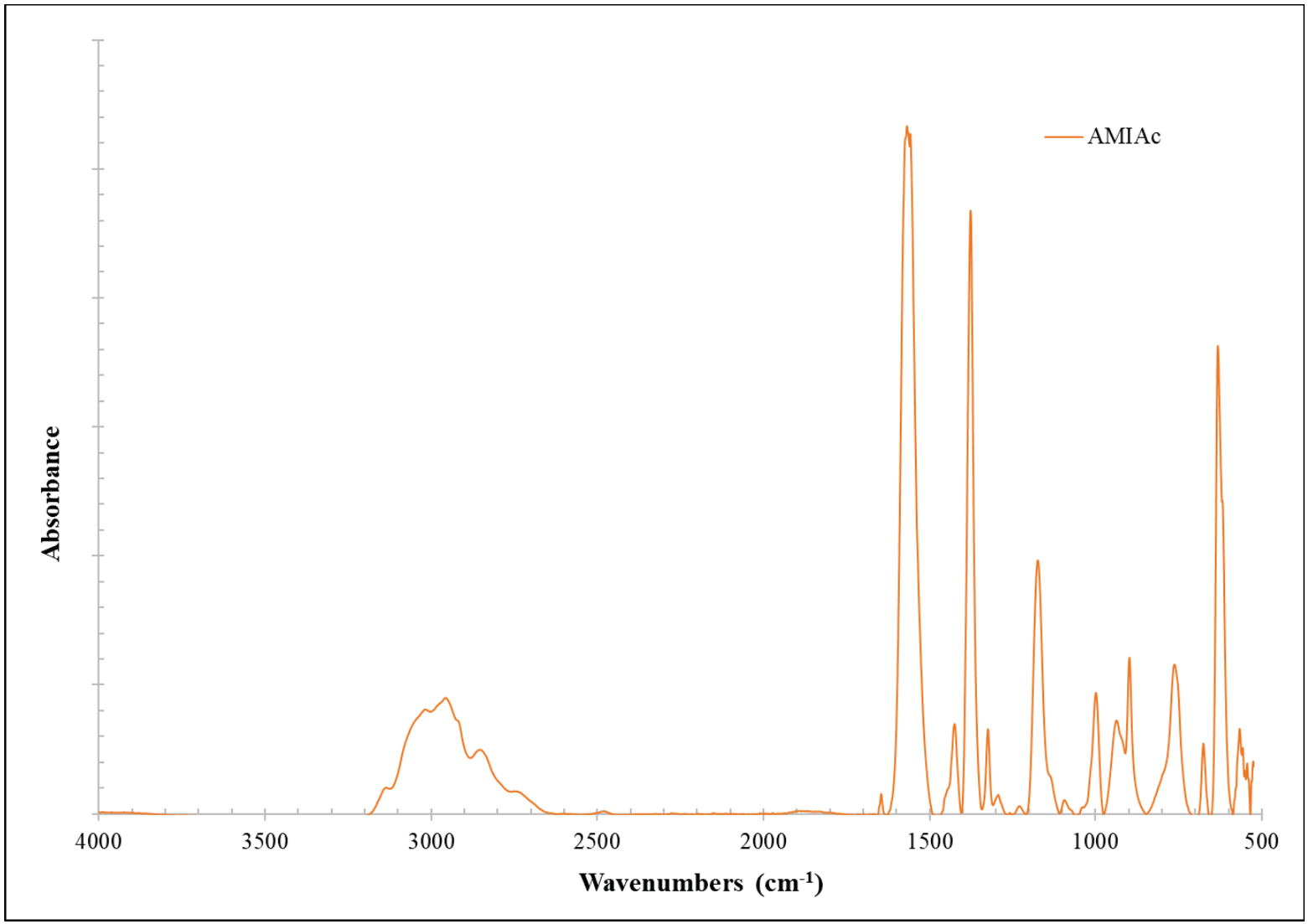

Figure A-20. Attenuated Total Reflectance-Fourier Transform Infrared Spectroscopy (ATR-FTIR) of of 1-allyl-3-methylimidazolium acetate (AMIAc).

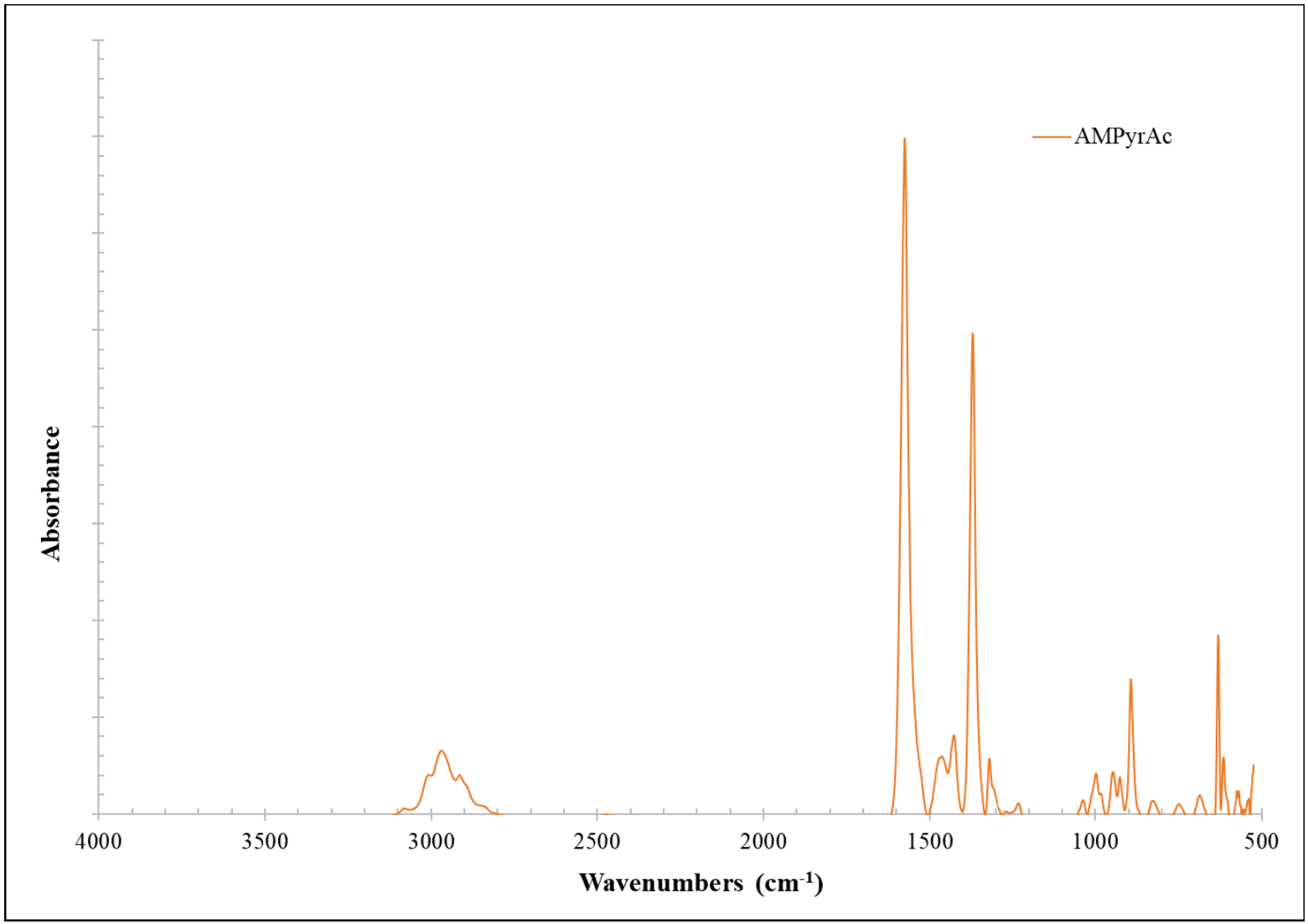

Figure A-21. Attenuated Total Reflectance-Fourier Transform Infrared Spectroscopy (ATR-FTIR) of of 1-allyl-1-methylpyrrolidinium acetate (AMPyrAc).

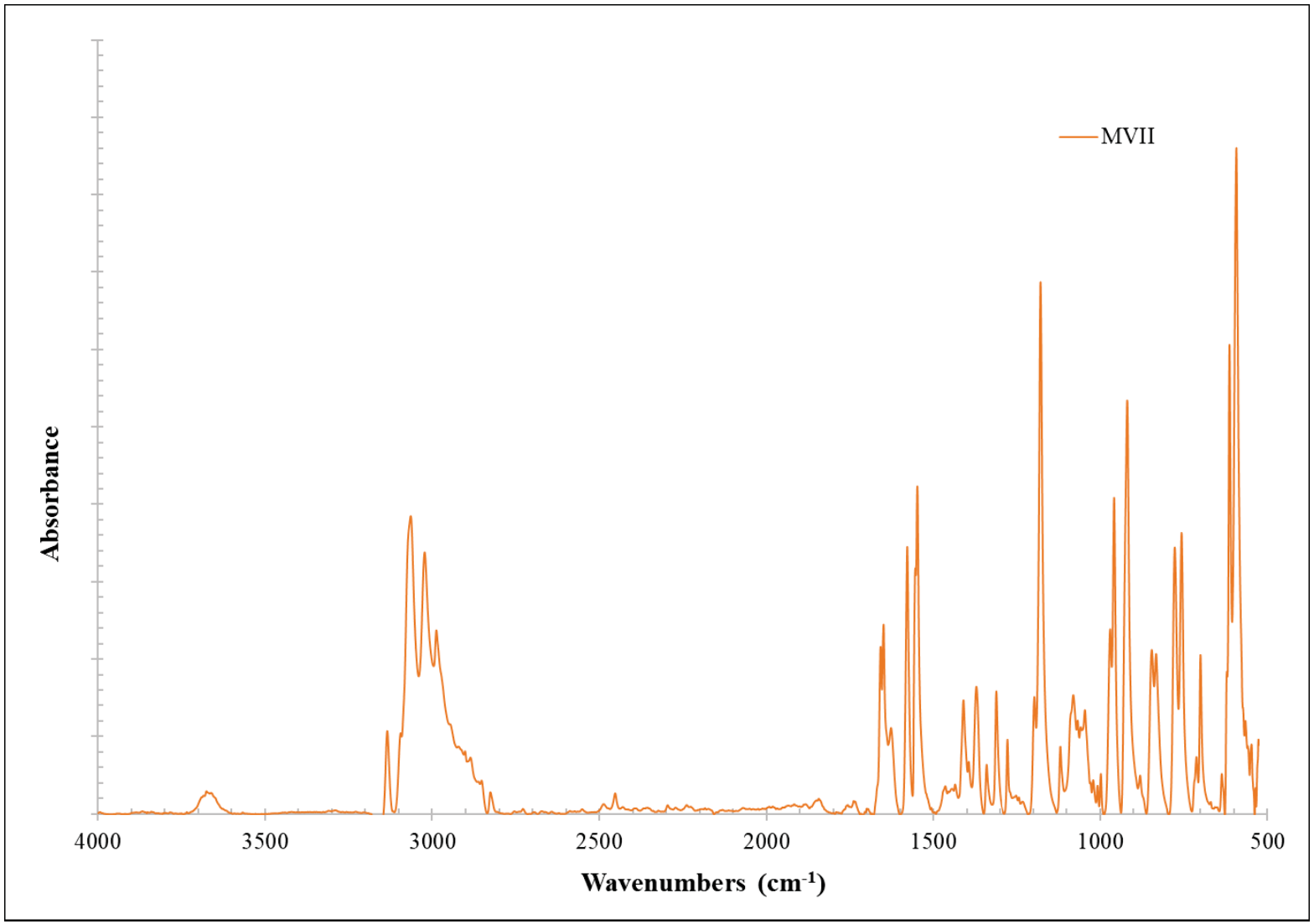

Figure A-22. Attenuated Total Reflectance-Fourier Transform Infrared Spectroscopy (ATR-FTIR) of of 1-methyl-3-vinyllimidazolium iodide (MVII).

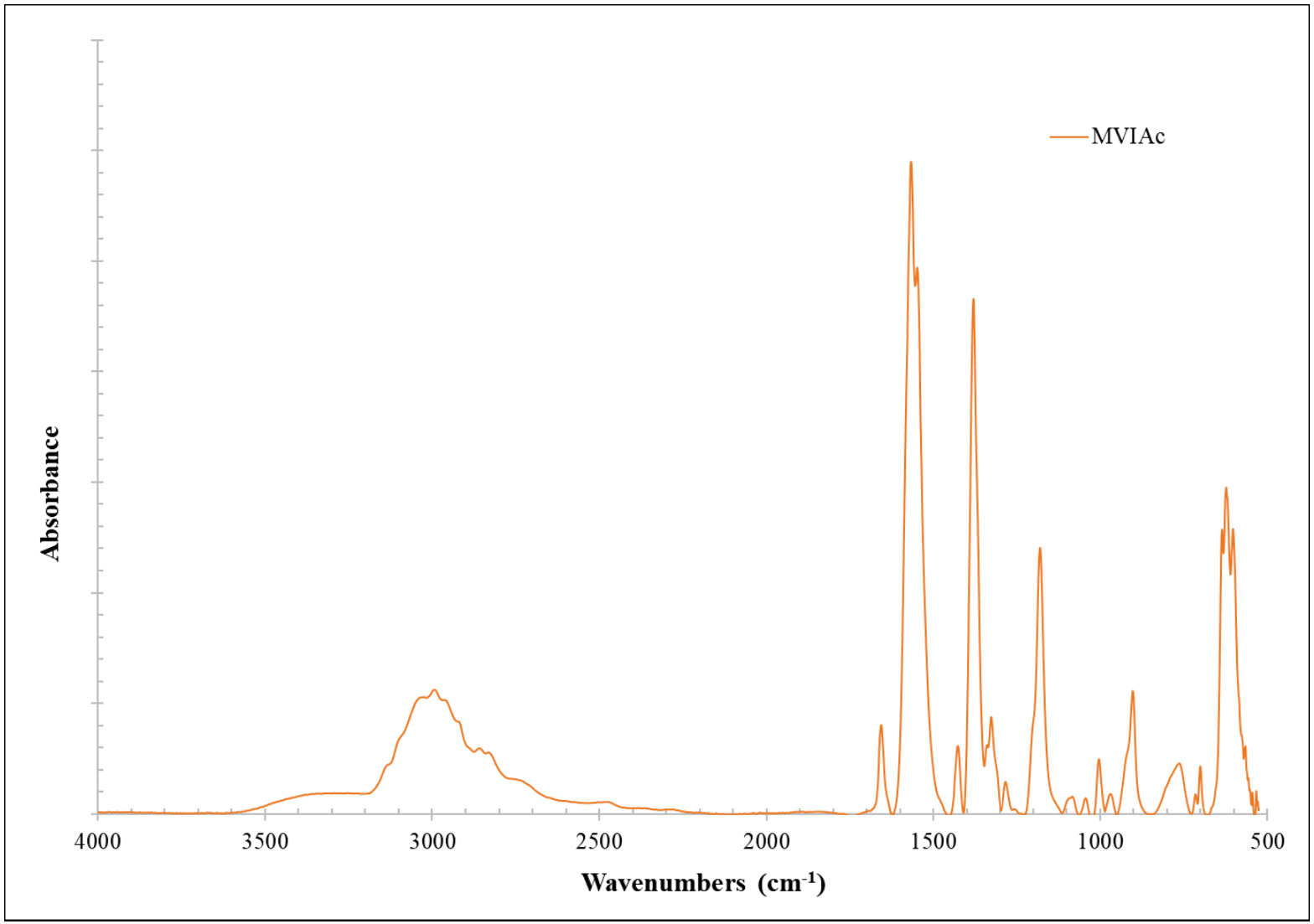

Figure A-23. Attenuated Total Reflectance-Fourier Transform Infrared Spectroscopy (ATR-FTIR) of of 1-methyl-3-vinylimidazolium acetate (MVIAc).

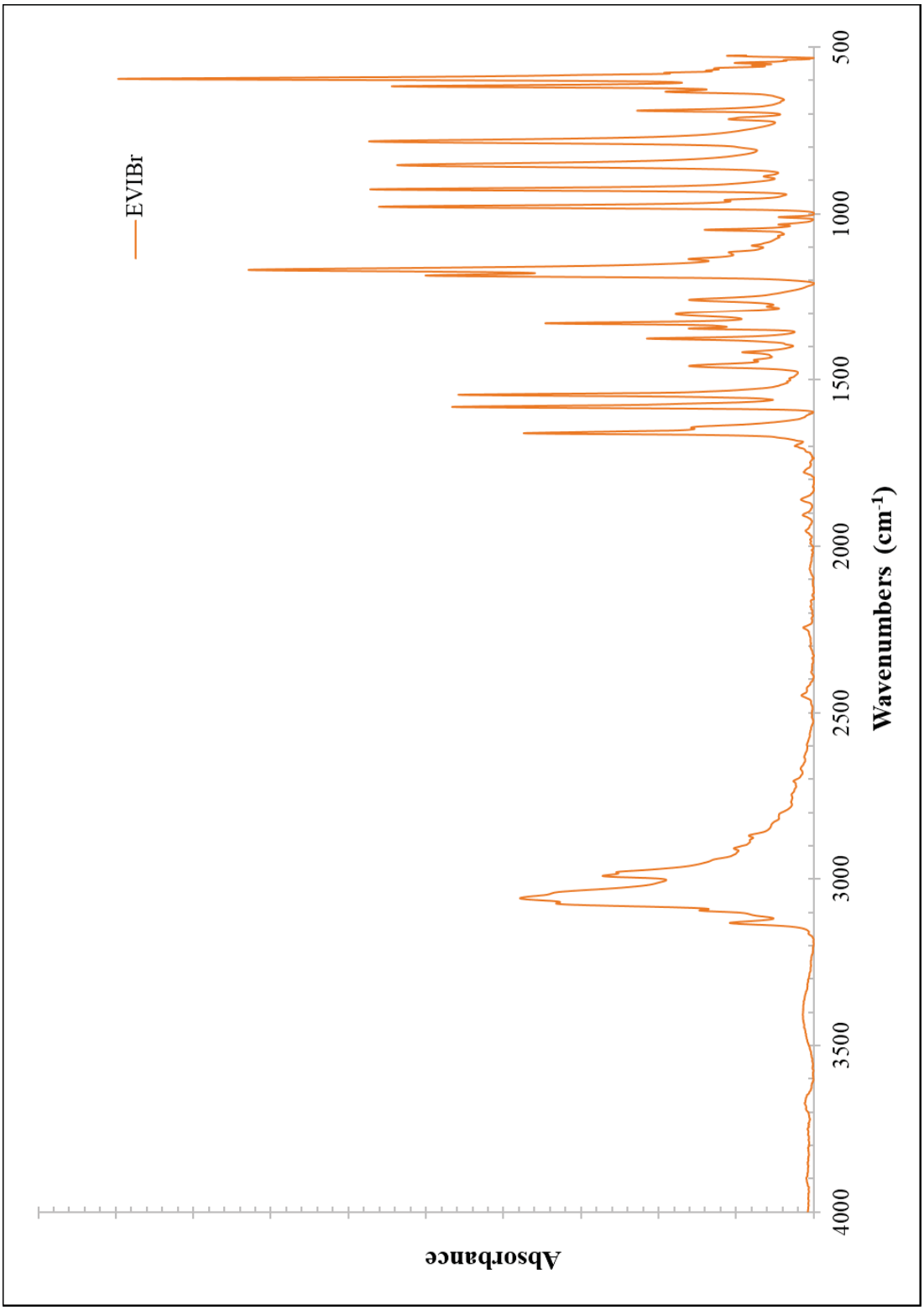

Figure A-24. Attenuated Total Reflectance-Fourier Transform Infrared Spectroscopy (ATR-FTIR) of of 1-ethyl-3-vinylimidazolium bromide (EVIBr).

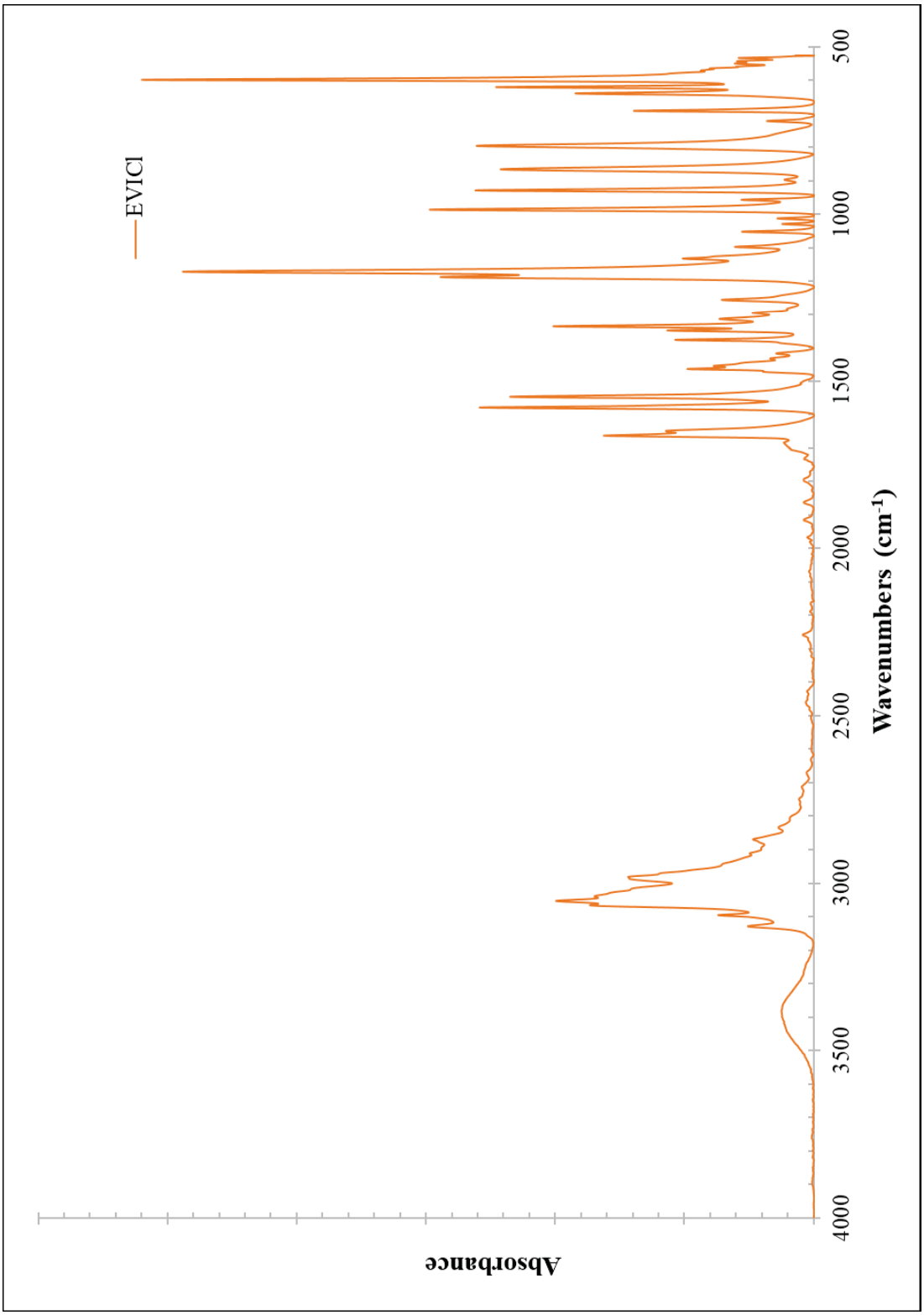

Figure A-25. Attenuated Total Reflectance-Fourier Transform Infrared Spectroscopy (ATR-FTIR) of of 1-ethyl-3-vinylimidazolium chloride (EVICl).

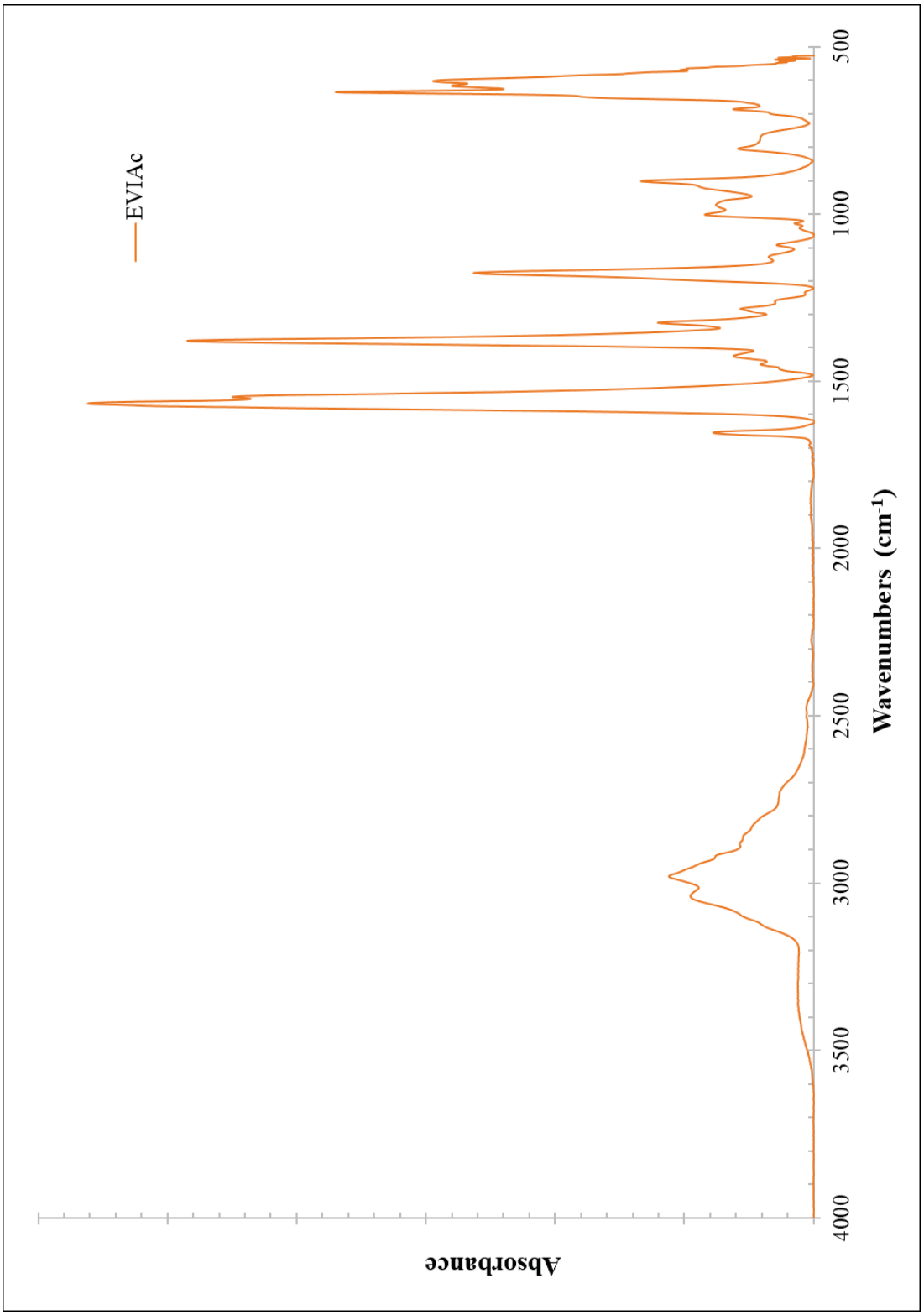

Figure A-26. Attenuated Total Reflectance-Fourier Transform Infrared Spectroscopy (ATR-FTIR) of of 1-ethyl-3-vinylimidazolium acetate (EVIAc).

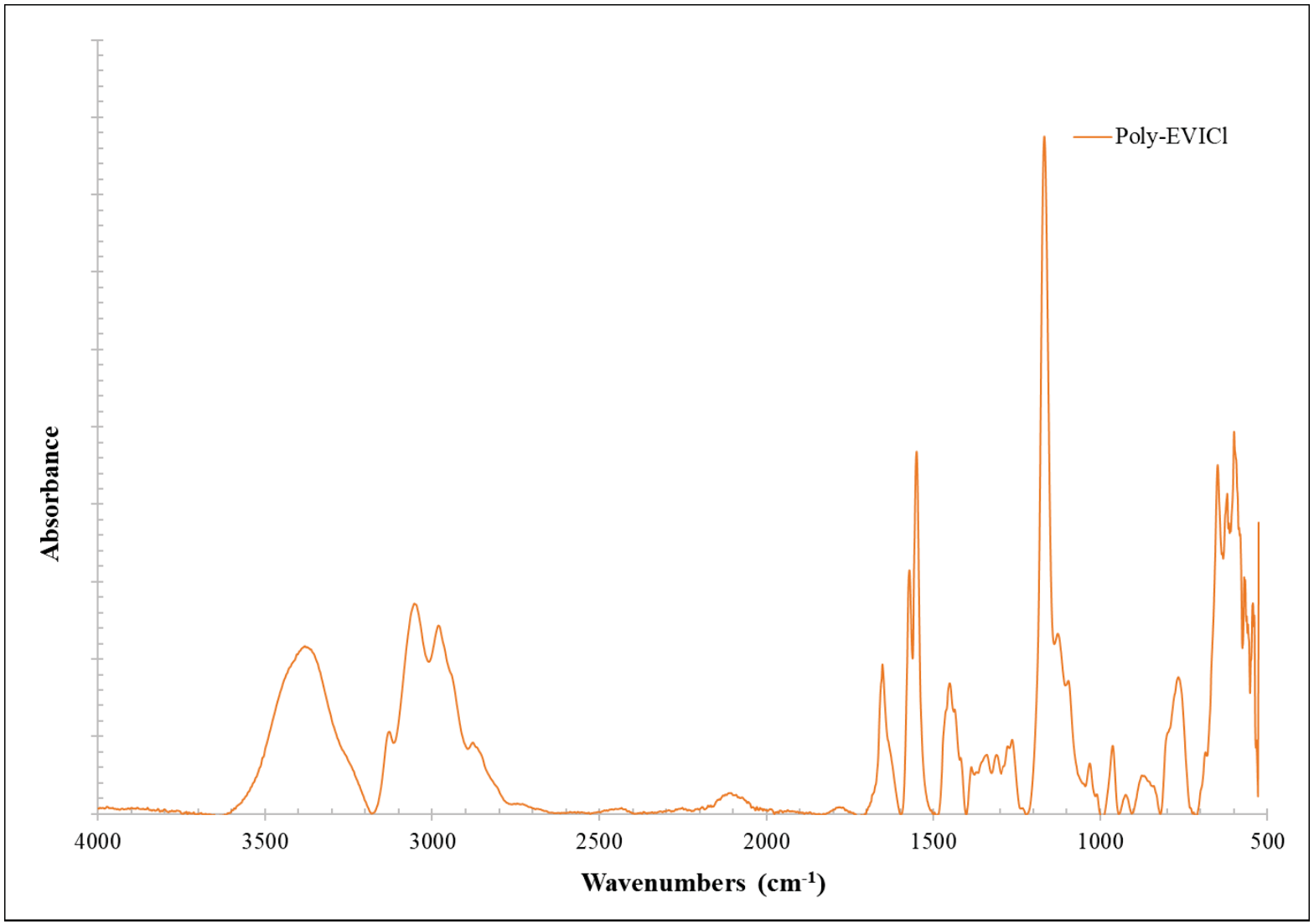

Figure A-27. Attenuated Total Reflectance-Fourier Transform Infrared Spectroscopy (ATR-FTIR) of polymerized 1-ethyl-3-vinylimidazolium chloride (Poly-EVICl).

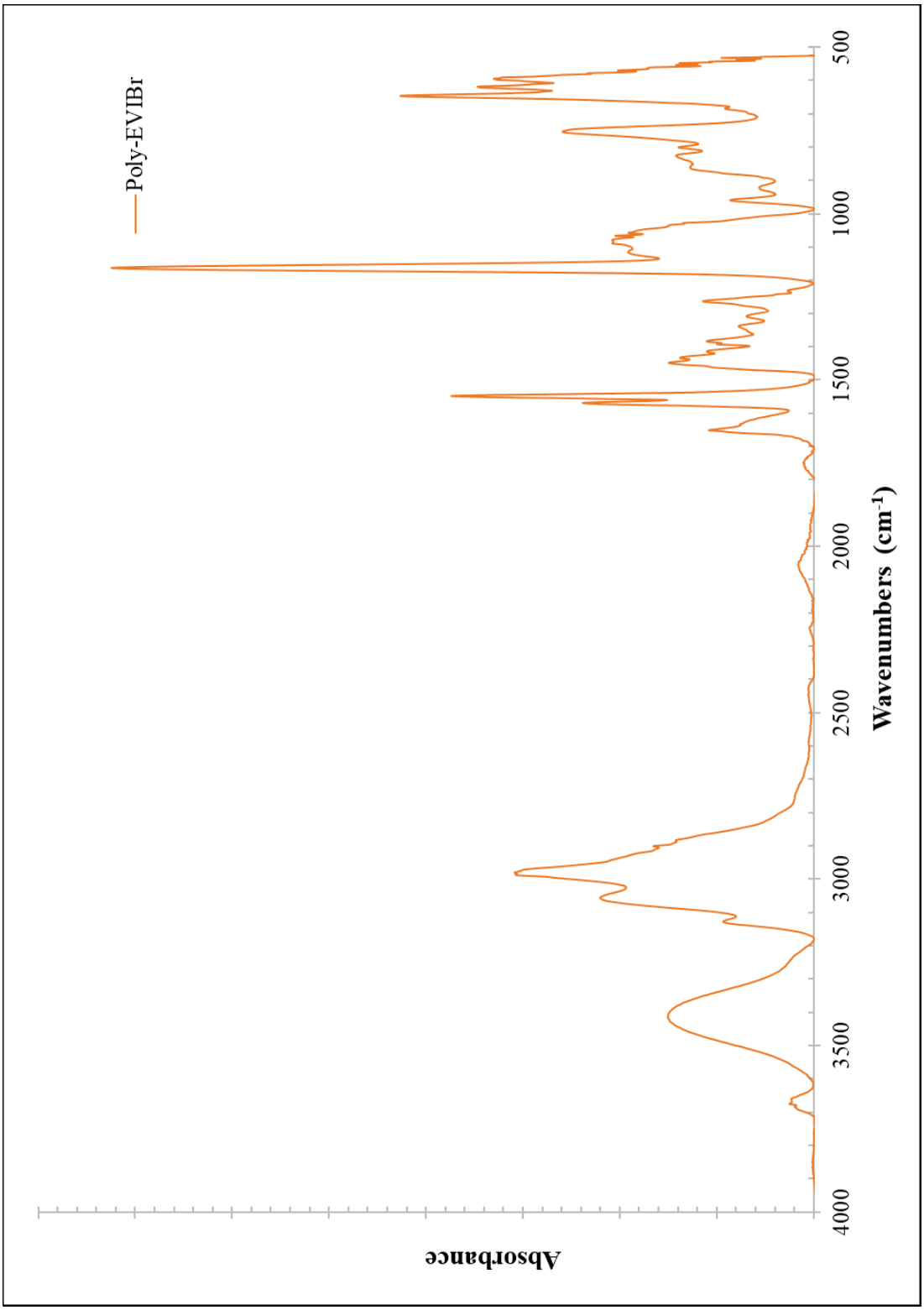

Figure A-28. Attenuated Total Reflectance-Fourier Transform Infrared Spectroscopy (ATR-FTIR) of polymerized 1-ethyl-3-vinylimidazolium bromide (Poly-EVIBr).